Synthesis of novel 2-thiohydantoin derivatives as potential anti-diabetic drugs

A dissertation submitted to the faculty of

Science, Engineering, and Agriculture

Department of Chemistry

As the minimum requirements for the fulfilment of

Master of Science degree in Chemistry at the

University of Venda

By

Tshishonga Unarine

15000291

Supervisor: Prof S.S Mnyakeni-Moleele

Co-supervisor: Dr M.V Bvumbi

DECLARATION

I ***Tshishonga Unarine*** hereby declare that the work presented in this dissertation titled ***'Synthesis of novel 2-thiohydantoin derivatives as potential anti-diabetic drugs'*** 'is my own, unaided work carried out exclusively by me under the supervision of ***Dr Simon Mnyakeni-Moleele*** and the co-supervision of ***Dr Victoria Bvumbi***. It is being submitted for the Degree **Master of science in Chemistry** in the University of Venda, Faculty of science, engineering and agriculture at the department of chemistry. It has not been submitted before for any degree or examination in this or any other University.

Student signature  Date 03 July 2024

ABSTRACT

Thiohydantoin is a hydantoin with one carbonyl group replaced with a thiocarbonyl group. In this study five series (glycinates, alaninates, butanoates, vallinates and norvalinates) of thiohydantoin derivatives (**21a-v**) were successfully synthesized and characterized using known analytical characterization techniques. The synthesis of these compounds followed four reaction steps using conventional methods from step one with nucleophilic substitution to Knoevenagel condensation reaction as the final step. All twenty two compounds were obtained in good to excellent yields and were subjected to *in vitro* screening for their inhibitory activity against α-glucosidase.

Among the five series of thiohydantoin derivatives, the alaninate derivative **21f** exhibited the highest inhibition at both concentrations of 65 µM and 130 µM, with values of 71.13±0.61 and 64.20±0.54, respectively. The glycinate derivative **21j** exhibited the highest inhibition of 60.95±1.07 at 130 µM, while butanoate derivatives showed a consistant moderate inhibition. Only compound **21z** exhibited concentration-dependent trends of moderate inhibition on the norvallinates derivatives and the vallinates exhibited negligible inhibition.

ACKNOWLEDGEMENTS

I would like to give thanks to the almighty **God** for his grace and presence throughout the course of this study.

I would like to thank and appreciate the following people:

- My supervisor **Prof. SS Mnyakeni-Moleele** for his continuous support, encouragement and motivation throughout the great and sad times towards this study. You were the best leader and supervisor during the course of this study. May you continue with this wonderful supervision to your all your upcoming students.
- My Co-supervisor **Dr MV Bvumbi** for her efforts and contributions in this dissertation.
- Our NMR operator **Mr P Pandelani** for making sure we received our results in time and for making sure that NMR is always running smoothly.
- **Prof. NE Madala**, thank you so much for running our mass spectral analysis (HRMS) of all our synthesized compounds.
- our Lab technicians **Mr FB Mutshaeni** and **Ms NR Maseko**, thank you so much for keeping the labs in a much safer conditions and for your assistance in providing the much-needed resources to carry out this study.
- **Univen Drug synthesis and isolation** (DSI) and **Chemistry department** in general, thank you so much for all your assistance and for the opportunity to work with you guys.
- Prof Maryna van de Venter from the Nelson Mandela Metropolitan University Bioassaix, for screening our compounds for their anti-diabetic activities.
- My mother **Ms TJ Munyai** for all your prayers, support, motivation and love.
- Mr **F Tshishonga** for your guidance and support throughout my masters' study.
- To my life partner **Mr AI Nemudzivhadi**, thank you very much for your help, support and motivation towards this study. You carried me through to the end, I'm grateful.
- My son **Mukundi Theodore Nemudzivhadi** for his love and presence in my life.
- My friends, **Miss Ramusetha Rolivhuwa**, **Miss Awelani sinyegwe** and **miss Nyeleti Mbokazi**, thank you for your support.

I would also like to thank the following organisations:

- **University of Venda** for giving an opportunity to undertake this study.
- To the **National Research Foundation of South Africa** (NRF), thank so much for your financial assistance towards the successful completion of this dissertation.

Glossary of Abbreviations/Acronyms

α: Alpha

AC2O: Acetic Anhydride

ATP: Adenosine Triphosphate

β: Beta

^{13}C NMR: Carbon 13 Nuclear Magnetic Resonance

$CDCl_3$: Deuterated chloroform

DM: Diabetes mellitus

DMSO: Deuterated Dimethyl sulfoxide

DNA: Deoxyribonuclei acid

EGCG: Epigallocatechin gallate

FFA: Free fatty acid

FTIR: Fourier transform infrared spectroscopy

GAD65: Glutamic acid decarboxylase

GDM: Gestational diabetes mellitus

HRMS: High resolution mass spectroscopy

Hz: Hertz

IAA: Insulin Antibodies

IA-2: insulinoma-associated 2

IAPP: Islet amyloid polypeptide

ICA: Islet cell cytoplasmic antibodies

IC50: Half Maximal Inhibitory Concentration

IDF: International diabetes federation

IR: Insulin resistance

IR: Infrared spectroscopy

MGAM: maltase-glucoamylase

MHz: Mega hertz

m.p: Melting point

ml: millilitre

mmol: millimole

NMR: Nuclear Magnetic Resonance

PPAR: Peroxisome proliferator-activated receptor

PPAR-α: Peroxisome Proliferator Activated Receptor alpha

PPAR-γ: Peroxisome Proliferator Activated Receptor Gamma

PPRE: Proliferator response elements

SI: Sucrose-isomaltase

SC: Subcutaneous injection

SAR: Structure activity relationship

SUR: Sulphonylurea receptors

T1D: Type 1 diabetes

T2D: Type 2 diabetes

TLC: Thin layer chromatography

TMS*:* Tetramethylsilane

TZDs: Thiazolidinediones

ZnT8: Zinc transporter 8

Table of Contents

CHAPTER ONE

1. INTRODUCTION

1.1 Diabetes

Diabetes is a metabolic disorder that manifests as chronic hyperglycaemia due to a lack of insulin, defective insulin action, or both. [1] Insulin is an important hormone that aids the body's use of glucose for energy. Glucose is a type of sugar that is derived primarily from the foods we eat. Insulin allows glucose to enter cells in the body where it is needed and stores excess glucose for later use. [2] Diabetes is a non-communicable disease that has a significant impact on fatality and mortality worldwide. [3] Diabetes is divided into three main types: type 1, type 2 and gestational diabetes, with type 2 accounting for 90% of all diabetes cases. [4]

Type 1 diabetes (T1D) is distinguished by the autoimmune destruction of pancreatic beta-cells, which results in insulin insufficiency. Obesity, decreased insulin production, and insulin resistance are commonly related with type 2 diabetes (T2D). [5] There are other rare types of diabetes, such as neonatal diabetes and maturity-onset diabetes of the young. [6] Even though the etiology of T1D and T2D may be different, both have been demonstrated to make cardiovascular problems more common. [7] Many diabetics will experience long-term organ issues, which often manifest gradually and may eventually cause irreversible damage. [8]

1.2 Metabolic role of Insulin

Insulin, a hormone made up of 51 amino acids, is essential for glucose balance, cell development, and metabolism. [9] Insulin, often known as the primary hormone, regulates blood glucose levels in our bodies by transporting glucose from the blood to the tissues. [3] The hormone potentially coordinates with glucagon to modulate blood glucose levels; insulin acts via an anabolic pathway, while glucagon performs catabolic functions. [10] When the concentration of glucose rises, cells secrete insulin. Insulin lowers blood glucose levels by either decreasing glucose production from the liver via

glycogenolysis or increasing glucose uptake by the liver, muscle, and adipose tissue via gluconeogenesis. [11]

In addition to the aforementioned functions, insulin also stimulates the synthesis of fat, encourages the storage of triglycerides in fat cells, stimulates the synthesis of protein in the liver and muscles, and promotes cell growth. [12] Insulin is not secreted if the blood glucose concentration is ≤ 3.3 mmol/l, [13] but is secreted in increasing amounts as glucose concentrations increase beyond this threshold. [14] Insulin secretion occurs in two stages postprandially: an initial quick release of preformed insulin, followed by greater insulin synthesis and release in response to blood glucose. [10] Glucose control is an intricate orchestration of numerous hormones, including pancreatic and gastrointestinal hormones, that have an impact on a variety of target tissues, including muscle, brain, liver, and adipocyte. [15]

1.3 Incidence and prevalence of diabetes

1.3.1 Around the world

Diabetes had reached pandemic proportions globally, with the IDF's 9th edition reporting a prevalence of 9% (463 million adults) in 2019. [16] The increased prevalence of diabetes has been linked primarily to population aging. [17] However, decreasing diabetes-related mortality as a consequence of better medical care as well as rises in diabetes incidence in some nations as a result of rising rates of diabetes risk factors, particularly obesity, are also significant contributors to higher prevalence. [18]

The prevalence of diabetes in adults globally increased to 8.8% of the adult population in 2017, and it is predicted that this number will grow to 9.9% by 2045. This represents a total of 424.9 million people with diabetes globally in 2017 and is projected to rise to 628.6 million by 2045, a 48% increase. [19]. Contrary to this alarming prevalence of DM, there is still a lack of diagnosis affecting about 193 million people globally with the largest proportion, over 120 million in the Southeast. [20]

Recently the 10th IDF Diabetes Atlas records that 537 million adults (20-79 years) are living with diabetes. This number is predicted to rise to 643 million by 2030 and 783 million by 2045. [16] The African continent accounts for just 4.5% (24 million) of adults with diabetes on a global scale, but this figure is expected to climb to 55 million by 2045, a 134% increase. [21]

1.3.2 In South Africa

Diabetes was South Africa's second-greatest underlying cause of death in 2016 and 2017. [22] Diabetes prevalence in South Africa has reached 11.3%, the highest in Africa and had an estimated 96,000 deaths in 2021. [Error! Bookmark not defined.] According to recent assessment from the International Diabetes Federation (IDF), there are 1.8 million people in South Africa who have diabetes. The IDF also predicts that 69% of all diabetics are undiagnosed. [23] The most significant cause of variability in T2D prevalence in South Africa was the population group. T2D prevalence was highest among Indians, followed by Coloureds, and lowest among Black Africans, which may represent South Africa's status of health transition and noncommunicable disease death rates. [24]

1.4 Classification of diabetes

1.4.1 Type 1 diabetes

Type 1 diabetes is a complex autoimmune illness defined by the loss of insulin-producing pancreatic beta cells; however, the causes of autoimmunity and disease remain poorly understood. [25] The development of β cell autoantibodies is thought to be induced after a genetically susceptible individual is exposed to a presumed environmental factor that triggers a loss of immune regulation. [26] β-Cell destruction results in decreased insulin secretion, hyperglycaemia and, eventually, clinical type 1 diabetes. [27] The asymptomatic phase in which multiple autoantibodies to β cell antigens are detectable in serum is termed islet autoimmunity. [26] Islet cell cytoplasmic antibodies (ICA), insulin antibodies (IAA), glutamic acid decarboxylase (GAD65), insulinoma-associated 2 or protein tyrosine phosphatase antibodies (IA-2) and zinc transporter 8 (ZnT8) are among these antibodies. The more detectable antibodies there are and the higher their titers, the greater the risk of developing T1DM. [28]

Type 1 diabetes is also known as insulin-dependent diabetes mellitus (IDDM) or juvenile-onset diabetes. [29] T1DM is one of the most common chronic diseases among children, but it can begin at any age. The incidence and prevalence of T1DM have steadily increased, particularly the incidence of childhood T1D. [30] T1D treatment should aim to decrease cell autoimmunity while also protecting and restoring remaining cell mass. There are currently no clinically approved interventional treatments for addressing the underlying autoimmune and increasing cell survival in

T1D. [31] As previously stated, the presence of diabetes-related autoantibodies validates the diagnosis of type 1. However, type 1 DM can arise in obese patients with one or more risk factors for insulin resistance, therefore screening for markers of autoimmunity is advised in all cases of new-onset DM. [29]

1.4.2 Type 2 diabetes

Type 2 diabetes (T2D) usually arises in middle or late adulthood, often in people who have a number of health problems, such as high blood pressure, obesity, and inactivity. [32] Given the global obesity pandemic, it is not surprising that the incidence of T2D in adolescents and young adults has recently increased. [33] Type 2 diabetes usually appears gradually as muscle and liver cells lose sensitivity to the glucose-lowering actions of endogenous insulin. Insulin resistance is followed by elevated blood glucose levels and, eventually, increasing beta cell damage. [34]

T2DM is typically caused by either inadequate insulin production by β-cells or insulin resistance following a progressive decline in β cell function and accumulation of islet amyloid polypeptide (IAPP, or amylin) in the pancreatic islets. [35] Although the causes of insulin resistance are numerous, one of the reasons is the accumulation of excess lipids and fatty acids in the circulation and skeletal muscle tissue. This causes the transporters that deliver glucose from the bloodstream into the cells to become blocked when insulin is activated. [36] T2DM pathogenesis is predominantly driven by the induction of insulin resistance in skeletal muscle, liver and adipose tissue. [37] Since skeletal muscle is the primary organ responsible for postprandial glucose disposal, insulin resistance in skeletal muscle severely limits glucose clearance capacity in T2DM patients. [38]

Insulin resistance in the liver is related with high rates of hepatic glucose synthesis during fasting, which is due in part to inadequate insulin-mediated inhibition of gluconeogenesis. [39] Liver insulin resistance is also related with a failure to regulate postprandial hepatic glucose production due to inadequate suppression of gluconeogenesis and glycogenolysis. [40] Ultimately, insulin resistance in adipose tissue is characterized by impaired insulin-mediated glucose transport, decreased lipid absorption capacity, and a failure to control lipolysis and inflammation, leading in increased plasma free fatty acids (FFAs) and cytokines. [41] There are numerous candidate genes involved in modulating insulin secretion and action, all of which are likely to play a role in the development of type 2 diabetes. [42]

1.4.3 Gestational diabetes

Gestational diabetes mellitus (GDM) is described as glucose intolerance that develops during pregnancy. Around the world, the incidence of GDM is rising and could impact up to 18% of pregnancies. [43] GDM is linked not only to prenatal morbidity but also to a higher risk of diabetes and cardiovascular disease in the mother later in life, as well as childhood obesity in kids. [44] Large amounts of hormones are created during pregnancy; these hormones may impair insulin activity in the mother's body, resulting in insulin resistance. [29] Throughout the first trimester of pregnancy, both fasting and postprandial blood glucose levels are typically lower than normal; however, blood glucose levels rise during the third trimester of pregnancy, reaching diabetes levels in certain cases. [45]

Insulin resistance (IR) increases during pregnancy due to an increase in numerous IR hormones generated by the placenta (such as estrogen, progesterone, human placental prolactin, and so on). Adipocytokines released by adipose tissue (such as adiponectin, leptin, and others) are also implicated in IR. [46] Normal pregnant women's islet cells may undergo adaptive alterations that enhance insulin output to compensate for increased insulin demand. Insulin secretion in GDM pregnant women rises accordingly, but not enough to compensate for the growing IR, resulting in clinically observable aberrant glucose metabolism. One of the most significant etiologies of GDM is IR. [47]

GDM occurs more commonly in certain racial or ethnic groups than others, and the impact of ethnicity on the risk of GDM is significant and well known. Asian Indians have the highest frequency of GDM, followed by aboriginal Australians, Middle Eastern (Lebanese, Syrian, Iranian, Iraqi, or Afghan), Filipina, Pacific Islanders, Chinese, Japanese, Korean, and Mexican women. Blacks have a lower prevalence, as do non-Hispanic white women. [48]

1.5 Available therapeutic methods for diabetes

Diabetes mellitus continues to be an important medical problem due to its increasing prevalence worldwide, but there are established treatments to control the disease. [3]

1.5.1 Insulin therapy

Insulin was discovered in 1921 by Dr Frederick G Banting and Charles Best. [49] It was first administered to a patient in 1922 and, since then, has been commercially available for the treatment of diabetes mellitus. [50] Insulin treatment replaces or supplements the body's own insulin with the goal of achieving normal or near-normal blood sugar levels and preventing or minimizing complications. [51] If one has type 1 diabetes, insulin therapy is vital for replacing the insulin one's body doesn't produce. [52] When a patient with type 2 diabetes or gestational diabetes is diagnosed, insulin therapy may be used as the first line of treatment if metabolic decompensation, a glycosylated hemoglobin level greater than 9.0%, or symptoms of hyperglycemia are present. [53] Insulin therapy may also be necessary if a type 2 diabetic patient is unable to reach the target glycemic goal despite receiving appropriate oral hypoglycemic treatment. [3]

Insulin is not available in pill form because the digestive system would break it down before it could operate. [53] However, there are various insulin administration options, including shots or pens, in which insulin is injected into the fat immediately beneath one's skin with a syringe and needle, or a pen-like device that holds insulin with a needle attached. An insulin pump, which sends small, consistent doses of rapid-acting insulin into a thin tube that can be implanted beneath the skin, is also utilized. [54] There are many types of insulin therapy such as Regular insulin type, rapid-acting insulins and mixtures of intermediate and rapid-acting insulins. [52]

1.5.1.1 Short-Acting insulin

Short-acting insulin is also commonly referred to as Regular or Neutral insulin. Regular insulin is metabolized in the liver, spleen, kidney and muscle. [55] Regular insulin has a start of action of 30-60 minutes after a subcutaneous (SC) injection, a peak effect of 2-4 hours, and a duration of action of 4-8 hours. The higher the Regular insulin dosage, the faster the start of action, but the longer the time to peak effect and the duration of the impact. [56]

1.5.1.2 Basal insulin

Intermediate-acting and long-acting insulins are often termed background or basal insulins. The intermediate-acting insulins are cloudy in nature and need to be mixed well. These insulins begin to work about 60 to 90 minutes after injection, peak between 4 to 12 hours and last for between 16 to 24 hours. [57] Long-acting insulin works to

establish a healthy baseline blood sugar level. This means that when food enters the body, blood glucose will increase from a lower and more regular point, making it easier to manage. [58]

1.5.1.3 Rapid-Acting Insulin

Rapid-acting insulins are insulin analogues that were created to better manage blood glucose excursions after a meal by obtaining a pharmacokinetic profile that is more akin to mealtime endogenous insulin than human unmodified insulin. [59] If the patient is also taking a long-acting or intermediate-acting insulin (basal insulins), rapid-acting insulin should be administered three times daily before each meal. [60]

1.5.1.4 Premixed Insulins

Premixed insulins are a predetermined ratio of short-acting insulin (Regular/Neutral) or rapid-acting analogue insulin mixed with intermediate-acting insulin. [61] Premixed insulin is thought to provide a number of benefits over self-mixed insulin, including greater dose precision, effectiveness, and patient convenience. These benefits may lead to higher compliance and improved long-term diabetes control. [62]

1.5.2 Anti-diabetic drugs

1.5.2.1 Alpha-glucosidase inhibitors

Alpha-glucosidase inhibitors are used to treat type 2 diabetes by competitively and reversibly decreasing the activity of intestinal alpha-glucosidase enzymes. [4]

Mechanism of action

Alpha-glucosidase is an enzyme that cleaves glucosidic bonds. [63]. In the small intestine, alpha-glucosidase inhibitors reversibly limit the enzymatic breakdown of complex carbohydrates to simple absorbable sugars. [64] Consequently, the digestion of carbohydrates and absorption of monosaccharides in the proximal jejunum are decreased or incomplete in the distal jejunum and ileum. [65] This leads to less sugar being absorbed, resulting in lower postprandial glucose levels and reducing hyperglycemia. Examples of Inhibitors of α-Glucosidases are acarbose (**1**) and miglitol (**2**) [**Figure 1**]. [63]

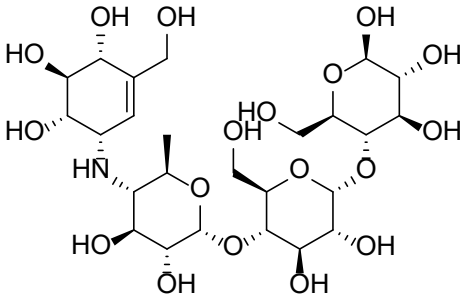

1

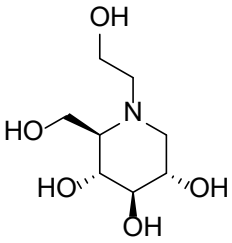

2

Figure 1: Examples of Inhibitors of α-Glucosidases.

1.5.2.2 Biguanides

Biguanides' antihyperglycemic activity is mostly due to the suppression of hepatic gluconeogenesis, which results in decreased blood glucose levels with little danger of inducing hypoglycaemia in type 2 diabetes patients. [66]

Mechanism of action

Biguanides work by reducing the assembly of glucose from digestion. [67] They are insulin-sensitizing drugs that have antihyperglycemic actions by inhibiting hepatic gluconeogenesis through gluconeogenic flux control. [65] As a result, plasma glucose and lactate levels are lowered, as are liver gluconeogenesis, hepatic glucose secretion, and endogenous glucose production. Examples of biguanides are metformin (**3**) and phenformin (**4**) [**Figure 2**]. [63]

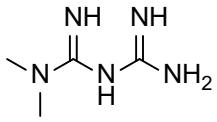

3

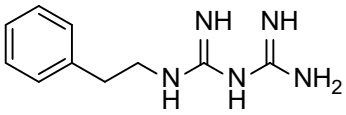

4

Figure 2: Examples of biguanides.

1.5.2.3 Sulphonylureas

Sulphonylureas reduce blood sugar levels by stimulating insulin secretion from pancreatic cells. As a result, this class has the highest risk of causing hypoglycemia, especially in the elderly, those with impaired kidney function, or those on insulin at the same time. [68]

Mechanism of action

Sulphonylureas mimic the effect of ATP in pancreatic beta cells and act as insulin-secreting agents. [69] Sulphonylurea compounds bind to sulphonylurea receptors (SURs) on beta cell surfaces, inhibiting ATP-dependent inward-rectifier potassium ion

channels. [70] As a result, the intracellular concentration of potassium cations rises, resulting to depolarization of the plasma membrane. These circumstances cause voltage-gated calcium channels to open, and an increase in cytosolic calcium cation concentration causes an increase in insulin production. [71] Examples of sulphonylureas are glipizide (**5**) and tolbutamide (**6**) [**Figure 3**]. [68]

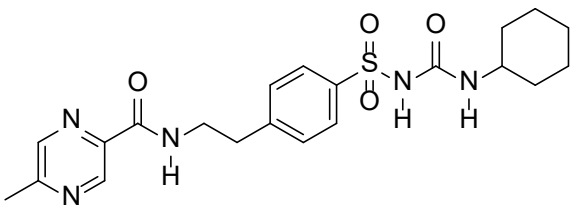

5

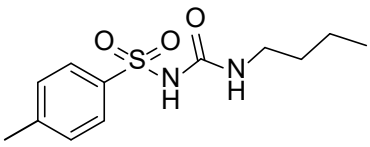

6

Figure 3: Examples of sulfonylureas.

1.5.2.4 Thiazolidinediones

Thiazolidinediones (TZDs) are also known as glitazones and are used for the treatment of type 2 diabetes. [3] Thiazolidinediones (TZDs) are insulin sensitizers that activate peroxisome proliferator-activated receptors (PPARs), a nuclear receptor family. [63] They are used in conjunction with other forms of oral diabetes medications, such as sulfonylureas, metformin, and acarbose, to reduce the amount of insulin required in insulin-dependent patients. [4]

Mechanism of action

TZD molecules can interact with PPAR-α and PPAR-γ isoforms, which are mostly found in fatty tissues and skeletal muscle. This activates these receptors and stimulates complexation with another important component, the retinoid X receptor. [72] The triple complex has the ability to bind selectively to DNA via peroxisome proliferative response elements (PPRE) and operate as a target gene promoter, therefore promoting gene expression. [63] This treatment technique increases adiponectin levels, decreases gluconeogenesis, and increases glucose absorption in muscle and fat. Adiponectin is a hormone released in adipose tissue that modulates glucose levels through enhancing insulin sensitivity. [72] Examples of thiazolidinediones are pioglitazone (**7**) and rosiglitazone (**8**) [**Figure 4**]

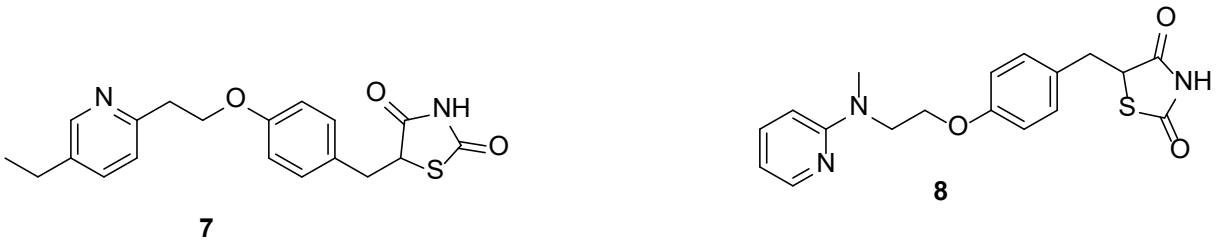

Figure 4: Examples of thiazolidinediones.

1.6 Thiohydantoins

Thiohydantoins are an important family of chemicals in pharmaceutical chemistry because they occur in a variety of pharmacologically active molecules with high bioactivities and are used in therapeutic medications. [73] The chemistry of thiohydantoins has gained increased interest in both synthetic organic chemistry and biological fields. [74] Thiohydantoins are hydantoins (2,4-imidazolidinediones) having one or both carbonyl groups substituted by thiocarbonyl groups. Thiohydantoin's backbone may be easily changed to favour one structural type over another by adding groups to provide steric bulk, more hydrophilic or hydrophobic interactions, or π-π stacking. [75] Therefore, their ability to form hydrogen-bonded arrays can be controlled in the solid-state, which is crucial in the pharmaceutical industry. [76] There are three known thiohydantoins: 2-thiohydantoin (**9**), 4-thiohydantoin (**10**), and 2,4-dithiohydantoin (**11**) [**Figure 5**]. [77]

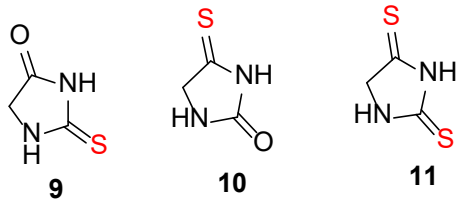

Figure 5: Structures of thiohydantoins.

The 2-thiohydantoins (2-thioxoximidazolin-4-ones) are well-known analogues because of their numerous uses as intermediates and reagents in organic synthesis, pharmaceuticals, and agricultural processes. [76] The nature of the substituents on the heterocyclic ring influences their biological action. The properties of the molecule are affected by the substitution of the 2-thiohydantoin core at N-1, N-3, or C-5. [77] The nucleophilic centre of the five-membered ring 2-thiohydantoin is position 5, and numerous substituents can be inserted at this location. 5-substituted thiohydantoins are also utilized in therapeutic practice. [78] The introduction of an exocyclic double

C=C bond into position 5 of the thiohydantoin ring renders the molecules amenable for electrophilic and nucleophilic addition, 1,3-dipolar cycloaddition and Diels-Alder reaction. [79] The olefination of thiohydantoins with exocyclic arylidene or alkylidene substituents at the C5 atom results in the creation of tri- or tetrasubstituted exocyclic C=C bonds. However, attempts to synthesize thiohydantoins containing exocyclic methylidene (CH2=) fragments are uncommon. [80]

1.6.1 Synthetic methods for 2-Thiohydantoin derivatives

Due to the biological importance of 2-thiohydantoins, different methods have been used to prepare various derivatives from these compounds.

- From the reaction of acyl α -amino acid derivatives with thiocyanate in acetic anhydride (**scheme 1**). [81]

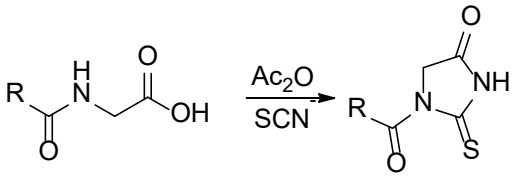

Scheme 1: Synthesis of 2-thiohydantoin derivative.

- From the reaction of α -amino acids and thiourea (**scheme 2**). [82]

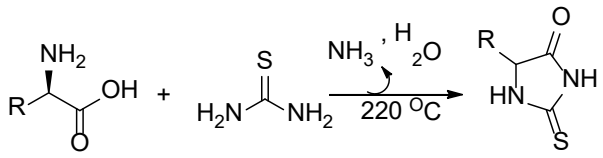

Scheme 2: The general procedure for 2-thiohydantoins synthesis from amino acids and thiourea.

- From the reaction of amino acid ester and aldehyde (**scheme 3**). [77]

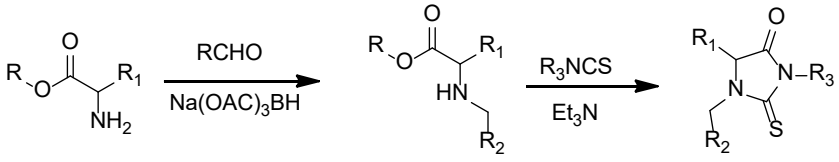

Scheme 3: synthesis of 2-thiohydantoin derivatives from the reaction of amino acid ester and aldehyde.

- From the reductive amination reaction of glyoxylic acid (**scheme 4**). [77]

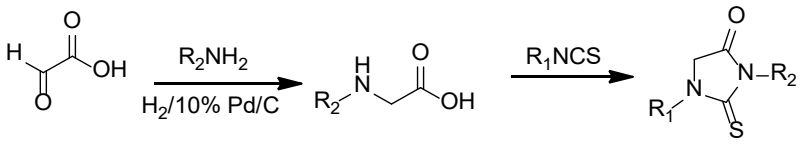

Scheme 4: synthesis of 2-thiohydantoins from N-substituted amino acids.

1.7 Pharmacological applications of 2-Thiohydantoins

1.7.1 Antiparasitic activity

In 2017, Buchynskyy et al. discovered the thiohydantoins 1-benzyl-3-aryl-2-thiohydantoins as anti-Trypanosoma brucei agents. The two synthesized analogues 1-(4-fluorobenzyl)-3-(4-dimethylamino-3-chlorophenyl)-2-thiohydantoin (**12**) and 1-(2-chloro-4-fluorobenzyl)-3-(4-dimethylamino-3-methoxyphenyl)-2-thiohydantoin (**13**) [**Figure 6**] displayed a high antiparasitic activity with IC_{50} 3.2 and 1.9 µM respectively. [83]

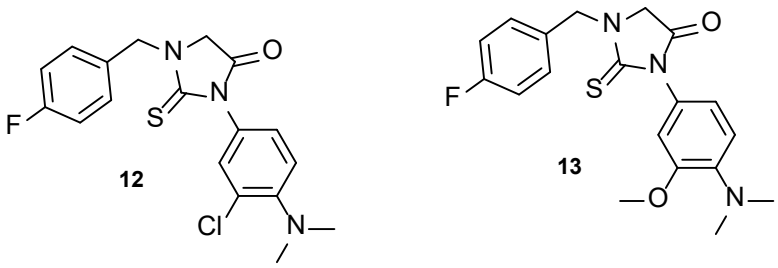

Figure 6: Compounds with parasitic activity

1.7.2 Antimalarial activity

In 2014, Raghu Raj and co-workers reported the synthesis of a series of 7-chloroquinoline-thiohydantoins derivatives as antimalarial agents. Compounds **14a-d** exhibited inhibitory activity against P. falciparum with promising low IC_{50} values of 39.84-57.21 µM and low toxicity. [84]

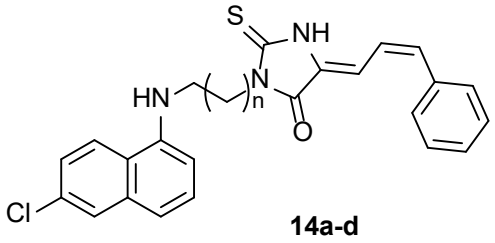

14a-d

14a; n=1, **14b**; n=2, **14c**; n=3, **14d**; n=6

Figure 7: compounds with antimalarial activity.

1.7.3 Antibacterial Activity

In 2002, K. Kiec´-Kononowicz reported 5-arylidine-2-thiohydantoins as mycobacterial agents. These compounds (**15**) and (**16**) displayed more than 90% inhibition of Mycobacterium tuberculosis growth with IC_{50} of 6.7 and 4.5 μM respectively. [85]

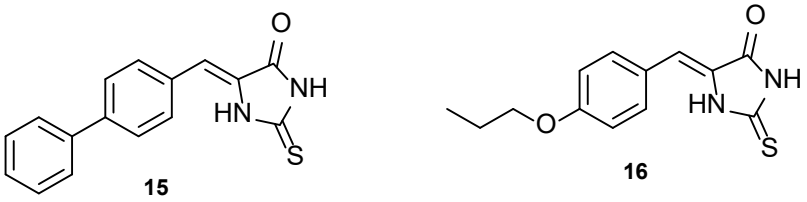

15 **16**

Figure 8: Structures of thiohydantoins derivatives with antibacterial activity.

1.7.4 Antifungal activity

Han J and co-workers synthesized 5-Arylidene-2-thiohydantoin derivatives with a substituent sulfonyl group in position 4 as a linker between two phenyl groups (**17** and **18**) and they exhibited high antifungal activity. [86]

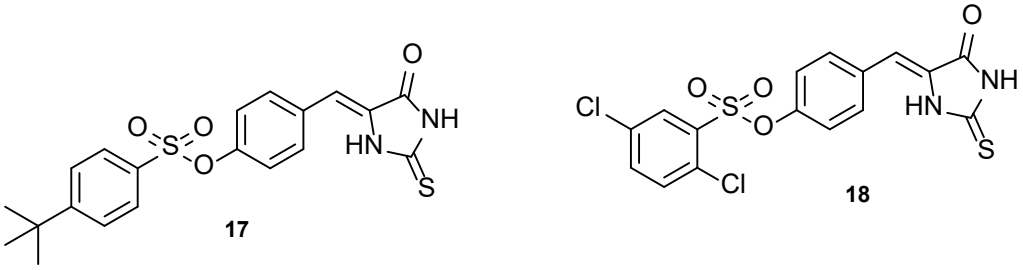

17 **18**

Figure 9: Compounds of thiohydantoins derivatives with antifungal activity.

1.8 Aims, origin and objectives of the project

Diabetes mellitus, ranked ninth among the leading causes of death worldwide, is a severe chronic metabolic disease that necessitates extensive healthcare resources. It has been recorded to have affected more than 578 million individuals in 2023. [87]

Hence, it is imperative to expedite the development of novel therapeutic strategies to prevent and manage diabetes. Different therapeutic approaches for managing diabetes encompass enhancing insulin secretion from pancreatic β cells, augmenting insulin activity, decreasing hepatic glucose production, or inhibiting the glucosidase digestive enzyme. [88]To regulate elevated blood glucose levels, one can suppress the activity of the enzymes α-amylase and α-glucosidase, which play a role in breaking down carbohydrates. [89]

The α-amylase enzyme initially hydrolyzes the elongated chains found in polysaccharides, while the enzyme α-glucosidase ultimately facilitates the conversion of disaccharides and starch into glucose. [90]Therefore, the suppression of α-amylase and α-glucosidase enzymes is a beneficial therapeutic approach for managing diabetes mellitus. This intervention aids in slowing down the absorption of glucose following meals. Currently, several inhibitors of these enzymes, including voglibose, acarbose, and miglitol, are being utilised in clinical practice to treat type II diabetes. [91] Recent, structure-activity relationship (SAR) investigation and biological evaluation of a novel series of synthesised 5-substituted 2-thiohydantion analogues (19) showed that hydroxyl group was an optimal R_1 substituent. For R_2, smaller alkyl groups such as methyl and ethyl showed poor inhibitory activity. Therefore, the main aim of this study was to synthesize novel thiazolidinediones analogues **20** as potential diabetic drugs.

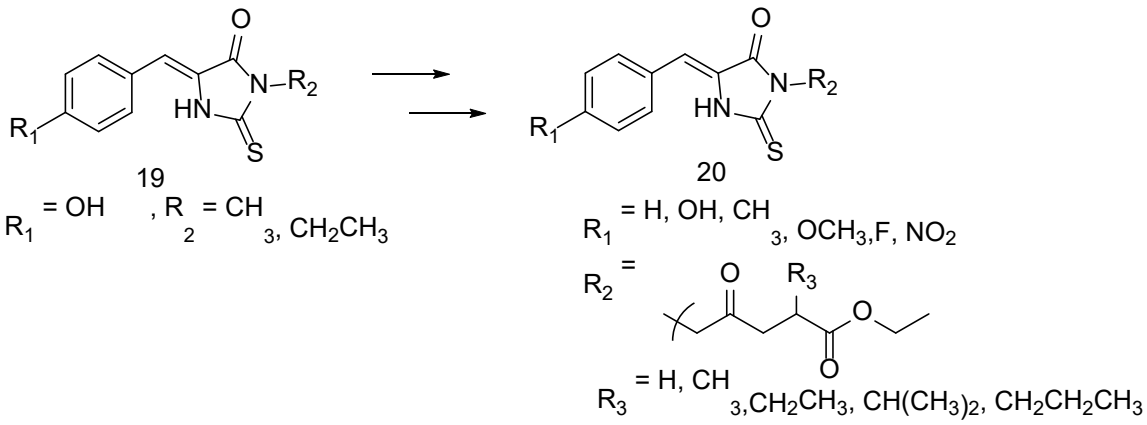

Scheme 5:

Our main objectives were as follows:

- Synthesis and purification of final compounds using recrystallization techniques and column chromatography.
- Characterization of final target compounds using a combination of NMR (^{1}H and ^{13}C), IR Spectroscopies as well as HRMS.
- In-vitro anti-diabetic evaluation of targeted synthesized compounds.

CHAPTER TWO

2.0 Results and discussion

In this section, we examine the various characterization techniques that were employed throughout the course of this project, as well as the detailed results and discussions that emerged from them.

2.1 Chemistry

In this study, the preparation of hydantoins analogues was carried out using the general synthetic method. The hydantoins derivatives were synthesised using the following retrosynthetic analysis.

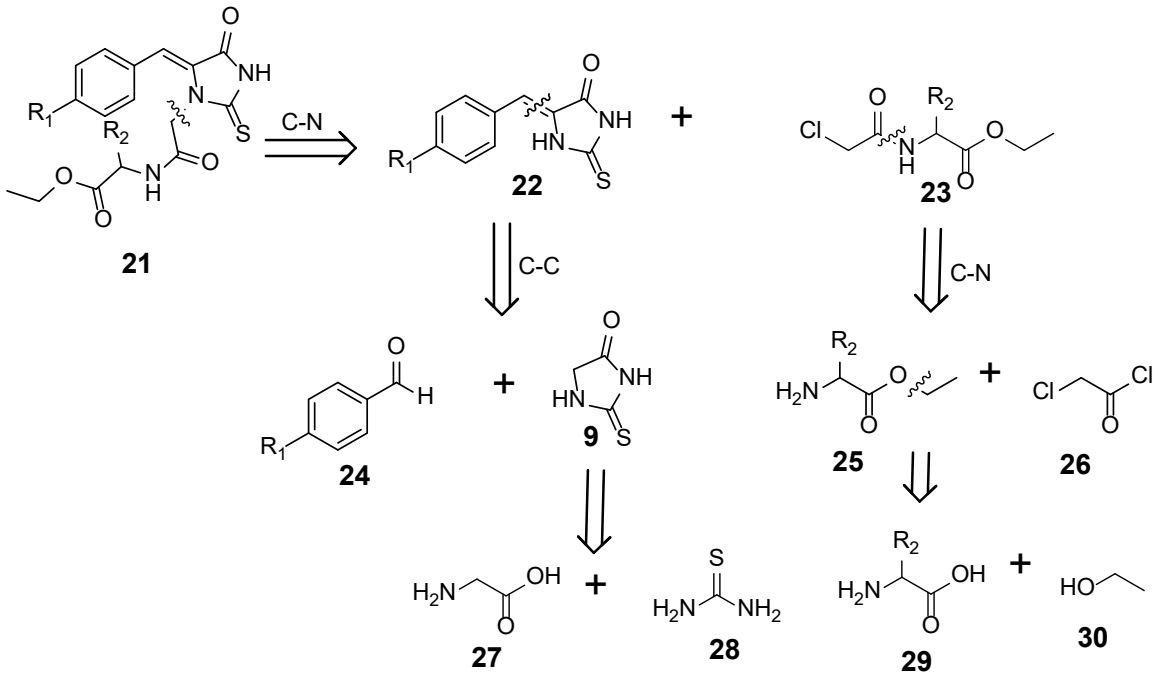

Scheme 6: Retrosynthesis of target thiohydantoin derivatives.

Target compounds **21** are retro synthesized to 5-benzylidene-2-thioxoimidazolidin-4-one **22** and amino esters **23** as depicted in **scheme 1.** It showed further a feasible retrosynthesis in disconnection of a carbon-carbon double bond of compound **22** producing benzaldehydes **24** and 2 thiohydantoin **9**. Carbon nitrogen bond on 2 thiohydantoin was further disconnected to give glycine **27** and thiourea **28**. ethyl 2-(2-chloro acetamido) esters **23** were cleaved of the carbon-nitrogen bond to give protected amino acids **25** and chloro acetyl chloride **26**. Compound was disconnected at carbon-oxygen bond to give amino acids **29** and alcohol **30**.

2.2 Synthesis of 2-thiohydantoin

2.2.1 Synthesis of 2-thiohydantoin from thiourea and glycine

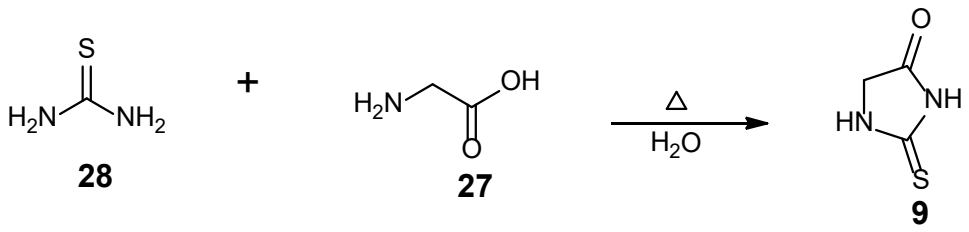

Scheme 7: Synthesis of 2-thiohydantoin from thiourea and glycine

The study began by synthesising 2-thiohydantoin through a one-step process. This involved reacting thiourea **28** and glycine **27** under stirring to directly condense and produce 2-thiohydantoin **9**. [82] The product was confirmed through various analytical techniques, including TLC, ^{1}H NMR, and ^{13}C NMR. However, the yields obtained were relatively low, ranging from 5-10%. As a result of unsatisfactory yields obtained from this synthetic method, an alternative approach was utilised to enhance the yields.

2.2.2 Synthesis of 2-thiohydantoin using acylation method

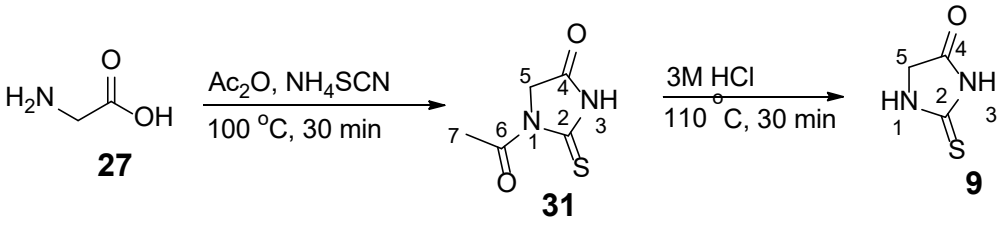

Scheme 8: Synthesis of 2-thiohydantoin using acylation method

The synthesis of compound **9** involved a two-step process. In the first step, glycine **27** and ammonium thiocyanate were combined using acetic anhydride as a solvent and heated under reflux. This reaction resulted in the formation of acylated compound **31**. After acidifying compound **31**, the acyl group was removed, resulting in a 79% yield of 2-thiohydantoin **9**. [81] This product was used as is, without any additional purification. Compounds **31** and **9** were verified through ^{1}H NMR, ^{13}C NMR, and melting point analysis.

Regarding compound **31**, ^{1}H NMR spectrum displayed three singlet peaks, with the N-H peak (**H-3**) registering at 12.60 ppm and integrating for a single hydrogen. The methylene protons (**H-5**) were identified at 4.40 ppm, while the methyl protons (**H-7**) of the acyl group were found at 2.68 ppm. The ^{13}C NMR spectrum displayed a total of five peaks, including the thiocarbonyl group **C-2** at 182.95 ppm and the two carbonyl

groups **C-4** and **C-6** at 170.81 and 169.77 ppm respectively. The methylene carbon **C-5** resonated at 52.63 ppm while the methyl carbon **C-7** at 27.05 ppm. The melting point of compound **31** ranged from 166 - 168 °C, which aligns with the literature value of 167 - 169 °C. [81] This provides further evidence supporting the formation of the compound.

Compound **9** exhibited a ^{1}H NMR spectrum with a total of 3 singlet peaks. The presence of three peaks indicates the successful deacylation process, thus confirming the formation of 2-thiohydantoin. Observations of N-H peaks **H-3** and **H-1** can be made at 11.67 and 9.87 ppm respectively, while the methylene protons **H-5** peak is observed at 4.09 ppm. The ^{13}C NMR spectrum displays three peaks, each with its own assigned resonance value. These peaks correspond to the thiocarbonyl carbon **C-2** at 183.83 ppm, the carbonyl carbon **C-4** at 174.99 ppm, and the methylene carbon **C-5** at 50.75 ppm. The product was also verified using the melting point, which was found to be 227 - 229 °C. [81] This value is in line with the reported literature value of 229-231 °C.

2.3 Synthesis of amino esters 3a-e.

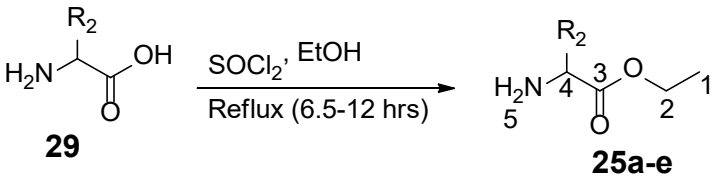

29 **25a-e**

Scheme 8: Synthesis of amino esters.

Amino ester acids **25a-d** were synthesised through a reaction between amino acids (alanine, butanoate, valine, and norvaline) and thionyl chloride, using ethanol as the solvent under reflux conditions (**scheme 4**). [92] Compound **25a** was acquired as a white solid, while compounds **25b** and **25e** were obtained as colourless oils. On the other hand, compounds **25c** and **25d** were obtained as light brown oils. The percentage yield of compounds **25a-e** varied between 79% and 93% (**Table 1**).

Table 1: percentage yields and colours of ester protected amino acids (**25a-e**).

Compound	R_2	Percentage Yields (%)	Colour	Melting point (°C)	Literature melting point (°C)
25a	H	89	White solid	89-91	91-93 [93]
25b	CH_3	91	Colourless	-	-

25c	CH_2CH_3	93	Light brown	-	-
25d	$CH(CH_3)_2$	79	Light brown	-	-
25e	$CH_2CH_2CH_3$	79	colourless	-	-

The amino esters **25a-e** were confirmed using ^{1}H, ^{13}C NMR and IR spectroscopies. The ^{1}H NMR spectra showed the emergence of a distinct signal in the range of 3.64 - 4.12 ppm. This signal confirmed the existence of methylene (**H-2**) protons, which were observed as a quartet and accounted for two hydrogens. Additional signals were detected at 1.09, 1.05, 1.19, 1.21, and 1.21 ppm for compound **25a**, **25b**, **25c**, **25d**, and **25e** respectively, indicating the existence of methyl protons (**H-1**). These peaks appeared as a triplet and had an integration value of 3Hs. The attachment of the ethoxy group to the amino acid was confirmed by these two signals, providing strong evidence for the formation of product **25a-e**.

The ^{13}C NMR spectra of compounds **25a-e** displayed a methyl (**C-1**) peak and a methylene (**C-2**) peak, with chemical shifts ranging from approximately 13.23-14.48 ppm and 60.99-63.47 ppm, respectively. This observation confirms the presence of the ethoxy group. In the ^{13}C NMR spectrum of compound **25b**, a new signal emerged at 16.17 ppm, suggesting the presence of alanine. Compound **25c** displayed two additional signals at approximately 23.26 and 8.43 ppm, indicating the presence of methylene and methyl carbons associated with butanoate. In addition, compound **25d** ^{13}C NMR spectrum revealed the presence of three additional peaks. These peaks correspond to two methyl carbons at approximately 19.27 and 18.39 ppm, as well as one methylene carbon at around 29.32 ppm. These findings suggest the presence of valine. Lastly, the ^{13}C NMR spectrum of compound **25e** revealed three extra peaks. Two of these peaks correspond to methylene carbons at approximately 29.31 ppm and 27.64 ppm, while the third peak corresponds to a methyl carbon at 13.85 ppm. This confirms the presence of norvaline.

IR also confirmed the products as all functional groups were observed. The N-H stretching vibrations were observed at 3352-3397 cm^{-1}, the carbonyl stretching vibrations were observed 1710-1761cm^{-1} and lastly the C-O stretched at 1121-1450 cm^{-1}.

2.4 Synthesis of ethyl 2-(2-chloroacetamido) esters

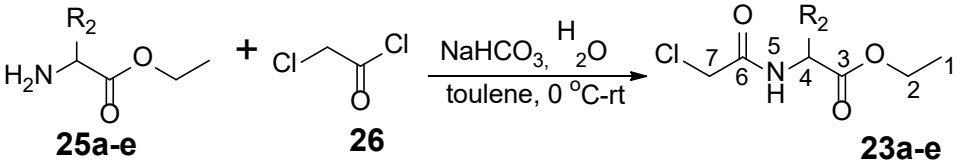

Scheme 9: Synthesis of ethyl 2-(2-chloroacetamido) esters

The synthesis of ethyl 2-(2-chloroacetamido) esters (23a-e) was achieved by reacting chloro acetyl chloride (26) with amino esters (25a-e) in a mixture of water and toluene in the presence of sodium hydrogen carbonate. The reactions were performed at room temperature for 12 hours. (**scheme 5**). [94] Compound **23**a was acquired as a white solid, while compounds **23b-e** were obtained as brown oils. The compounds **23a-e** were obtained with high yields (**Table 2**).

Table 2: percentage yields and melting point for ethyl 2-(2-chloroacetamido) esters

Compound	R_2	Percentage yields (%)	Melting point (°C)	Literature melting point (°C)	colours
23a	H	87	75 - 77	77.50 [94]	White
23b	CH_3	91	-	-	Brown
23c	CH_2CH_3	91	-	-	Brown
23d	$CH(CH_3)_2$	88	-	-	Brown
23e	$CH_2CH_2CH_3$	87	-	-	Brown

The presence of a singlet methylene H-7 protons signal integrating for 2H at 3.75 - 4.21 ppm in the ^{1}H NMR spectra confirmed compounds **23a-e.** Another important observation was the identification of an N-H **H-5** signal in the range of approximately 8.58 - 8.78 ppm, which integrated for 1H and appeared as a doublet. The ^{1}H NMR spectra of compounds **23b-e** revealed the presence of three additional signals. Firstly, there was a quartet signal at approximately 3.96 - 4.13 ppm, indicating the presence of 2H. Secondly, a quintet signal appeared at around 4.09 - 4.25 ppm, suggesting the presence of 1H. Lastly, a triplet signal appeared at approximately 1.19 - 1.22 ppm, integrating for 3H.

The ^{13}C NMR spectra exhibited the presence of two additional peaks, one corresponding to carbonyl (**C-6**) carbon at 166.65-168.96 ppm, and the other corresponding to methylene (**C-7**) carbon at 33.40 - 42.60 ppm. In addition, ester carbon signals were observed at 169.76 - 172.30 ppm in the spectra of compounds **23a-e**. Furthermore, **C-2** signals appeared at around 60.96 - 62.10 ppm, and the methyl carbon **C-1** was also detected at approximately 14.28 - 16.77 ppm. At last, a new carbon signal C-7 emerged at approximately 33.40 - 42.67 ppm, in contrast to the unreacted chloro acetyl chloride which appeared at around 49.01 ppm.

IR spectroscopy was also applied to further characterize the products. The N-H stretching vibrations were observed at 3386-3397 cm^{-1}, the carbonyl stretching vibrations were observed 1615-1747 cm^{-1} and lastly the C-O stretched at 1526-1548 cm^{-1}.

2.5 Synthesis of (Z)-5-benzylidene-2-thioxoimidazolidin-4-ones using Knoevenagel condensation reactions

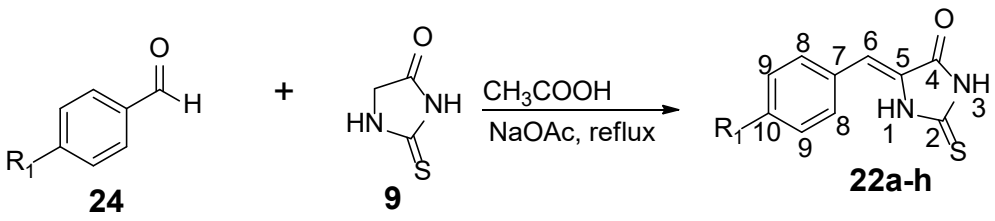

Scheme 10: Synthesis of (Z)-5-benzylidene-2-thioxoimidazolidin-4-ones using Knoevenagel condensation reactions.

(Z)-5-Benzylidene-2-thioxoimidazolidin-4-ones **22a-h** were synthesized from reacting equimolar amounts of substituted benzaldehydes **24** and thiohydantoin **9** in acetic acid and sodium acetate as the base. [95] The (Z)-5-benzylidene-2-thioxoimidazolidin-4-ones were synthesised with high efficiency, resulting in melting points within the range of 210-289 ^oC (**Table 3**).

Table 3: Percentage yields and melting points of 5-benzylideneimidazolidine-2,4-dione (**22a-h**)

Compound	R_1	Percentage yields (%)	Melting point (^oC)	Literature melting point ^oC
22a	H	81	257.2-259.1	258-260 [95]

22b	CH_3	69	247.1-248.9	246-248 [96]
22c	OH	87	280.6-282.1	280 [95]
22d	OCH_3	89	210.1-211.7	211-213 [97]
22e	F	74	252.1-253.8	253-257 [98]
22f	NO_2	77	283.8-286.1	284-286 [99]
22g	C_3H_3O	60	253.8-256.7	258-262 [100]
22h	C_4H_4	93	287.9-289.5	289-291 [101]

The compounds (**22a-h**) were characterised using ^{1}H NMR, ^{13}C NMR, and IR spectroscopies. The ^{1}H NMR spectra of compounds **22a-h** exhibited a total of five signals. The products (**22a-h**) were additionally characterised by the absence of the distinctive aldehydic proton peak resonating at approximately 9 ppm, which indicates that all aldehydes were completely consumed in the reaction. Another significant confirmation was the emergence of a new arylidene signal (**H-6**) at 6.41 - 6.63 ppm as a singlet, which confirms the occurrence of the condensation reaction. Another factor that contributed to the confirmation of compounds (**22a-h**) is the shift in the proton signals **(H-1** and **H-3**) towards higher frequencies (downfield) after the reaction. Prior to the reaction, these signals were observed at 9.87 and 11.67 ppm, whereas after the reaction, they were observed at 11.95 – 12.58 ppm, indicating a change in their chemical environment.

^{13}C NMR Spectra of compounds (**22a-h**) were characterised by the absence of a signal indicating the presence of the aldehydic carbon peak at approximately 190 ppm. This observation confirms that the aldehydes were completely reacted. Nevertheless, a distinct arylidene carbon (**C-6**) peak emerged at approximately 99.54 - 116.31 ppm, confirming the success of the reaction and the formation of the condensation product. Additionally, a novel quaternary carbon peak **(C-5**) was observed within the range of 125.62 - 139.62 ppm. Lastly, shielded carbons (**C-2**) and (**C-4**) were detected at around 178.48 - 179.75 and 165.79 -166.41 ppm, respectively.

The compounds **22c**, **22d**, **22e**, and **22f** exhibited intriguing observations in their 1H NMR and 13C NMR spectra. Compound **22e** exhibited the propensity to combine signals from both protons and carbons located at the ipso-, ortho-, meta-, and para-positions of the phenyl ring. The observed coupling in this compound (**22e**) is

heteronuclear coupling, as the fluorine is bonded to a different atom, specifically carbon C-10. The ipso C-10 displayed a peak at 162.79 ppm with a coupling constant (Jc-f) of 248.8 Hz. The carbon C-9, located ortho to the fluorine, also showed a peak with a coupling constant of 21.7 Hz. The carbon C-8, positioned meta to the fluorine, exhibited a peak with a coupling constant of 8.5 Hz. Lastly, the carbon C-7, located on the para position, displayed a peak of doublet of doublet due to the influence of C-8 and C-9 with coupling constants $J_{c\text{-}f}$ = 143.1 & 2.6 Hz. A significant finding revealed that the coupling constant decreases as the positions of the carbons move further away from the Fluorine atom. Another significant consequence of the presence of a fluorine atom is the greater downfield shift of carbon C-10 in comparison to other compounds, owing to its enhanced electron withdrawing capacity. Upon the attachment of R_1 to compounds **22b-h**, the energy of signal C-10 experiences an increase. Compounds **22c**, **22d**, and **22f** have an electron withdrawing group, specifically oxygen attached to C-10. As a result, the chemical shifts of both the protons and carbon signals in these compounds are down shielded. The IR spectra indicated the existence of N-H stretching vibrations within the range of 3115 - 3319 cm-1. In addition, the vibrations associated with the stretching of C-H bonds were detected within the frequency range of 2750 - 3002 cm-1. In addition, the carbonyl stretching vibrations were observed within the range of 1705 – 1739 cm-1. The C=C stretching vibrations were detected within the spectral range of 1590 - 1649 cm-1. Finally, the stretching vibrations of the C=S bond were observed at a wavenumber range of 1226 – 1252 cm^{-1}. The IR spectra unambiguously demonstrated the existence of all functional groups in compounds **22a-h**, thereby confirming the formation of the products.

2.6 Synthesis of target compounds (21a-v)

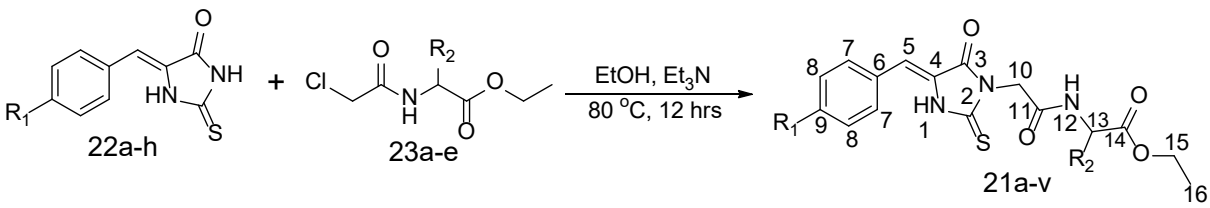

Scheme 11: Synthesis of novel 2-thiohydantoin derivatives.

The target compounds (**21a-v**) were synthesised by dissolving the Knoevenagel condensation products (**22a-h**) in ethanol with triethylamine and stirring for 15 minutes. Following the completion of the designated time period, ethyl amino esters (**23a-e**)

were introduced into the reaction mixture, which was subsequently subjected to reflux for a duration of 12 hours. The resulting target compounds were purified using column chromatography, resulting in efficient yields.

The characterization of the target compounds (**21a-v**) was confirmed using ^{1}H NMR, ^{13}C NMR, IR, and HRMS spectroscopic techniques. The ^{1}H NMR spectra exhibited a total of 9 peaks. The products were identified by the specific absence of the second N-H peak **N-3**, previously detected between 12.20-12.58 ppm, confirming the successful bonding of the ethyl amino esters (**23a-e**). Furthermore, it is noted that the proton **H-1** has experienced upshielding, indicating the impact of the energy alteration on the magnetic field. Another N-H proton that exhibited alteration is **H-12**, which experienced deshielding (indicating an increase in signal energy) in products containing the glycinate, alaninate, butanoate, and norvalinate moieties. However, it only underwent upshielding in the vallinate moieties. It can be inferred that when branched ethyl amino esters are attached to compounds (**22a-h**), they cause a shielding effect, resulting in a decrease in the chemical shift of **H-12**. Another notable observation in the ^{1}H NMR spectra is the downfield shift of **H-5**. In previous compounds (**22a-h**), it ranged from 6.41-6.53 ppm, whereas in the products (**21a-v**), it ranged from 6.73-6.85 ppm. It was evident that when R_1 was a potent electron withdrawing group (such as F and O), **H-5** experienced even greater downshifting compared to other groups. The ^{13}C NMR spectra of the target compounds (**21a-v**) displayed 14 peaks, providing confirmation of the occurrence of the reaction. In the ^{13}C NMR spectra, we can see that the thiocarbonyl group **C-2** becomes upshielded, moving from a range of 179.02 – 180.50 ppm in compounds **22a-h** to a range of 169.97 – 171.01 ppm upon the attachment of compounds **23a-e**. Upon further observations it was noted that on glycinate containing compounds **C-2** has upshielded more compared to alaninate, butanoate, vallinate and norvalinate containing compounds. The **C-10** carbon is further up field on the final compounds compared to before the reaction. The compounds containing glycinate show minimal change in comparison to the other ethyl 2-(2-chloroacetamido) esters (**12b-e**). Therefore, it can be inferred that the introduction of straight and/or branched alkyl groups to **C-13** causes a significant decrease in the chemical shift of **C-10**. Another notable alteration is the massive downshield of carbon **C-5**, where before reaction it was at 99.54-114.84 ppm and after reaction it was observed at 120.37-123.98 ppm. The observed effect is attributed to the presence of

a significant number of oxygen atoms in the introduced compound **23a-e**, which acts as a potent electron withdrawing group.

The ^{13}C NMR spectra of the fluorine-containing products exhibited signal splitting into doublets for the ipso, ortho-, meta-, and para- carbons of the phenyl ring. The coupling constant J_{C-F} for the ipso carbon **C-9** is 11.4, 22.2, 29.7, 32.4, and 23.7 Hz for the glycinate, alaninate, butanoate, valinate, and norvalinate moieties of the fluorine-containing products, respectively. The coupling constant for the ortho-, meta- and para-carbons in all ethyl 2-(2-chloroacetamido) esters remains constant at 21.5, 8.3, and 3.1 Hz, respectively. The observed phenomenon was the rise in the coupling constant of ispo **C-9** as the R_2 chain lengthens.

These compounds were also characterized by IR which showed all final novel compounds **21a-v** indicated characteristic peaks for N-H stretching in the range of 3021 - 3312 cm^{-1}, C-H stretch at 2805 - 2977 cm^{-1}, C=O stretch at 1537-1753 cm^{-1}, C=C at 1315 -1605 cm^{-1}, C=S stretch at 1206 - 1337 cm^{-1} and the C-O stretch at 1112 - 1190 cm^{-1}. HRMS of compounds **21a-v** gave further evidence of the successful synthesis of the compounds with the molecular ion corresponding to the calculated values and the data is shown in **table 4**.

Table 4:

compounds	R_1	R_2	% Yields	Melting point (°C)	HRMS (m/z $[M + H]^+$)
21a	H	H	64	187-189	348.1018 (found), 348.0939 (calcd.)
21e	CH_3		66	165-167	362.1581 (found), 362.4215 (calcd.)
21j	F		69	231-232	366.0918 (found), 366.0845 (calcd.)
21o	OCH_3		48	201-202	378.1114 (found), 378.1045 (calcd.)
21b	H	CH_3	58	180-182	362.1175 (found), 362.1096 (calcd.)
21f	CH_3		50	203-205	376.1321 (found), 376.1252 (calcd.)
21k	F		60	222-224	380.1068 (found), 380.1002 (calcd.)
21p	OCH_3		14	174-176	392.1267 (found), 392.1209 (calcd.)
21t	NO_2		67	232-234	407.1475 (found), 407.1409 (calcd.)
21c	H	CH_2CH_3	71	182-184	376.1333 (found), 376.1252 (calcd.)
21g	CH_3		69	167-169	390.1473 (found), 390.1426 (calcd.)
21l	F		81	209-211	394.1224 (found), 394.1158 (calcd.)
21q	OCH_3		68	162-164	406.1423 (found), 406.1358 (calcd.)

21u	NO_2		25	237-239	421.1170 421.1103 (calcd.)	(found),
21h	CH_3	$CH(CH_3)_2$	59	208-210	404.1630 404.1565 (calcd.)	(found),
21m	F		53	175-177	408.1384 408.1303 (calcd.)	(found),
21r	OCH_3		62	184-186	420.1582 420.1514 (calcd.)	(found),
21d	H	$CH_2CH_2CH_3$	56	175-177	390.1474 390.1409 (calcd.)	(found),
21i	CH_3		78	201-203	404.1630 404.1565 (calcd.)	(found),
21n	F		72	196-198	408.1384 408.1303 (calcd.)	(found),
21s	OCH_3		48	214-216	420.1582 420.1514 (calcd.)	(found),
21v	NO_2		62	211-213	435.1324 435.1260 (calcd.)	(found),

CHAPTER THREE

3.1 Background

This chapter presents a brief summary of the extensive biological evaluation carried out on the synthesised compounds. The α-glucosidase assay method was used to perform the biological testing for α-glucose activity. Ms C Rudolph from the bioassay department at Nelson Mandela University conducted the screening tests.

3.1.1 α-glucosidase

α-Glucosidase is an enzyme that plays a crucial role in the final stages of starch digestion. It facilitates the process of breaking down oligosaccharides by catalysing the hydrolysis of glucose molecules located at the non-reducing ends. This leads to the production of glucose units that can be readily absorbed. The enzyme is predominantly situated at the brush border of epithelial cells in the small intestine, where it exists in the form of maltase-glucoamylase (MGAM) and sucrose-isomaltase (SI). [102]

α-Glucosidase inhibitors are crucial for controlling elevated blood sugar levels after meals. By inhibiting the enzyme α-glucosidase, these inhibitors effectively slow down the process of breaking down carbohydrates, which leads to a delay in the release of glucose into the bloodstream. The gradual degradation of carbohydrates in the digestive system results in a reduction in the rate at which glucose is absorbed by the small intestine, effectively inhibiting abrupt spikes in blood sugar levels. In order to achieve the best possible outcomes, it is of utmost importance that inhibitors effectively impede the breakdown of oligosaccharides by attaching to all four catalytic domains of the enzyme. [103] Competitive inhibition arises when an inhibitor and substrate compete for the identical active site on an enzyme, leading to a decrease in the catalytic activity of α-glucosidase. α-Glucosidase inhibitors, such as oral antidiabetic drugs, are frequently employed in the early stages of type 2 diabetes (T2D) to specifically target postprandial hyperglycemia and obesity. Acarbose is a specific medication in this context. [104]

The α-glucosidase inhibitory activities of all synthesised compounds **21a-z** were assessed by comparing them to the standard drug EGCG at concentrations of 65 and 130 µM. (**table 5**).

3.2 Results

At a concentration of 200 µM, the standard drug EGCG exhibits a significant inhibition of 84.84±2.45%. This serves as a standard for evaluating the synthesised compounds, indicating their relative effectiveness in inhibiting alpha-glucosidase.

For the butanoates derivatives with different substituted benzaldehydes, the furfural at both 65 µM and 130 µM concentrations, exhibits substantial alpha-glucosidase inhibition, with percentages of 48.37±0.78 and 45.56±2.50, respectively. This suggests that furfural is effective at inhibiting the enzyme at both concentrations. At 65 µM, the fluorine substituted phenyl butanoate derivative showed lower inhibition (16.30±1.03). However, at 130 µM, the inhibition significantly increased to 61.19±1.48. This indicates a concentration-dependent effect, with higher concentrations resulting in greater inhibition. Methoxy substituted phenyl derivative demonstrates relatively moderate inhibition at both concentrations (38.06±0.74 at 65 µM and 35.12±2.80 at 130 µM), suggesting a consistent inhibitory effect. Naphthaldehyde exhibited moderate to high inhibition, with a decrease from 36.31±2.76 at 65 µM to 25.10±3.09 at 130 µM. This could indicate a concentration-dependent effect, with the inhibitory potential decreasing at higher concentrations. The nitro, methyl and benzaldehyde substituted phenyl derivatives showed relatively low to none inhibition as showed in **table 5**.

At 65 µM, compound **21f** exhibited a high percentage inhibition of 71.13±0.61 for the alaninate derivatives. This suggests that alpha-glucosidase is strongly inhibited at the lower concentration. At 65 µM and 130 µM, respectively, compound **21x** demonstrates a significant inhibition of 38.64±6.05 and 22.74±2.01. Like compound **21f**, this molecule shows moderate inhibition, with a drop at higher concentrations. The inhibitory effect of compound **21k** diminishes with increasing concentration, and it exhibited weak inhibition at both concentrations.

The glycinate derivatives exhibit varying degrees of alpha-glucosidase inhibition, at a concentration of 130 µM, compound **21j** exhibited a significant increase of 60.95±1.07 in inhibition. At a concentration of 130 µM, compound 21j exhibited a significant increase of 60.95±1.07 in inhibition, while the other glycinates derivatives showed varying degrees of alpha-glucosidase inhibition. Compounds **21e** and **21a** continue to have reduced efficacy. At concentrations of 65 and 130 µM, there was a somewhat weak inhibition of α-glucosidase in relation to the vallinates. Only compound **21z** exhibited concentration-dependent trends of moderate inhibition on the norvallinate

derivatives, with values of 37.50±0.39 and 42.41±8.07 at 65 and 130 µM, respectively. Additionally, the vallinates exhibited negligible inhibition.

The alaninate derivative was the only methyl-containing compound to exhibit the highest inhibition at 65 µM and 130 µM, with values of 71.13±0.61 and 64.20±0.54, respectively, indicating that it may have an inhibitory effect on alpha-glucosidase. Table 5 shows that other derivatives have low inhibitory activities, with values fluctuating somewhat and varying in degree.

The glycinate and butanoate derivatives exhibited strong inhibition at 130 µM concentration among the fluorine-containing compounds, whereas the inhibition of the other derivatives was relatively low, ranging from 2.99±6.32 to 10.10±0.50 at 65 and 130 µM concentrations.

The produced 2-thiohydantoin derivatives **21a–v** exhibited low to high inhibition levels overall. At 65 µM and 130 µM, respectively, the para methyl phenyl alaninate showed the strongest inhibition of 71.13±0.61 and 64.20±0.54, respectively. At 65 µM, para fluoro phenyl glycinate showed a moderately high inhibition of 60.95±1.07 and butanoate showed 61.19±1.48.

Table 5: % α-glucosidase inhibition of final compounds **21a-z**.

Compounds	65 µM	130 µM
21a	5.15±0.51	8.91±6.56
21c	2.19±0.28	3.43±5.32
21d	2.84±1.74	1.89±0.59
21e	5.26±4.14	5.50±1.43
21f	71.13±0.61	64.20±0.54
21g	6.61±10.72	11.80±5.36
21h	10.82±5.66	14.89±1.00
21i	14.07±1.57	14.63±2.44
21j	17.17±2.53	60.95±1.07
21k	10.10±0.50	6.88±4.99
21l	16.30±1.03	61.19±1.48
21m	2.99±6.32	6.51±2.39
21n	6.76±1.70	5.80±5.03
21q	38.06±0.74	35.12±2.80

21r	17.99±3.96	14.52±0.65
21u	8.59±0.87	11.40±8.43
21v	4.66±1.75	4.40±3.16

**EGCG at 200 exhibited 84.84±2.45 inhibition.*

CHAPTER FOUR

4.0 Overall conclusion

This chapter looks at the main general conclusion of this study. The study has explored a series of glycinates, alaninates, butanoates, vallinates as well as norvalinates thiohydantoin analogous. The chemistry and biology of the target synthesized compounds were studied extensively and gave promising % α-glucosidase inhibition results.

4.1 Synthesis of novel (Z)-ethyl 2-(2-(4-benzylidene-5-oxo-2-thioxoimidazolidin-1-yl)acetyl) esters

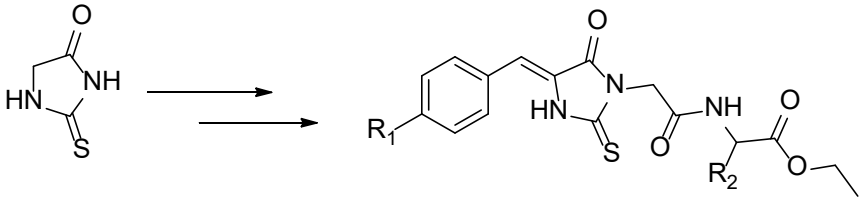

9 21

Scheme 12: Synthesis of novel 2-thiohydantoin derivatives.

This study was achieved through four reaction steps using conventional methods. All the novel compounds were characterized with different techniques. The ^{1}H NMR characterization of these compounds was confirmed with the absence of the second N-H peak and upon that there were other minor but effective changes to the spectra that supported that indeed the reactions were successful. The ^{13}C NMR technique was also used to confirm the products and the main sign that confirmed the products was the increase/decrease in the chemical positions of groups like thiocarbonyl group and ester carbonyl groups. The HRMS technique also proved that the target compounds have formed by having the found mass and the calculated mass being equal.

When the biological assays of these compounds were done, it was observed that some compounds exhibited high inhibition while others did not. At concentrations 65 µM and 130 µM, respectively, the para methyl phenyl alaninate **21f** showed the strongest inhibition of 71.13±0.61 and 64.20±0.54, respectively. At 130 µM, para fluoro phenyl glycinate **21j** showed a moderately high inhibition of 60.95±1.07 and **21l** butanoate showed 61.19±1.48. As much as there were high inhibition, extremely low inhibitions were also observed for compounds **21a**, **21c**, **21d**, **21e**, **21g**, **21m**, **21n**, **21u** and **21v** at both concentrations, while compounds **21q**, **21w**, **21x**, **21y** and **21z**

exhibited consistently moderate inhibition in both concentrations. Further research needs to be conducted in these compounds to establish conclusive SAR of these compounds.

CHAPTER FIVE

5. Experimental procedures

5.1 General procedures

All reagents used in this study were analytical grade from Fluka and Sigma Aldrich and were used without further purification.

5.1.1 Spectroscopic techniques

^{1}H NMR (400 MHz) and ^{13}C NMR (100 MHz) spectra were recorded on a Bruker 400 MHz spectrometer using DMSO-d_6, D_2O or $CDCl_3$ as solvents and TMS at 0.00 ppm as an internal standard. Values for the chemical shifts were expressed in parts per million (ppm), with the following abbreviations used to describe the spin multiplicities: br.s for broad singlet, s for singlet, d for doublet, dd for doublet of doublets, q for quartet, quint for quintet and m for multiplet and J as the coupling constant measured in Hertz (Hz).

All melting points were determined without correction on a Buchi melting point B-540 apparatus using capillary tubes.

Infrared spectra were run on a Bruker platinum 22 vector Fourier Transform spectrometer (FTIR).

Mass spectra (high resolution) were recorded on a Waters GCT mass spectrometer using a Restek Rxi Wintegra Guard column (15m, 0.25mm ID, 0.25µm film thickness). The samples were dissolved in methanol and water and were injected (1µL) in mode 10:1 at a temperature of 280°C. The source temperature was 100°C and the desolvation temperature was set at 300°C. Helium gas was used as the carrier gas. The software used to control the hyphenated system and to perform all data manipulation was MassLynx 4.1 (SCN 704).

5.1.2 Thin Layer Chromatography

Thin layer chromatography (TLC) was used to monitor the reactions using aluminium backed Macherey-Nagel ALUGRAM Sil G/UV254 plates or Aldrich or Merck TLC plates, silica gel on aluminium. The most used solvent system was a mixture of hexane and ethyl acetate.

5.1.3 Nomenclature of compounds

The compounds prepared during the course of this project are named in the following experimental sections according to systematic nomenclature wherever possible. The

numbering system used to illustrate the diagrams of these compounds is one adopted for convenience and it is not meant to reflect the systematic numbering of these compounds.

5.2 General method for protection of amino acids

A solution of an amino acid (1 mmol) in ethanol was cooled to 0-5 °C in an ice bath. To this reaction mixture thionyl chloride (1 mmol) was added dropwise. The resultant mixture was then allowed to warm up to room temperature before being refluxed for 24 hours and was further allowed to cool down to room temperature and a colourless liquid was obtained at reduced pressure (**25a-d**). The resultant products were used without further purification. [92]

5.2.1 Ethyl 2-aminoacetate (25a)

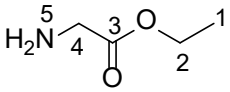

25a

A reaction of glycine (5.01 g, 66.74 mmol) and thionyl chloride (4.86 ml, 66.74 mmol) gave compound **25a** as a white solid (6.10 g, 89 %) %). m.p=89.1 – 91.2 ^{o}C (lit m.p = 91 - 93 ^{o}C), [105] **^{1}H NMR (400 MHz, DMSO-d$_6$) δ$_H$** (ppm) 7.48 (t, 2H, J = 5.3 Hz, H-5), 4.22 (t, 2H, J = 6.1 Hz, H-4), 3.64 (q, 2H, J = 5.6 Hz, H-2), 1.09 (t, 3H, J = 7.0 Hz, H-1); **^{13}C NMR (100 MHz, DMSO-d$_6$) δ$_C$** (ppm) 170.08 (C-3), 61.20 (C-2), 45.04 (C-4), 14.25 (C-1),), **IR** (KBr cm^{-1}): 3368 (N-H), 2898 (C-H), 1710 (C=O), 1450(C-O).

5.2.2 Ethyl 2-aminopropanoate (25b)

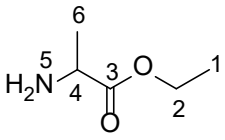

25b

A reaction of alanine (5.03 g, 56.15 mmol) and thionyl chloride (4.09 ml, 56.15 mmol) gave compound **25b** as a colourless liquid (6.01 g, 91 %), **^{1}H NMR (400 MHz, DMSO-d$_6$) δ$_H$** (ppm) 7.58 (d, 2H, J = 6.8 Hz, H-5), 4.19-4.16 (m, 1H, H-4), 3.74 (q, 2H, J = 5.6 Hz, H-2), 1.10 (d, 3H, J = 7.2 Hz, H-6), 1.05 (t, 3H, J = 7.0 Hz, H-1); **^{13}C NMR (100 MHz, DMSO-d$_6$) δ$_C$** (ppm) 170.27 (C-3), 62.14 (C-2), 58.3 (C-4), 16.17 (C-6), 14.36 (C-1), **IR** (KBr cm^{-1}): 3385 (N-H), 2978 (C-H), 1720 (C=O), 1314 (C-O).

5.2.3 Ethyl 2-amino butanoate (25c)

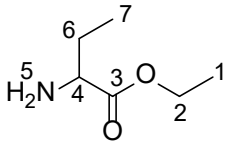

25c

A reaction of alpha amino butanoic acid (5.01 g, 48.51 mmol) and thionyl chloride (3.51 ml, 48.51 mmol) gave compound **25c** as a brown oil (5.91 g, 93 %), **^{1}H NMR (400 MHz, DMSO-d$_6$)** δ_H (ppm) 8.67 (d, 2H, *J* = 7.8 Hz, H-5), 4.22 (quint, 1H, J = 1.2 Hz, H-4), 3.99 (q, 2H, *J* = 6.4 Hz, H-2), 1.89 (quint, 2H, J = 7.2 Hz, H-6), 1.19 (t, 3H, *J* = 7.2 Hz, H-1), 0.91 (t, 3H, *J* = 7.6 Hz, H-7), **^{13}C NMR (100 MHz, DMSO-d$_6$)** δ_C (ppm) 170.30 (C-3), 63.47 (C-2), 54.07 (C-4), 23.26 (C-6), 13.23 (C-1), 8.43 (C-7), **IR** (KBr cm^{-1}): 3397 (N-H), 2875 (C-H), 1761 (C=O), 1171 (C-O).

5.2.4 Ethyl 2-amino-3-methylbutanoate (25d)

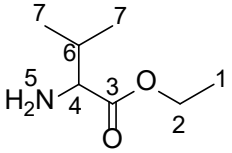

25d

A reaction of valine (10.0 g, 85.41 mmol) and thionyl chloride (5.01 ml, 85.41 mmol) gave compound **25d** as a light brown oil (9.88 g, 79 %), **^{1}H NMR (400 MHz, DMSO-d$_6$)** δ_H (ppm) 8.58 (d, 2H, *J* = 8.0 Hz, H-5), 4.17 (q, 1H, *J* = 5.6 Hz, H-4), 3.93 (q, 2H, *J* = 10.8 Hz, H-2), 2.06 (m, 1H, H-6), 1.21 (t, 2H, *J* = 7.2 Hz, H-1), 0.87 (d, 3H, *J* = 3.2 Hz, H-7), **^{13}C NMR (100 MHz, DMSO-d$_6$)** δ_C (ppm) 171.31 (C-3), 62.09 (C-2), 58.07 (C-4), 29.32 (C-6), 19.27 (C-7), 18.39 (C-7), 14.30 (C-1), **IR** (KBr cm^{-1}): 3352 (N-H), 2915 (C-H), 1745 (C=O), 1231 (C-O).

5.2.5 Ethyl 2-aminopentanoate (25e)

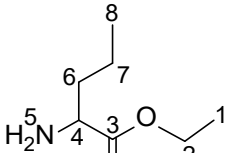

25e

A reaction of norvaline (10.0 g, 85.41 mmol) and thionyl chloride (5.01 ml, 85.41 mmol) gave compound **25e** as a colourless oil (9.76 g, 79%), **^{1}H NMR (400 MHz, DMSO-d$_6$)** δ_H (ppm) 8.66 (d, 2H, *J* = 6.2 Hz, H-5), 4.22 (quint, 1H, *J* = 4.8 Hz, H-4), 4.12 (q, 2H,

J = 7.2 Hz, H-2), 1.70 – 1.61 (m, 2H, H-6), 1.36 – 1.35 (m, 2H, H-7), 1.21 (t, 3H, *J* = 6.8 Hz, H-1), 0.89 (t, 3H, *J* = 7.2 Hz , H-8), **^{13}C NMR (100 MHz, DMSO-d$_6$) δ$_C$** (ppm) 172.18 (C- 3), 60.99 (C-2), 52.54 (C-4), 29.31 (C-6), 27.64 (C-7), 14.48 (C-1), 13.85(C-8), **IR** (KBr cm^{-1}): 3397 (N-H), 2986 (C-H),1732 (C=O), 1121 (C-O).

5.3 General procedure for the synthesis of ethyl 2-(2-chloro acetamido) esters

To a solution of protected amino acids **25a-e** (1 mmol) in water was added $NaHCO_3$ (1 mmol) at 0 °C portion-wise. This reaction mixture was treated with a solution of chloro acetyl chloride (2 mmol) in toluene dropwise before been stirred vigorously for 12h at room temperature. After this reaction time, the mixture was extracted with toluene, dried over magnesium sulphate and filtered before excess toluene was removed using rotary evaporator to obtain desired products as white solids (**23a-e**). [94]

5.3.1 ethyl 2-((2-chloroacetomido)acetate (23a)

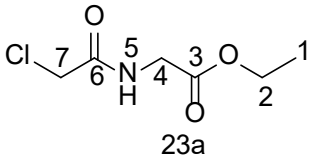

23a

A reaction of ethyl 2-aminoacetate (6.10 g, 5.91 mmol) with chloro acetyl chloride (9.41 ml, 11.83 mmol) in toluene gave compound **23a** as white solid (9.21g, 86.69%). m.p=75.4 – 77.2 °C (lit m.p = 77.5 °C [94]), **^{1}H NMR (400 MHz, DMSO-d$_6$) δ$_H$** (ppm) 8.58 (t, 1H, J = 5.58 Hz, H-5), 4.21 (s, 2H, H-7), 4.10 (q, 2H, J = 7.16 Hz, H-2), 3.90 (d, 2H, J = 5.84 Hz, H-4), 1.19 (t, 3H, J = 7.32 Hz, H-1), **^{13}C NMR (100 MHz, DMSO-d$_6$) δ$_C$** (ppm) 169.76 (C-3), 167.02 (C-6), 61.00 (C-2), 42.60 (C-7), 41.38 (C-4), 14.28 (C-1). **IR** (KBr cm^{-1}): 3396 (N-H), 1723 (C=O), 1646 (C=O), 1548 (C-O)

5.3.2 Ethyl 2-(2-chloroacetamido)propanoate (23b)

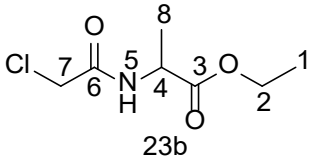

23b

A reaction of ethyl 2-aminopropanoate (6.01 g, 5.13 mmol) with chloroacetyl chloride (8.16 ml, 10.26 mmol) in toluene gave compound **23b** as brown oil (9.01g, 90.70%), **^{1}H NMR (400 MHz, DMSO-d$_6$) δ$_H$** (ppm) 8.78 (d, 1H, J = 6.76 Hz, H-5), 4.25 (quintet, 1H, J = 7.16 Hz, H-4), 4.09 (q, 2H, J = 5.2 Hz, H-2), 3.89 (s, 2H, H-7), 1.30 (d, 3H, J =

7.28 Hz, H-8), 1.19 (t, 3H, J = 6.88 Hz, H-1), **^{13}C NMR (100 MHz, DMSO-d$_6$) δ$_C$** (ppm) 172.30 (C-3), 168.96 (C-6), 61.09 (C-2), 48.50 (C-4), 42.24 (C-7), 16.77 (C-1), 13.70 (C-8). **IR** (KBr cm^{-1}): 3396 (N-H), 1746 (C=O), 1670 (C=O), 1548 (C-O).

5.3.3 Ethyl 2-(2-chloroacetamido)butanoate (23c)

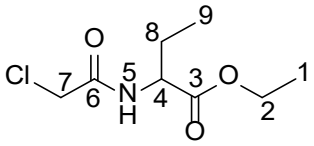

23c

A reaction of ethyl 2-aminobutanoate (5.91 g, 4.50 mmol) with chloroacetyl chloride (7.16 ml, 9.01 mmol) in toluene gave compound **23c** as brown oil (8.54g, 91.28%), **^{1}H NMR (400 MHz, DMSO-d$_6$) δ$_H$** (ppm) 8.60 (d, 1H, J = 7.32 Hz, H-5), 4.26 (s, 2H, H-7), 4.19 (q, 2H, J = 7.80 Hz, H-2), 4.09 (quintet, 1H, J = 4.68 Hz, H-4), 1.79 – 1.62 (m, 2H, H-8), 1.20 (d, 3H, J = 7.16 Hz, H-1), 0.89 (t, 3H, J = 7.44 Hz, H-9), **^{13}C NMR (100 MHz, DMSO-d$_6$) δ$_C$** (ppm) 171.97 (C-3), 166.65 (C-6), 61.02 (C-2), 54.14 (C-4), 42.67 (C-7), 24.67 (C-8), 14.46 (C-1), 10.51 (C-9). **IR** (KBr cm^{-1}): 3387 (N-H), 1720 (C=O), 1650 (C=O), 1538 (C-H).

5.3.4 ethyl 2-(2-chloroacetamido)-3-methylbutanoate (23d)

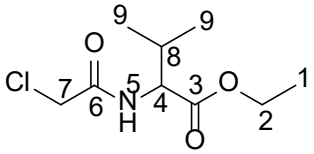

23d

A reaction of ethyl 2-amino-3-methylbutanoate (9.88 g, 6.80 mmol) with chloroacetyl chloride (10.82 ml, 13.60 mmol) in toluene gave compound **23d** as brown oil (13.25g, 87.84%), **^{1}H NMR (400 MHz, DMSO-d$_6$) δ$_H$** (ppm) 8.62 (d, 1H, J = 8.16 Hz, H-5), 4.14 (m, 1H, H-4), 4.04 (s, 2H, H-7), 3.96 (q, 2H, J = 9.20 Hz, H-2), 2.10 – 2.01 (m, 1H, H-8), 1.20 (t, 3H, J = 6.08 Hz, H-1), 0.89 (d, 6H, J = 3.24 Hz, H-9), **^{13}C NMR (100 MHz, DMSO-d$_6$) δ$_C$** (ppm) 171.51 (C-3), 166.95 (C-6), 60.96 (C-2), 58.12 (C-4), 40.54 (C-7), 29.35 (C-8), 19.29 (C-9), 18.43 (C-9), 14.53 (C-1). **IR** (KBr cm^{-1}): 3386 (N-H), 1740 (C=O), 1615 (C=O), 1526 (C-O).

5.3.5 ethyl 2-(2-chloroacetamido)pentanoate (23e)

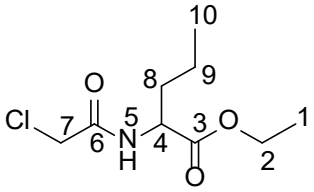

23e

A reaction of ethyl 2-aminopentanoate (9.76 g, 6.72 mmol) with chloroacetyl chloride (10.69 ml, 13.44 mmol) in toluene gave compound **23e** as brown oil (12.98g, 87.11%), **^{1}H NMR (400 MHz, DMSO-d$_6$) δ$_H$** (ppm) 8.68 (d, 1H, *J* = 3.6 Hz, H-5), 4.22 (quint, 1H , *J* = 4.8 Hz, H-4), 4.13 (q, 2H, *J* = 4.0 Hz, H-2), 3.93-3.89 (m, 2H, *J* = 6.8 Hz, H-8), 3.75 (s, 2H, H-7), 1.70-1.64 (2H, m, H-9), 1.22 (t, 3H, *J* = 2.0 Hz, H-1), 0.88 (t, 3H, *J* = 7.2 Hz, H-10), **^{13}C NMR (100 MHz, DMSO-d$_6$) δ$_C$** (ppm) 172.18 (C-3), 166.68 (C-6), 62.10 (C-2), 52.54 (C-4), 33.40 (C-7), 29.32 (C-9), 18.92 (C-8), 14.48 (C-1), 13.85 (C-10). **IR** (KBr cm^{-1}): 3389 (N-H), 1747 (C=O), 1630 (C=O), 1534 (C-O).

5.4 Synthesis of 1-acetyl-2-thioxoimidazolidin-4-one (31).

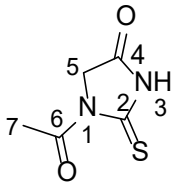

31

2-aminoacetic acid (1 mmol) and ammonium thiocyanate (1 mmol) were mixed in acetic anhydride (6 mmol) in a round-bottom flask. The resulting mixture was heated in an oil bath at 100 °C for 3 hours, during which time all solids dissolved. The reaction was poured into a beaker of ice water and stirred. The resultant reaction solution was filtered through vacuum filtration, washed with cold water and recrystallized from methanol to give an orange solid (10.61g, 50.52 %). m.p=166.9 – 168.4 ^{o}C (lit m.p = 167 – 169 ^{o}C). [81] **^{1}H NMR (400 MHz, DMSO-d$_6$) δ$_H$** (ppm) 12.60 (s, 1H, H-3), 4.40 (s, 2H, H-5), 2.68 (s, 3H, H-7), **^{13}C NMR (100 MHz, DMSO-d$_6$) δc** (ppm) 182.95 (C-2), 170.81 (C-4), 169.77 (C-6), 52.63 (C-5), 27.05 (C-7). **IR** (KBr cm^{-1}): 3104 (N-H), 1755 (C=O), 1667 (C=O), 1223 (C=S).

5.5 Synthesis of 2-thioxoimidazolidin-4-one (9)

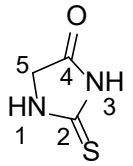

9

1-acetyl-2-thioxoimidazolidin-4-one (1 mmol) was dissolved in 3M HCl and refluxed for 2 hours at 120 °C. The resulting clear, yellow solution was extracted with 4 x 10 mL of ethyl acetate. The combined ethyl acetate extracts were dried over Na_2SO_4, concentrated, and dried under vacuum to give 2-thioxoimidazolidin-4-one as a brown solid (1.17 g, 79,59%) m.p = 227.9 – 229.4 °C (lit m.p = 229 – 231 °C). [81] **^{1}H NMR (400 MHz, DMSO-d$_6$) δ$_H$** (ppm) 11.67 (s, 1H, H-3), 9.87 (s, 1H, H-1), 4.09 (s, 2H, H-5), **^{13}C NMR (100 MHz, DMSO-d$_6$) δ$_C$** (ppm) 183.83 (C-2), 174.99 (C-4), 50.75 (C-5). **IR** (KBr cm^{-1}): 3146 (N-H), 1783 (C=O), 1289 (C=S).

5.5 General synthetic procedure for the Knoevenagel condensation reaction.

A solution of thiohydantoin (1 mmol) in glacial acetic acid was treated with benzaldehyde (1 mmol) and sodium acetate (8 mmol). This reaction mixture was heated under reflux overnight. After been allowed to cool down to room temperature and treated with water, a precipitate was formed and filtered before been recrystallized from ethanol to obtain products as white crystalline solids. (**22a-h**). [95]

5.5.1 (Z)-5-benzylidene-2-thioxoimidazolidin-4-one (22a)

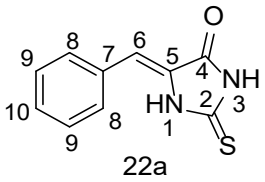

22a

A mixture of benzaldehyde (3.50 mL, 34.44 mmol), thiohydantoin (4.00 g, 34.44 mmol) and sodium acetate (22.69 g, 275.53 mmol) in glacial acetic acid yielded compound **22a** as a brown solid (5.71 g, 81,24 %); m.p 257.2-259.1 °C (lit m.p 258-260 °C); [95] **^{1}H NMR (400 MHz, DMSO-d$_6$) δ$_H$** (ppm) 12.29 (s, 2H, H-1 & H-3), 7.76 (d, 2H, J = 6.88 Hz, H-8), 7.61–7.27 (m, 3H, H9 & H-10), 6.50 (s, 1H, H-6), **^{13}C NMR (100 MHz, DMSO-d$_6$) δ$_C$** (ppm) 179.73 (C-2), 166.25 (C-4), 132.79 (C-5), 130.62 (C-8), 129.67

(C-9), 129.23 (C-10), 128.21 (C-7), 112.01 (C-6). **IR** (KBr cm^{-1}): 3187 (N-H), 2956 (C-H), 1716 (C=O), 1638 (C=C), 1249 (C=S).

5.5.2 (Z)-5-(4-methylbenzylidene)-2-thioxoimidazolidin-4-one (22b)

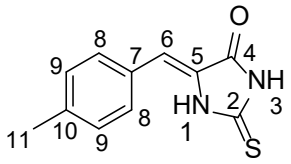

22b

A mixture of 4-methylbenzaldehyde (4.06 mL, 34.44 mmol), thiohydantoin (4.00 g, 34.44 mmol) and sodium acetate (22.69 g, 275.53 mmol) in glacial acetic acid yielded compound **22b** as a green solid (5.20 g, 69.17%); m.p 247.1-248.9 °C (lit m.p 246-248 °C); [96] **^{1}H NMR (400 MHz, DMSO-d_6) δ_H** (ppm 12.37 (s, 1H, H-3), 12.11 (s, 1H, H-1), 7.66 (d, *J* = 8.1 Hz, 2H, H-8), 7.24 (d, *J* = 8.0 Hz, 2H, H-9), 6.47 (s, 1H, H-6), 2.34 (s, 3H, H-11). **^{13}C NMR (100 MHz, DMSO-d_6) δ_C** (ppm) 179.42 (C-2), 166.27 (C-4), 139.76 (C-10), 130.69 (C-8), 129.98 (C-5), 129.91 (C-9), 127.42 (C-7), 112.36 (C-6), 21.52 (C-11). **IR** (KBr cm^{-1}): 3164 (N-H), 2815 (C-H), 1719 (C=O), 1644 (C=C), 1250 (C=S).

5.5.3 (Z)-5-(4-hydroxybenzylidene)-2-thioxoimidazolidin-4-one (22c)

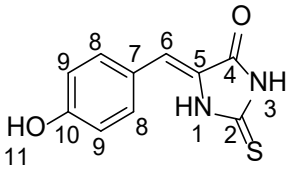

22c

A mixture of 4-hydroxybenzaldehyde (4.21g, 34.44mmol), thiohydantoin (4.00 g, 34.44 mmol) and sodium acetate (22.69 g, 275.53 mmol) in glacial acetic acid yielded compound **22c** as a yellow solid (6.62g, 87.27 %); m.p 280.6-282.1 °C (lit m.p 280 °C); [95] **^{1}H NMR (400 MHz, DMSO-d_6) δ_H** (ppm) 12.26 (s, 1H, H-3), 12.02 (s, 1H, H-1), 10.10 (s, 1H, H-11), 7.65 (d, *J* = 8.6 Hz, 2H, H-8), 6.83 (d, *J* = 8.5 Hz, 2H, H-9), 6.45 (s, 1H, H-6). **^{13}C NMR (100 MHz, DMSO-d_6) δ_C** (ppm) 178.72 (C-2), 166.30 (C-4), 159.45 (C-10), 132.86 (C-8), 125.62 (C-5), 123.79 (C-7), 116.31 (C-6), 113.35 (C-9). **IR** (KBr cm^{-1}): 3319 (O-H), 3102 (N-H), 2750 (C-H), 1705 (C=O), 1649 (C=C), 1252 (C=S).

5.5.4 (Z)-5-(4-methoxybenzylidene)-2-thioxoimidazolidin-4-one (22d)

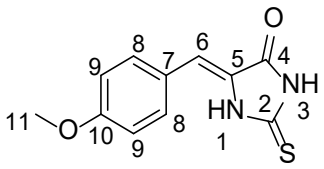

22d

A mixture of 4-methoxybenzaldehyde (4.18 mL, 34.44 mmol), thiohydantoin (4.00 g, 34.44 mmol) and sodium acetate (22.69 g, 275.53 mmol) in glacial acetic acid yielded compound **22d** as a brown solid (7.25g, 89.86%); m.p 210.1-211.7 ^{o}C (lit m.p 211-213 ^{o}C) [97] **^{1}H NMR (400 MHz, DMSO-d$_6$) δ$_H$** (ppm) 12.20 (s, 2H, H-1 & H-3), 7.75 (d, *J* = 8.8 Hz, 2H, H-8), 6.99 (d, *J* = 8.8 Hz, 2H, H-9), 6.49 (s, 1H, H-6), 3.82 (s, 3H, H-11). **^{13}C NMR (100 MHz, DMSO-d$_6$) δc** (ppm) 179.03 (C-2), 166.28 (C-4), 160.69 (C-10), 132.59 (C-8), 126.33 (C-5), 125.32 (C-7), 114.82 (C-6), 112.63 (C-9), 55.80 (C-11). **IR** (KBr cm^{-1}): 3115 (N-H), 2815 (C-H), 1735 (C=O), 1617 (C=C), 1235 (C=S).

5.5.5 (Z)-5-(4-fluorobenzylidene)-2-thioxoimidazolidin-4-one (22e)

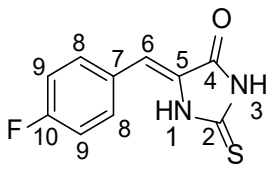

22e

A mixture of 4-fluorobenzaldehyde (4.27g, 34.44 mmol), thiohydantoin (4.00 g, 34.44 mmol) and sodium acetate (22.69 g, 275.53 mmol) in glacial acetic acid yielded compound **22e** as a black solid (5.68g, 74.20%); m.p 252.1-253.8 ^{o}C (lit m.p 253-257 ^{o}C); [98] **^{1}H NMR (400 MHz, DMSO-d$_6$) δ$_H$** (ppm) 12.28 (s, 2H, H-1 & H-3), 7.80 (dd, J_{HH} = 8.0 Hz, $^{4}J_{FH}$ 6.0 Hz, 2H, H-8), 7.24 (dd, J_{HH} = 8.4 Hz, $^{3}J_{FH}$ 16.8 Hz, 2H, H-9), 6.49 (s, 1H, H-6). **^{13}C NMR (100 MHz, DMSO-d$_6$) δc** (ppm) 179.73 (C-2), 166.23 (C-4), 162.79 (d, $^{1}J_{FC}$ 248.0 Hz, C-10), 132.94 (d, $^{3}J_{FC}$ 9.0 Hz C-8), 129.41 (d, $^{6}J_{FC}$ 2.0 Hz, C-5), 127.99 (d, $^{4}J_{FC}$ 3.0 Hz C-7), 116.24 (d, $^{2}J_{FC}$ 22.0 Hz C-9), 110.90 (C-6). **IR** (KBr cm^{-1}): 3201 (N-H), 2765 (C-H), 1725 (C=O), 1595 (C=C), 1230 (C=S).

5.5.6 (Z)-5-(4-nitrobenzylidene)-2-thioxoimidazolidin-4-one (22f)

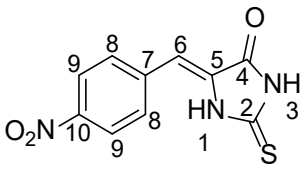

22f

A mixture of 4-nitrobenzaldehyde (5.20 g, 34.44 mmol), thiohydantoin (4.00 g, 34.44 mmol) and sodium acetate (22.69 g, 275.53 mmol) in glacial acetic acid yielded compound **22f** as a brown solid (6.64g, 77.35%); m.p 283.8-286.1 °C (lit m.p 284-286 °C); [99] **^{1}H NMR (400 MHz, DMSO-d$_6$) δ$_H$** (ppm) 12.58 (s, 1H, H-3), 12.42 (s, 1H, H-1), 8.20 (d, *J* = 8.0 Hz, 2H, H-8), 7.94 (d, *J* = 8.2 Hz, 2H, H-9), 6.53 (s, 1H, H-6). **^{13}C NMR (100 MHz, DMSO-d$_6$) δc** (ppm) 180.50 (C-2), 166.10 (C-4), 147.05 (C-10), 139.62 (C-5), 131.34 (C-8), 130.70 (C-7), 124.10 (C-9), 108.47 (C-6). **IR** (KBr cm^{-1}): 3196 (N-H), 3001 (C-H), 1739 (C=O), 1590 (C=C), 1249 (C=S).

5.5.7 (Z)-5-(furan-2-ylmethylene)-2-thioxoimidazolidin-4-one (22g)

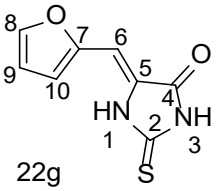

22g

A mixture of furan-2-carbaldehyde (2.85 mL, 34.44 mmol), thiohydantoin (4.00 g, 34.44 mmol) and sodium acetate (22.69 g, 275.53 mmol) in glacial acetic acid yielded compound **22g** as a brown solid (4.26g, 60.56 %); m.p 253.9-256.7 °C (lit m.p 258-262 °C); [100] **^{1}H NMR (400 MHz, DMSO-d$_6$) δ$_H$** (ppm) 12.23 (s, 1H, H-3), 11.95 (s, 1H, H-1), 7.85 (s, 1H, H-10), 7.14 (d, *J* = 3.3 Hz, 1H, H-8), 6.88 – 6.54 (m, 1H, H-9), 6.41 (s, 1H, H-6). **^{13}C NMR (100 MHz, DMSO-d$_6$) δc** (ppm) 178.48 (C-2), 165.79 (C-4), 149.32 (C-7), 146.23 (C-8), 125.94 (C-5), 115.99 (C-9), 113.62 (C-10), 99.54 (C-6). **IR** (KBr cm^{-1}): 3187 (N-H), 2948 (C-H), 1716 (C=O), 1638 (C=C), 1242 (C=S).

5.5.8 (Z)-5-(naphthalen-2-ylmethylene)-2-thioxoimidazolidin-4-one (22h)

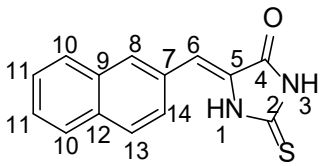

22h

A mixture of 2-naphthaldehyde (5.38g, 34.44 mmol), thiohydantoin (4.00 g, 34.44 mmol) and sodium acetate (22.69 g, 275.53 mmol) in glacial acetic acid yielded compound **22h** as a brown solid (8.16g, 93.19 %); m.p 287.9-289.5 °C (lit m.p 289-291 °C); [101] **^{1}H NMR (400 MHz, DMSO-d$_6$) δ$_H$** (ppm) 12.35 (s, 2H, H-1 & H-3), 8.38 (s, 1H, H-8), 7.97 (d, *J* = 4.6 Hz, 1H, H-14), 7.93 (d, *J* = 8.6 Hz, 2H, H-10), 7.81 (d, *J* = 8.6 Hz, 1H, H-13), 7.67 – 7.44 (m, 2H, H-11), 6.63 (s, 1H, H-6). **^{13}C NMR (100 MHz, DMSO-d$_6$) δc** (ppm) 179.75 (C-2), 166.41 (C-4), 133.40 (C-12), 133.28 (C-7), 130.45

(C-5), 130.10 (C-10), 128.90 (C-13), 128.74 (C-9), 128.63 (C-10), 128.01 (C-14), 127.94 (C-11), 127.65 (C-8), 127.07 (C-11), 111.94 (C-6). **IR** (KBr cm^{-1}): 3189 (N-H), 2870 (C-H), 1715 (C=O), 1630 (C=C), 1226 (C=S).

5.6 General synthetic procedure for target compounds (21a-v)

A mixture of Knoevenagel condensation reaction products (1 mmol) (**22a-h**) dissolved in ethanol and triethylamine (2 mmol) was agitated for 15 minutes at 80 °C. The reaction mixture was then refluxed for 12 hours with ethyl amino esters (**23a-e**) (1 mmol). When the reaction had cooled to room temperature, the solvent was removed and the product was purified using column chromatography.

5.6.1(Z)-Ethyl2-(2-(4-benzylidene-5-oxo-2-thioxoimidazolidin-1-yl) acetamido)acetate (21a)

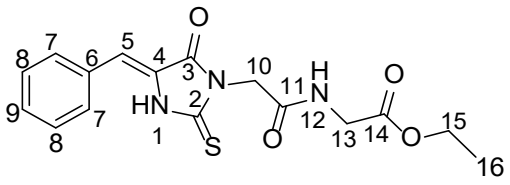

21a

A reaction of (Z)-5-benzylidene-2-thioxoimidazolidin-4-one **22a** (0.50 g, 2.48 mmol) and ethyl 2-(2-chloroacetamido) acetate **23a** (0.44g, 2.48 mmol) gave compound **21a** as a yellow solid (0.53g, 63.79 %); m.p 187-189 °C; **^{1}H NMR (400 MHz, DMSO-d_6) δ_H** (ppm) 11.89 (s, 1H, H-1), 8.83 (t, 1H, J = 5.64 Hz, H-12), 8.17 (d, 2H, J = 7.32 Hz, H-7), 7.45-7.37 (m, 3H, H-9 & H-8), 6.76 (s, 1H, H-5), 4.14 (s, 2H, H-10), 4.09(q, 2H, J = 7.12 Hz, H-15), 3.90 (d, 2H, J = 5.72 Hz, H-13), 1.17 (t, 3H, J = 7.08 Hz, H-16), **^{13}C NMR (100 MHz, DMSO-d_6) δ_C** (ppm) 171.02 (C-14), 169.97 (C-2), 167.57 (C-11), 164.26 (C-3), 139.52 (C-4), 134.62 (C-6), 132.06 (C-7), 130.02 (C-8), 129.07 (C-9), 121.70 (C-5), 60.99 (C-15), 41.63 (C-10), 33.80 (C-13), 14.47 (C-16). **IR** (KBr cm^{-1}): 3215 (N-H), 2977 (C-H), 2860 (C-H), 1753 (C=O), 1708 (C=O), 1663 (C=O), 1605 (C=C), 1226 (C=S),1170 (C-O). **HRMS** (ESI-TOF): m/z $[M + H]^+$ calculated for $C_{16}H_{17}N_3O_4S$: 348.0939; found: 348.1018.

5.6.2 (Z)-ethyl 2-(2-(4-benzylidene-5-oxo-2-thioxoimidazolidin-1-yl)acetamido) propanoate (21b)

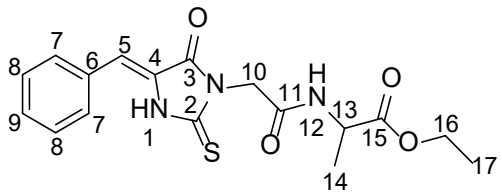

21b

A reaction of (Z)-5-benzylidene-2-thioxoimidazolidin-4-one **22a** (0.5g, 2.48 mmol) and ethyl 2-(2-chloroacetamido)propanoate **23b** (0.47g, 2.48 mmol) gave compound **21b** as a grey solid (0.51g, 57.95 %); m.p 180-182 ^{o}C; **^{1}H NMR (400 MHz, DMSO-d$_6$) δ_H** (ppm) 11.94 (s, 1H, H-1), 8.81 (d, 1H, J = 6.8 Hz, H-12),8.18 (d, 2H, J = 7.12, H-7), 7.37-7.45 (m, 3H, H-8 & H-9), 6.76 (s, 1H, H-5), 4.28 (quintet, 1H, J = 7.12 Hz, H-13), 4.18 (s, 2H, H-10), 4.06 (q, 2H, J = 3.2 Hz, H-16), 1.30 (d, 3H, J = 7.2 Hz, H-14), 1.15 (t, 3H, J = 7.04 Hz, H-17), **^{13}C NMR (100 MHz, DMSO-d$_6$) δ_C** (ppm) 172.71 (C-15), 171.01 (C-2), 166.86 (C-11), 164.40 (C-3), 139.52 (C-4), 134.64 (C-6), 132.08 (C-7), 130.62 (C-8), 129.23 (C-9), 121.60 (C-5), 60.99 (C-16), 40.61 (10), 33.83 (C-13), 17.50 (C-14), 14.43 (C-17). **IR** (KBr cm^{-1}): 3312 (N-H), 2921 (C-H), 2851 (C-H), 1732 (C=O), 1710 (C=O), 1637 (C=O),1535 (C=C), 1272 (C=S),1190 (C-O). **HRMS** (ESI-TOF): m/z [M + H]$^{+}$ calculated for $C_{17}H_{19}N_3O_4S$: 362.1096; found: 362.1175.

5.6.3 (Z)-ethyl 2-(2-(4-benzylidene-5-oxo-2-thioxoimidazolidin-1-yl)acetamido)butanoate (21c)

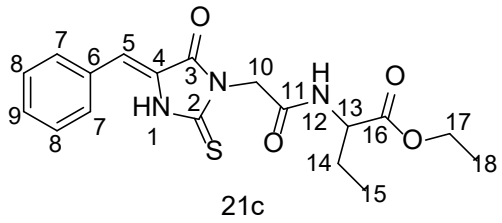

21c

A reaction of (Z)-5-benzylidene-2-thioxoimidazolidin-4-one **22a** (0.5g, 2.48 mmol) and ethyl 2-(2-chloroacetamido)butanoate **23c** (0.51g, 2.48 mmol) gave compound **21c** as a white solid (0.65g, 71.30 %); m.p 182-184 ^{o}C; **^{1}H NMR (400 MHz, DMSO-d$_6$) δ_H** (ppm) 11.64 (s, 1H, H-1), 8.72 (d, 1H, J = 7.32 Hz, H-12),8.18 (d, 2H, J = 7.20, H-7), 7.38-7.45 (m, 3H, H-8 & H-9), 6.76 (s, 1H, H-5), 4.20 (quintet, 1H, J = 7.02 Hz, H-13), 4.14 (s, 1H, H-10), 4.07 (q, 2H, J = 5.76 Hz, H-17), 1.78-1.53 (m, 2H, H-14), 1.17 (q, 3H, J = 7.20 Hz, H-15), 1.15 (t, 3H, J = 7.32 Hz, H-18), **^{13}C NMR (100 MHz, DMSO-d$_6$) δ_C** (ppm) 172.08 (C-16), 171.00 (C-2), 167.18 (C-11), 164.41 (C-3), 139.48 (C-4),

134.60 (C-6), 132.08 (C-7), 130.62 (C-8), 129.01 (C-9), 121.64 (C-5), 61.02 (C-17), 54.33 (C-13), 46.11 (C-10), 24.63 (C-14), 14.48 (C-18), 10.57 (C-15). **IR** (KBr cm^{-1}): 3296 (N-H), 2910 (C-H), 2805 (C-H), 1746 (C=O), 1711 (C=O), 1656 (C=O),1595 (C=C), 1255 (C=S),1173 (C-O). **HRMS** (ESI-TOF): m/z $[M + H]^+$ calculated for $C_{18}H_{23}N_3O_4S$: 376.1252; found: 376.1333.

5.6.4 (Z)-ethyl 2-(2-(4-benzylidene-5-oxo-2-thioxoimidazolidin-1-yl)acetamido)pentanoate (21d)

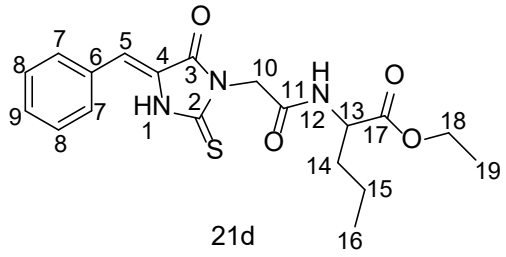

21d

A reaction of (Z)-5-benzylidene-2-thioxoimidazolidin-4-one **22a** (0.5g, 2.48 mmol) and ethyl 2-(2-chloroacetamido)pentanoate **23e** (0.54g, 2.48 mmol) gave compound **21d** as a white solid (0.53g, 55.79 %), m.p 175-177 ^oC; **^{1}H NMR (400 MHz, DMSO-d_6) δ_H** (ppm) 11.90 (s, 1H, H-9), 8.72 (d, 1H, J = 7.48 Hz, H-12),8.18 (d, 2H, J = 7.24, H-3), 7.39-7.45 (m, 3H, H-1 & H-2), 6.77 (s, 1H, H-5), 4.24 (quintet, 1H, J = 7.88 Hz, H-13), 4.17 (s, 1H, H-10), 4.06 (q, 2H, J = 6.08 Hz, H-18), 1.69-1.51 (m, 2H, H-14),1.32-1.22 (m, 2H, H-15), 1.15 (t, 3H, J = 7.08 Hz, H-19), 0.75 (t, 3H, J = 7.24 Hz, H-16), **^{13}C NMR (100 MHz, DMSO-d_6) δ_C** (ppm) 172.29 (C-17), 170.99 (C-2), 167.17 (C-11), 164.36 (C-3), 139.46 (C-4), 134.60 (C-6), 132.09 (C-7), 130.62 (C-8), 129.07 (C-9), 121.70 (C-5), 60.90 (C-18), 52.57 (C-13), 46.01 (C-10), 33.61 (C-14), 18.95 (C-15), 14.46 (C-19),13.79 (C-16). **IR** (KBr cm^{-1}): 3295 (N-H), 2956 (C-H), 2840 (C-H), 1709 (C=O), 1638 (C=O), 1537 (C=O), 1505 (C=C), 1248 (C=S),1174 (C-O). **HRMS** (ESI-TOF): m/z $[M + H]^+$ calculated for $C_{19}H_{23}N_3O_4S$: 390.1409; found: 390.1474.

5.6.5 (Z)-ethyl 2-(2-(4-(4-methylbenzylidene)-5-oxo-2-thioxoimidazolidin-1-yl)acetamido)acetate (21e)

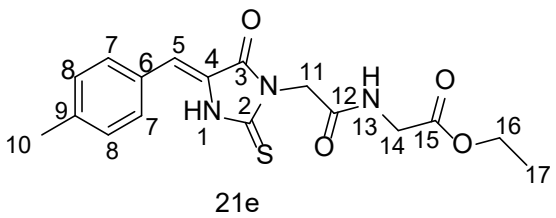

21e

A reaction of (Z)-5-(4-methylbenzylidene)-2-thioxoimidazolidin-4-one **22b** (0.5g, 2.29 mmol) and ethyl 2-(2-chloroacetamido)acetate **23a** (0.41g, 2.29 mmol) gave compound **21e** as a yellow solid (0.54g, 65.64%); m.p 165-167 °C; **^{1}H NMR (400 MHz, DMSO-d$_6$) δ$_H$** (ppm) 11.83 (s, 1H, H-1), 8.80 (t, *J* = 5.5 Hz, 1H, H-13), 8.06 (d, *J* = 7.8 Hz, 2H, H-7), 7.24 (d, *J* = 7.9 Hz, 2H, H-8), 6.73 (s, 1H, H-5), 4.12 (s, 2H, H-11), 4.08 (q, *J* = 7.1 Hz, 1H, H-16), 3.91 (d, *J* = 5.7 Hz, 2H, H-14), 2.35 (s, 3H, H-10), 1.18 (t, *J* = 7.1 Hz, 3H, H-17). **^{13}C NMR (100 MHz, DMSO-d$_6$) δ$_C$** (ppm) 171.02 (C-15), 169.98 (C-2), 167.60 (C-12), 163.46 (C-3), 140.05 (C-4), 138.86 (C-9), 132.10 (C-7), 131.92 (C-6), 129.76 (C-8), 121.96 (C-5), 60.98 (C-16), 41.64 (C-14), 33.75 (C-11), 21.63 (C-10), 14.48 (C-17). **IR** (KBr cm^{-1}): 3297 (N-H), 2915 (C-H), 2805 (C-H), 1757 (C=O), 1711 (C=O), 1664 (C=O),1605 (C=C), 1315 (C=S),1171 (C-O). **HRMS** (ESI-TOF): m/z [M + H]$^+$ calculated for $C_{17}H_{19}N_3O_4S$: 362.4215; found: 362.1851.

5.6.6 (Z)-ethyl 2-(2-(4-(4-methylbenzylidene)-5-oxo-2-thioxoimidazolidin-1-yl)acetamido)propanoate (21f)

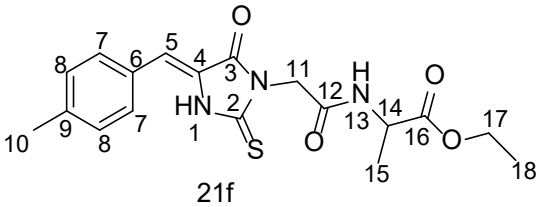

21f

A reaction of (Z)-5-(4-methylbenzylidene)-2-thioxoimidazolidin-4-one **22b** (0.5g, 2.29 mmol) and ethyl 2-(2-chloroacetamido)propanoate **23b** (0.44g, 2.29 mmol) gave compound **21f** as a yellow solid (0.43g, 49.79 %); m.p 203-205 °C; **^{1}H NMR (400 MHz, DMSO-d$_6$) δ$_H$** (ppm) 11.82 (s, 1H, H-1), 8.80 (d, *J* = 6.8 Hz, 1H, H-13), 8.08 (d, *J* = 7.8 Hz, 2H, H-7), 7.24 (d, *J* = 7.8 Hz, 2H, H-8), 6.74 (s, 1H, H-5), 4.28 (p, *J* = 6.9 Hz, 1H, H-14), 4.12 (s, 2H, H-11), 4.09 (m, *J* = 7.1 Hz, 2H, H-17), 2.35 (s, 3H, H-10), 1.30 (d, *J* = 7.2 Hz, 3H, H-15), 1.16 (t, *J* = 7.1 Hz, 3H, H-18). **^{13}C NMR (100 MHz, DMSO-d$_6$) δ$_C$** (ppm) 172.71 (C-16), 171.01 (C-2), 166.90 (C-12), 163.57 (C-3), 140.04 (C-4), 138.85 (C-9), 132.12 (C-7), 131.92 (C-6), 129.77 (C-8), 121.92 (C-5), 61.00 (C-17), 48.67 (C-14), 33.78 (C-11), 21.65 (C-10), 17.50 (C-15), 14.42 (C-18). **IR** (KBr cm^{-1}): 3310 (N-H), 2975 (C-H), 2840 (C-H), 1732 (C=O), 1708 (C=O), 1640 (C=O),1603 (C=C), 1273 (C=S),1190 (C-O). **HRMS** (ESI-TOF): m/z [M + H]$^+$ calculated for $C_{18}H_{21}N_3O_4S$: 376.1252; found: 376.1321.

5.6.7 (Z)-ethyl 2-(2-(4-(4-methylbenzylidene)-5-oxo-2-thioxoimidazolidin-1-yl)acetamido)butanoate (21g)

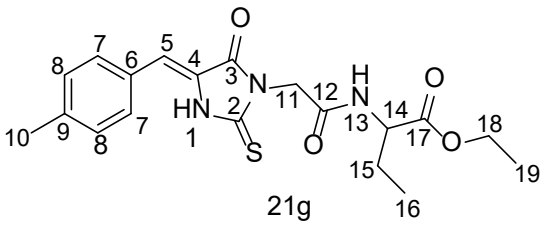

21g

A reaction of (Z)-5-(4-methylbenzylidene)-2-thioxoimidazolidin-4-one **22b** (0.5g, 2.29 mmol) and ethyl 2-(2-chloroacetamido)butanoate **23c** (0.48g, 2.29 mmol) gave compound **21g** as a brown solid (0.61g, 69.22%); m.p 167-169 °C; **^{1}H NMR (400 MHz, DMSO-d$_6$) δ$_H$** (ppm) 11.85 (s, 1H,H-1), 8.72 (d, *J* = 7.4 Hz, 1H, H-13), 8.07 (d, *J* = 8.1 Hz, 1H, H-7), 7.24 (d, *J* = 8.1 Hz, 2H, H-8), 6.73 (s, 1H, H-5), 4.19 (q, *J* = 7.9 Hz, 1H, H-14), 4.15 (s, 2H, H-11), 4.07 (q, *J* = 5.2 Hz, 2H, H-18), 2.34 (s, 3H, H-10), 1.83 – 1.52 (m, 2H, H-15), 1.20 (t, *J* = 7.3 Hz, 3H, H-19), 0.85 (t, *J* = 7.4 Hz, 3H, H-16). **^{13}C NMR (100 MHz, DMSO-d$_6$) δ$_C$** (ppm) 172.08 (C-17), 170.98 (C-2), 167.21 (C-12), 163.61 (C-3), 140.02 (C-4), 138.82 (C-9), 132.12 (C-7), 131.90 (C-6), 129.76 (C-8), 121.93 (C-5), 60.95 (C-18), 54.32 (C-14), 33.72 (C-11), 24.88 (C-15), 21.66 (C-10), 14.48 (C-16), 10.57 (C-19). **IR** (KBr cm^{-1}): 3021 (N-H), 2896 (C-H), 2810 (C-H), 1724 (C=O), 1650 (C=O), 1598 (C=O),1476 (C=C), 1229 (C=S),1155 (C-O). **HRMS** (ESI-TOF): m/z [M + H]$^+$ calculated for $C_{19}H_{23}N_3O_4S$: 390.1426; found: 390.1473.

5.6.8 (Z)-ethyl 3-methyl-2-(2-(4-(4-methylbenzylidene)-5-oxo-2-thioxoimidazolidin-1-yl)acetamido)butanoate (21h)

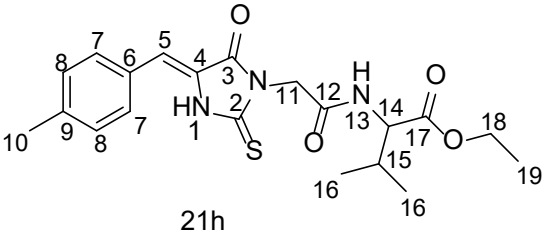

21h

A reaction of (Z)-5-(4-methylbenzylidene)-2-thioxoimidazolidin-4-one **22b** (0.5g, 2.29 mmol) and ethyl 2-(2-chloroacetamido)-3-methylbutanoate **23d** (0.51g, 2.29 mmol) gave compound **21h** as a white solid (0.54g, 58.94%); m.p 208-210 °C; **^{1}H NMR (400 MHz, DMSO-d$_6$) δ$_H$** (ppm) 11.83 (s, 1H, H-1), 8.57 (d, *J* = 8.2 Hz, 1H, H-13), 8.07 (d, *J* = 7.8 Hz, 2H, H-7), 7.24 (d, *J* = 7.9 Hz, 2H, H-8), 6.74 (s, 1H, H-5), 4.23 (t, *J* = 4.4 Hz, 1H), 4.20 (s, 2H, H-11), 4.08 (q, *J* = 6.2 Hz, 2H, H-18), 2.34 (s, 3H, H-10), 2.04 (m, 1H, H-15), 1.16 (t, *J* = 7.1 Hz, 3H, H-19), 0.86 (d, *J* = 6.8 Hz, 6H, H-16). **^{13}C NMR**

(100 MHz, DMSO-d$_6$) δc (ppm) 171.61 (C-17), 171.00 (C-2), 167.42 (C-12), 163.68 (C-3), 140.02 (C-4), 138.81 (C-9), 132.10 (C-7), 131.88 (C-6), 129.78 (C-8), 121.99 (C-5), 60.92 (C-18), 58.28 (C-14), 33.66 (C-11), 30.56 (C-15), 21.65 (C-10), 19.28 (C-16), 18.49 (C-16), 14.50 (C-19). **IR** (KBr cm^{-1}): 3280 (N-H), 2965 (C-H), 2820 (C-H), 1736 (C=O), 1699 (C=O), 1673 (C=O),1555 (C=C), 1271 (C=S),1175 (C-O). **HRMS** (ESI-TOF): m/z [M + H]$^+$ calculated for $C_{20}H_{24}N_3O_4S$: 404.1565; found: 404.1630.

5.6.9 (Z)-ethyl 2-(2-(4-(4-methylbenzylidene)-5-oxo-2-thioxoimidazolidin-1-yl)acetamido)pentanoate (21i)

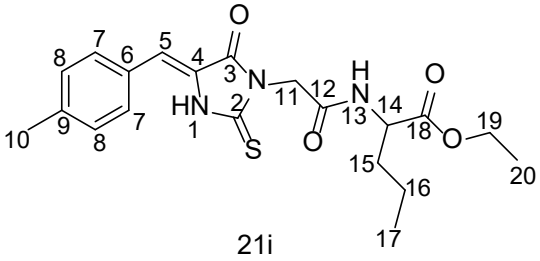

21i

A reaction of (Z)-5-(4-methylbenzylidene)-2-thioxoimidazolidin-4-one **22b** (0.5g, 2.29 mmol) and ethyl 2-(2-chloroacetamido)pentanoate **23e** (0.51g, 2.29 mmol) gave compound **21i** as a white solid solid (0.72g, 78.31 %); m.p 201-203 ^{o}C; **^{1}H NMR (400 MHz, DMSO-d$_6$) δH** (ppm) 11.83 (s, 1H, H-1), 8.69 (d, *J* = 7.5 Hz, 1H, H-13), 8.07 (d, *J* = 7.8 Hz, 2H, H-7), 7.24 (d, *J* = 7.9 Hz, 2H, H-8), 6.73 (s, 1H, H-5), 4.24 (q, *J* = 7.7 Hz, 1H, H-14), 4.18 (s, 2H, H-11), 4.07 (q, *J* = 4.7 Hz, 2H, H-19), 2.34 (s, 2H, H-10), 1.73 – 1.48 (m, 2H, H-15), 1.31-1.29 (m, 3H, H-16), 1.15 (t, *J* = 7.1 Hz, 3H, H-20), 0.77 (t, *J* = 7.3 Hz, 3H, H-17). **^{13}C NMR (100 MHz, DMSO-d$_6$) δc** (ppm) 172.30 (C-18), 171.01 (C-2), 167.19 (C-12), 163.62 (C-3), 139.98 (C-4), 138.81 (C-9), 132.02 (C-7), 129.76 (C-8), 121.92 (C-5), 60.96 (C-19), 52.74 (C-14), 33.68 (C-11), 33.63 (C-15), 21.65 (C-10), 18.98 (C-16), 14.47 (C-20), 13.82 (C-17). **IR** (KBr cm^{-1}): 3302 (N-H), 2957 (C-H), 2921 (C-H), 1732 (C=O), 1709 (C=O), 1640 (C=O),1603 (C=C), 1284 (C=S), 1142 (C-O). **HRMS** (ESI-TOF): m/z [M + H]$^+$ calculated for $C_{20}H_{24}N_3O_4S$: 404.1565; found: 404.1630.

5.6.10 (Z)-ethyl 2-(2-(4-(4-fluorobenzylidene)-5-oxo-2-thioxoimidazolidin-1-yl)acetamido)acetate(21j)

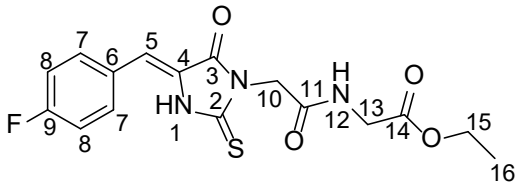

21j

A reaction of (Z)-5-(4-fluorobenzylidene)-2-thioxoimidazolidin-4-one **22e** (0.50g, 2.24 mmol) and ethyl 2-(2-chloroacetamido)acetate **23a** (0.40g, 2.24 mmol) gave compound **21j** as a yellow solid (0.55g, 68.89%); m.p 231-232 ^{o}C; **^{1}H NMR (400 MHz, DMSO-d$_6$) δ$_H$** (ppm) 11.86 (s, 1H, H-1), 8.80 (t, *J* = 5.6 Hz, 1H, H-12), 8.25 (dd, J_{HH} = 7.2 Hz, $^{4}J_{FH}$ 6.4 Hz Hz, 2H, H-7), 7.26 (t, J_{HH} = 8.4 Hz, $^{3}J_{FH}$ 17.2 Hz, 2H, H-8), 6.78 (s, 1H, H-5), 4.12 (s, 2H, H-10), 4.07 (q, *J* = 7.1 Hz, 1H, H-15), 3.91 (d, *J* = 5.7 Hz, 2H, H-13), 1.17 (t, *J* = 7.0 Hz, 3H, H-16). **^{13}C NMR (100 MHz, DMSO-d$_6$) δc** (ppm) 170.95 (C-2), 170.01 (C-14), 167.57 (C-11), 164.32 ($^{1}J_{FC}$ 258.0 Hz, C-9), 161.79 (C-3), 139.19 (C-4), 134.37 ($^{3}J_{FC}$ 8.0 Hz, C-7), 131.35 (C-6), 120.42 (C-5), 116.10 ($^{2}J_{FC}$ 8.0 Hz, C-8), 60.97 (C-15), 41.63 (C-13), 33.77 (C-10), 14.47 (C-16). **IR** (KBr cm^{-1}): 3279 (N-H), 2920 (C-H), 2852 (C-H), 1749 (C=O), 1709 (C=O), 1662 (C=O),1597 (C=C), 1220 (C=S), 1155 (C-O). **HRMS** (ESI-TOF): m/z [M + H]$^{+}$ calculated for $C_{16}H_{16}N_3O_4FS$: 366.0845; found: 366.0918.

5.6.11 (Z)-ethyl 2-(2-(4-(4-fluorobenzylidene)-5-oxo-2-thioxoimidazolidin-1-yl)acetamido)propanoate (21k)

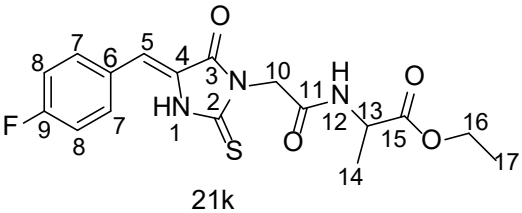

21k

A reaction of (Z)-5-(4-fluorobenzylidene)-2-thioxoimidazolidin-4-one **22e** (0.50g, 2.24 mmol) and ethyl 2-(2-chloroacetamido)propanoate **23b** (0.44g, 2.24 mmol) gave compound **21k** as a white solid (0.49g, 59.81%); m.p 222-224 ^{o}C; **^{1}H NMR (400 MHz, DMSO-d$_6$) δ$_H$** (ppm) 11.88 (s, 1H, H-1), 8.80 (d, *J* = 6.9 Hz, 1H, H-12), 8.36 (dd, J_{HH} = 7.6 Hz, $^{4}J_{FH}$ 6.4 Hz Hz, 2H, H-7), 7.25 (t, J_{HH} = 8.8 Hz, $^{3}J_{FH}$ 17.6 Hz, 2H, H-8), 6.78 (s, 1H, H-5), 4.28 (quintet, *J* = 7.1 Hz, 1H, H-13), 4.12 (s,2H, H-10), 4.06 (dd, *J* = 7.1, 3.8

Hz, 2H, H-16), 1.28 (d, *J* = 7.2 Hz, 3H, H-14), 1.15 (t, *J* = 7.1 Hz, 3H, H-17). **^{13}C NMR (100 MHz, DMSO-d$_6$) δ$_C$** (ppm) 172.72 (C-15), 170.93 (C-2), 166.85 (C-11), 164.35 ($^1J_{FC}$ 269.0 Hz, C-9), 161.76 (C-3), 139.21 (C-4), 134.41 ($^3J_{FC}$ 8.0 Hz, C-7), 131.38 (C-6), 120.37 (C-5), 116.09 ($^2J_{FC}$ 21.0 Hz, C-8), 60.99 (C-16), 48.65 (C-13), 33.81 (C-10), 17.51 (C-14), 14.41 (C-17). **IR** (KBr cm^{-1}): 3305 (N-H), 2922 (C-H), 2851 (C-H), 1746 (C=O), 1713 (C=O), 1643 (C=O),1597 (C=C), 1206 (C=S),1159 (C-O). **HRMS** (ESI-TOF): m/z [M + H]$^+$ calculated for $C_{17}H_{18}N_3O_4FS$: 380.1002; found: 380.1068.

5.6.12 (Z)-ethyl 2-(2-(4-(4-fluorobenzylidene)-5-oxo-2-thioxoimidazolidin-1-yl)acetamido)butanoate (21l)

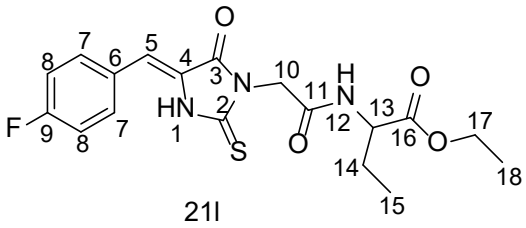

21l

A reaction of (Z)-5-(4-fluorobenzylidene)-2-thioxoimidazolidin-4-one **22e** (0.50g, 2.24 mmol) and ethyl 2-(2-chloroacetamido)butanoate **23c** (0.47g, 2.24 mmol) gave compound **21l** as a white solid (0.69g, 80.81%); m.p 209-211 ^{o}C; **^{1}H NMR (400 MHz, DMSO-d$_6$) δ$_H$** (ppm) 11.89 (s, 1H, H-1), 8.70 (d, *J* = 7.4 Hz, 1H, H-12), 8.53 (t, J_{HH} = 7.2 Hz, $^4J_{FH}$ 6.8 Hz, 2H, H-7), 7.25 (t, J_{HH} = 8.4 Hz, $^3J_{FH}$ 17.2 Hz, 2H, H-8), 6.78 (s, 1H, H-5), 4.20 (q, *J* = 8.4 Hz, 1H, H-13), 4.13 (s, 2H, H-10), 4.06 (q, *J* = 7.1 Hz, 2H, H-17), 1.89 – 1.46 (m, 2H, H-14), 1.15 (t, *J* = 7.1 Hz, 3H, H-18), 0.84 (t, *J* = 7.3 Hz, 3H, H-15). **^{13}C NMR (100 MHz, DMSO-d$_6$) δ$_C$** (ppm) 172.11 (C-2), 170.95 (C-16), 167.18 (C-11), 164.38 ($^1J_{FC}$ 248.0 Hz, C-9), 161.75 (C-3), 139.18 (C-4), 134.40 ($^3J_{FC}$ 8.0 Hz, C-7), 131.36 ($^3J_{FC}$ 3.0 Hz, C-6), 120.39 (C-5), 116.07 ($^2J_{FC}$ 21.0 Hz, C-8), 60.95 (C-17), 54.30 (C-13), 33.75 (C-10), 24.92 (C-14), 14.46 (C-18), 10.54 (C-15). **IR** (KBr cm^{-1}): 3303 (N-H), 2972 (C-H), 2852 (C-H), 1745 (C=O), 1711 (C=O), 1640 (C=O),1597 (C=C), 1292 (C=S),1159 (C-O). **HRMS** (ESI-TOF): m/z [M + H]$^+$ calculated for $C_{18}H_{20}N_3O_4FS$: 394.1158; found: 394.1224.

5.6.13 (Z)-ethyl 2-(2-(4-(4-fluorobenzylidene)-5-oxo-2-thioxoimidazolidin-1-yl)acetamido)-3-methylbutanoate (21m)

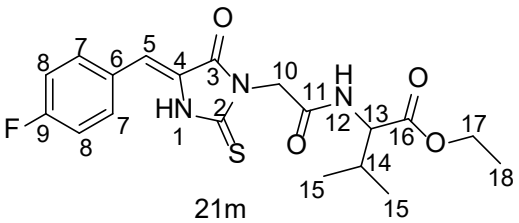

21m

A reaction of (Z)-5-(4-fluorobenzylidene)-2-thioxoimidazolidin-4-one **22e** (0.50g, 2.24 mmol) and ethyl 2-(2-chloroacetamido)-3-methylbutanoate **23d** (0.50g, 2.24 mmol) gave compound **21m** as a white solid (0.47g, 52.93%); m.p 175-177 ^{o}C; **^{1}H NMR (400 MHz, DMSO-d$_6$) δ$_H$** (ppm) 11.89 (s, 1H, H-1), 8.57 (d, *J* = 8.3 Hz, 1H, H-12), 8.38 (dd, J_{HH} = 7.2 Hz, $^{4}J_{FH}$ 6.8 Hz, 2H, H-7), 7.23 (dd, J_{HH} = 8.4 Hz, $^{3}J_{FH}$ 17.2 Hz, 2H, H-8), 6.78 (s, 1H, H-5), 4.23 (t, *J* = 4.3 Hz, 1H, H-13), 4.20 (s, 2H, H-10), 4.09 (q, *J* = 4.1 Hz, 2H, H-17), 2.03 (m, 1H, H-14), 1.15 (t, *J* = 7.0 Hz, 3H, H-18), 0.84 (d, *J* = 6.7 Hz, 6H, H-15). **^{13}C NMR (100 MHz, DMSO-d$_6$) δ$_C$** (ppm) 171.63 (C-17), 170.92 (C-2), 167.41 (C-11), 164.39 ($^{1}J_{FC}$ 248.0 Hz, C-9), 161.75 (C-3), 139.14 (C-4), 134.38 ($^{3}J_{FC}$ 8.0 Hz, C-7), 131.32 ($^{3}J_{FC}$ 3.0 Hz, C-6), 120.46 (C-5), 118.04 ($^{2}J_{FC}$ 22.0 Hz, C-8), 60.92 (C-17), 58.26 (C-13), 33.68 (C-10), 30.58 (C-14), 19.25 (C-15), 18.45 (C-15), 14.47 (C-18). **IR** (KBr cm^{-1}): 3259 (N-H), 2967 (C-H), 2885 (C-H), 1738 (C=O), 1715 (C=O), 1643 (C=O),1596 (C=C), 1307 (C=S), 1153 (C-O). **HRMS** (ESI-TOF): m/z [M + H]$^{+}$ calculated for $C_{19}H_{22}N_3O_4FS$: 408. 1303; found: 408.1384.

5.6.14 (Z)-ethyl 2-(2-(4-(4-fluorobenzylidene)-5-oxo-2-thioxoimidazolidin-1-yl)acetamido)pentanoate (21n)

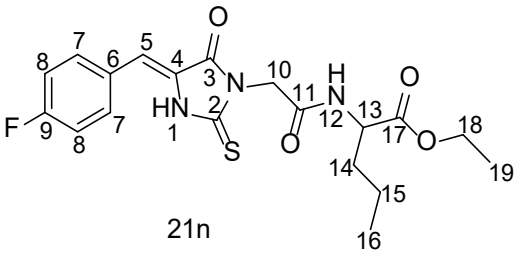

21n

A reaction of (Z)-5-(4-fluorobenzylidene)-2-thioxoimidazolidin-4-one **22e** (0.50g, 2.24 mmol) and ethyl 2-(2-chloroacetamido)pentanoate **23e** (0.50g, 2.24 mmol) gave compound **21n** as a white solid (0.65g, 72.51%); m.p 196-198 ^{o}C; **^{1}H NMR (400 MHz, DMSO-d$_6$) δ$_H$** (ppm) 11.73 (s, 1H, H-1), 8.71 (d, *J* = 7.5 Hz, 1H, H-12), 8.28 (dd, J_{HH} = 8.0 Hz, $^{4}J_{FH}$ 6.4 Hz Hz, 2H, H-7), 7.25 (dd, J_{HH} = 8.8 Hz, $^{3}J_{FH}$ 17.6 Hz, 2H, H-8), 6.79

(s, 1H, H-5), 4.26 (q, *J* = 7.9 Hz, 1H, H-13), 4.14 (s, 2H, H-10), 4.06 (q, *J* = 6.5 Hz, 2H, H-18), 1.94 – 1.47 (m, 2H, H-14), 1.34 – 1.21 (m, 2H, H-15), 1.16 (t, *J* = 7.2 Hz, 3H, H-19), 0.75 (t, *J* = 7.3 Hz, 3H, H-16). **^{13}C NMR (100 MHz, DMSO-d$_6$) δc** (ppm) 172.29 (C-17), 170.93 (C-2), 167.18 (C-11), 164.35 ($^{1}J_{FC}$ 247.0 Hz,C-9), 161.76 (C-3), 139.15 (C-4), 134.40 ($^{3}J_{FC}$ 8.0 Hz, C-7), 131.35 ($^{4}J_{FC}$ 3.0 Hz, C-6), 120.40 (C-5), 116.06 ($^{2}J_{FC}$ 21.0 Hz, C-8), 60.95 (C-18), 52.72 (C-13), 46.17 (14), 33.68 (C-10), 18.95 (C-15), 14.43 (C-19), 13.75 (C-16). **IR** (KBr cm^{-1}): 3286 (N-H), 2922 (C-H), 2852 (C-H), 1736 (C=O), 1711 (C=O), 1643 (C=O),1598 (C=C), 1269 (C=S), 1154 (C-O). **HRMS** (ESI-TOF): m/z [M + H]$^+$ calculated for $C_{19}H_{22}N_3O_4FS$: 408. 1303; found: 408.1384.

5.6.15 (Z)-ethyl 2-(2-(4-(4-methoxybenzylidene)-5-oxo-2-thioxoimidazolidin-1-yl)acetamido)acetate(21o)

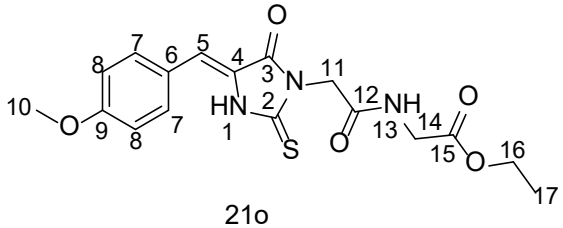

21o

A reaction of (Z)-5-(4-methoxybenzylidene)-2-thioxoimidazolidin-4-one **22d** (0.50g, 2.13 mmol) and ethyl 2-(2-chloroacetamido)acetate **23a** (0.38g, 2.13 mmol) gave compound **21o** as a yellow solid (0.38g, 47.51%); m.p 201-202 °C; **^{1}H NMR (400 MHz, DMSO) δH** 11.77 (s, 1H, H-1), 8.79 (t, *J* = 5.5 Hz, 1H, H-13), 8.15 (d, *J* = 8.4 Hz, 2H, H-7), 7.74 (d, *J* = 8.5 Hz, 2H, H-8), 6.74 (s, 1H, H-5), 4.12 (s, 2H, H-11), 4.10 (q, *J* = 5.7 Hz, 2H, H-16), 3.91 (d, *J* = 5.7 Hz, 2H, H-14), 3.81 (s, 3H, H-10), 1.17 (t, *J* = 7.1 Hz, 3H, H-17). **^{13}C NMR (101 MHz, DMSO) δc** (ppm) 171.02 (C-15), 170.00 (C-2), 167.65 (C-12), 162.43 (C-9), 160.94 (C-3), 137.74 (C-4), 133.98 (C-7), 127.29 (C-6), 122.07 (C-5), 114.83 (C-8), 60.98 (C-16), 55.80 (C-10), 41.65 (C-14), 33.72 (C-11), 14.47 (C-17). **IR** (KBr cm^{-1}): 3308 (N-H), 2979 (C-H), 2833 (C-H), 1759 (C=O), 1708 (C=O), 1662 (C=O),1598 (C=C), 1251 (C=S), 1164 (C-O). **HRMS** (ESI-TOF): m/z [M + H]$^+$ calculated for $C_{17}H_{19}N_3O_5S$: 378.1045; found: 378.1114.

5.6.16 (Z)-ethyl 2-(2-(4-(4-methoxybenzylidene)-5-oxo-2-thioxoimidazolidin-1-yl)acetamido)propanoate

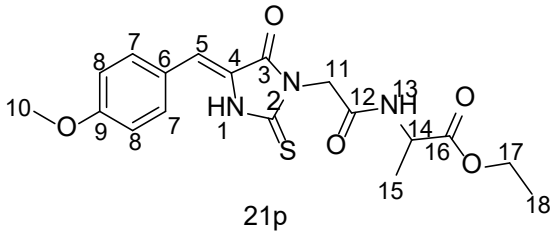

21p

A reaction of (Z)-5-(4-methoxybenzylidene)-2-thioxoimidazolidin-4-one **22d** (0.50g, 2.13 mmol) and ethyl 2-(2-chloroacetamido)propanoate **23b** (0.41g, 2.13 mmol) gave compound **21p** as a yellow solid (0.11g, 13.53%); m.p 174-176 °C; **^{1}H NMR (400 MHz, DMSO) δ_H** 11.77 (s, 1H, H-1), 8.81 (d, *J* = 6.8 Hz, 1H, H-13), 8.17 (d, *J* = 8.3 Hz, 2H, H-7), 6.99 (d, *J* = 8.3 Hz, 2H, H-8), 6.74 (s, 1H, H-5), 4.28 (quintet, *J* = 13.9, 6.9 Hz, 2H, H-14), 4.11 (s, 2H, H-11), 4.09 (q, *J* = 5.7 Hz, 2H, H-17), 3.82 (s, 3H, H-10), 1.15 (t, *J* = 7.0 Hz, 3H, H-18), 0.83 (d, *J* = 4.0 Hz, 3H, H-15). **^{13}C NMR (101 MHz, DMSO) δ_C** (ppm) 172.73 (C-16), 171.00 (C-2), 166.93 (C-12), 162.53 (C-9), 160.91 (C-3), 137.74 (C-4), 134.03 (C-7), 127.40 (C-6), 122.00 (C-5), 114.66 (C-8), 60.99 (C-17), 55.70 (C-14), 48.64 (C-10), 33.76 (C-11), 17.50 (C-15), 14.43 (C-18). **IR** (KBr cm^{-1}): 3285 (N-H), 2921 (C-H), 2851 (C-H), 1732 (C=O), 1708 (C=O), 1659 (C=O),1597 (C=C), 1254 (C=S), 1112 (C-O). **HRMS** (ESI-TOF): m/z [M + H]$^+$ calculated for $C_{18}H_{21}N_3O_5S$: 392.1209; found: 392.1267.

5.6.17 (Z)-ethyl 2-(2-(4-(4-methoxybenzylidene)-5-oxo-2-thioxoimidazolidin-1-yl)acetamido) butanoate (21q)

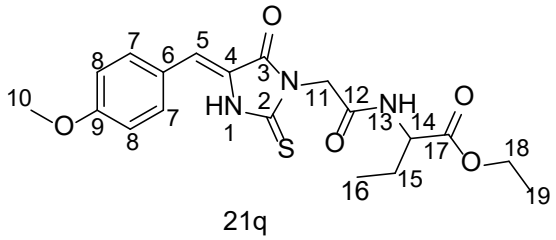

21q

A reaction of (Z)-5-(4-methoxybenzylidene)-2-thioxoimidazolidin-4-one **22d** (0.50g, 2.13 mmol) and ethyl 2-(2-chloroacetamido)butanoate **23c** (0.44g, 1 mmol) gave compound **21q** as a yellow solid (0.58g, 67.63%); m.p 162-164 °C; **^{1}H NMR (400 MHz, DMSO-d_6) δ_H** (ppm) 11.74 (s, 1H, H-1), 8.69 (d, *J* = 7.4 Hz, 1H, H-13), 8.16 (d, *J* = 8.3 Hz, 2H, H-7), 6.99 (d, *J* = 8.3 Hz, 2H, H-8), 6.74 (s, 1H, H-5), 4.20 (q, *J* = 5.8 Hz, 1H, H-13), 4.12 (s, 2H, H-11), 4.06 (q, *J* = 6.8 Hz, 2H, H-18), 3.81 (s, 3H, H-10),

1.80-1.68 (m, 2H, H-15), 1.15 (t, *J* = 7.1 Hz, 3H, H-19), 0.85 (t, *J* = 7.3 Hz, 3H, H-16). **^{13}C NMR (101 MHz, DMSO) δ_C** (ppm) 172.09 (C-17), 171.00 (C-2), 167.29 (C-12), 162.58 (C-9), 160.92 (C-3), 137.72 (C-4), 133.86 (C-7), 127.37 (C-6), 121.93 (C-5), 114.65 (C-8), 60.95 (C-18), 55.69 (C-14), 54.31 (C-10), 33.70 (C-11), 24.91 (C-15), 14.46 (C-19), 10.53 (C-16). **IR** (KBr cm^{-1}): 3306 (N-H), 2974 (C-H), 2901 (C-H), 1741 (C=O), 1707 (C=O), 1640 (C=O),1596 (C=C), 1251 (C=S),1139 (C-O). **HRMS** (ESI-TOF): m/z [M + H]$^+$ calculated for $C_{19}H_{23}N_3O_5S$: 406.1358; found: 406.1423.

5.6.18 (Z)-ethyl 2-(2-(4-(4-methoxybenzylidene)-5-oxo-2-thioxoimidazolidin-1-yl)acetamido)-3-methylbutanoate (21r)

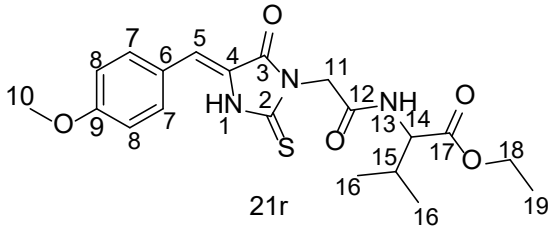

21r

A reaction of (Z)-5-(4-methoxybenzylidene)-2-thioxoimidazolidin-4-one **22d** (0.50g, 2.13 mmol) and ethyl 2-(2-chloroacetamido)-3-methylbutanoate **23d** (0.47g, 2.13 mmol) gave compound **21r** as a solid (0.55g, 61.59%); m.p 184-186 ^{o}C; **^{1}H NMR (400 MHz, DMSO) δ_H** 12.10 (s, 1H, H-1), 8.56 (d, *J* = 8.3 Hz, 1H, H-13), 8.15 (d, *J* = 8.6 Hz, 2H, H-7), 7.73 (d, *J* = 8.6 Hz, 2H, H-8), 6.74 (s, 1H, H-5), 4.21 (t, *J* = 8.5, 6.8 Hz, 1H, H-14), 4.15 (s, 2H, H-11), 4.08 (q, *J* = 9.8, 7.2 Hz, 2H, H-18), 3.81 (s, 3H, H-10), 1.15 (t, *J* = 7.0 Hz, 3H, H-19), 0.85 (d, *J* = 6.8 Hz, 6H, H-16). **^{13}C NMR (101 MHz, DMSO) δ_C** (ppm) 171.61 (C-17), 170.99 (C-2), 167.52 (C-12), 162.63 (C-9), 160.70 (C-3), 137.69 (C-4), 132.58 (C-7), 127.35 (C-6), 122.11 (C-5), 114.59 (C-8), 60.92 (C-18), 58.27 (C-14), 55.79 (C-10), 33.64 (C-11), 30.57 (C-15), 19.28 (C-16), 18.48 (C-16), 14.50 (C-19). **IR** (KBr cm^{-1}): 3198 (N-H), 2969 (C-H), 2891 (C-H), 1706 (C=O), 1630 (C=O), 1596 (C=O),1510 (C=C), 1226 (C=S),1167 (C-O). **HRMS** (ESI-TOF): m/z [M + H]$^+$ calculated for $C_{20}H_{25}N_3O_5S$: 420.1514; found: 420.1582.

5.6.19 (Z)-ethyl 2-(2-(4-(4-methoxybenzylidene)-5-oxo-2-thioxoimidazolidin-1-yl)acetamido)pentanoate(21s)

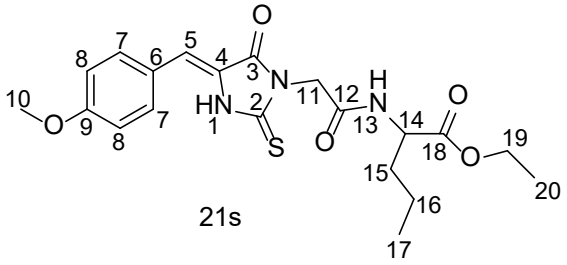

21s

A reaction of (Z)-5-(4-methoxybenzylidene)-2-thioxoimidazolidin-4-one **22d** (0.50g, 2.13 mmol) and ethyl 2-(2-chloroacetamido)pentanoate **23e** (0.47g, 2.13 mmol) gave compound **21s** as a yellow solid (0.43g, 48.05%); m.p 214-216 ^{o}C; **^{1}H NMR (400 MHz, DMSO-d$_6$) δ$_H$** (ppm) 12.01 (s, 1H, H-1), 8.68 (d, *J* = 7.5 Hz, 1H, H-13), 8.16 (d, *J* = 8.3 Hz, 2H, H-7), 7.74 (d, *J* = 8.3 Hz, 2H, H-8), 6.74 (s, 1H, H-5), 4.25 (q, *J* = 7.6 Hz, 1H, H-14), 4.14 (s, 2H, H-11), 4.07 (q, *J* = 5.2 Hz, 2H, H-19), 3.81 (s, 3H, H-10), 1.74 – 1.46 (m, 2H, H-15), 1.36 – 1.19 (m, 2H, H-16), 1.15 (t, *J* = 7.1 Hz, 3H, H-20), 0.76 (t, *J* = 7.2 Hz, 3H, H-17). **^{13}C NMR (101 MHz, DMSO) δ$_C$** (ppm) 172.30 (C-18), 171.00 (C-2), 167.28 (C-12), 162.55 (C-9), 160.92 (C-3), 137.69 (C-4), 134.01 (C-7), 127.37 (C-6), 122.07 (C-5), 114.66 (C-8), 60.96 (C-19), 55.83 (C-14), 52.73 (C-10), 46.31 (C-15), 33.63 (C-11), 18.96 (C-16), 14.45 (C-20), 13.81 (C-17). **IR** (KBr cm^{-1}): 3201 (N-H), 2962 (C-H), 2855 (C-H), 1707 (C=O), 1643 (C=O), 1597 (C=O),1505 (C=C), 1255 (C=S), 1167 (C-O). **HRMS** (ESI-TOF): m/z [M + H]$^{+}$ calculated for $C_{20}H_{25}N_3O_5S$: 420.1514; found: 420.1582.

5.6.20 (Z)-ethyl 2-(2-(4-(4-nitrobenzylidene)-5-oxo-2-thioxoimidazolidin-1-yl)acetamido)propanoate (21t)

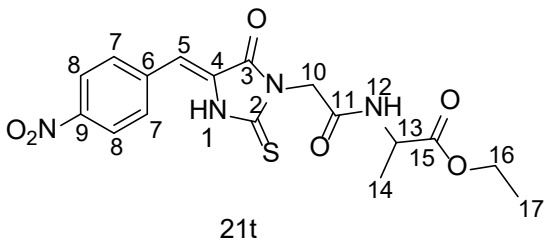

21t

A reaction of (Z)-5-(4-nitrobenzylidene)imidazolidine-2,4-dione **22f** (0.50g, 2.06 mmol) and ethyl 2-(2-chloroacetamido)propanoate **23b** (0.39g, 2.06 mmol) gave compound **21t** as a yellow solid (0.54g, 66.82%); m.p 232-234 ^{o}C; **^{1}H NMR (400 MHz, DMSO)**

δ_H 11.81 (s, 1H, H-1), 8.86 (d, *J* = 6.6 Hz, 1H, H-12), 8.45 (d, *J* = 8.1 Hz, 2H, H-7), 8.24 (d, *J* = 8.5 Hz, 2H, H-8), 6.85 (s, 1H, H-5), 4.35 – 4.24 (m, 1H), 4.15 (s, 2H, H-10), 4.06 (q, *J* = 6.6 Hz, 2H, H-16), 1.28 (d, *J* = 7.1 Hz, 3H, H-14), 1.19 (t, *J* = 8.0 Hz, 3H, H-17). **^{13}C NMR (101 MHz, DMSO) δ_c** (ppm) 172.42 (C-15), 170.29 (C-2), 167.19 (C-11), 166.56 (C-3), 146.87 (C-9), 142.11 (C-4), 141.24 (C-6), 132.41 (C-7), 122.99 (C-5), 117.47 (C-8), 60.16 (C-16), 48.70 (C-13), 33.84 (C-10), 17.55 (C-17), 14.40 (C-14). **IR** (KBr cm^{-1}): 3305 (N-H), 2920 (C-H), 2849 (C-H), 1750 (C=O), 1710 (C=O), 1650 (C=O), 1538 (C=C), 1305 (C=S),1150 (C-O). **HRMS** (ESI-TOF): m/z [M + H]$^+$ calculated for $C_{17}H_{18}N_4O_6S$: 407. 1409; found: 407. 1475.

5.6.21 (Z)-ethyl 2-(2-(4-(4-nitrobenzylidene)-5-oxo-2-thioxoimidazolidin-1-yl)acetamido)butanoate (21u)

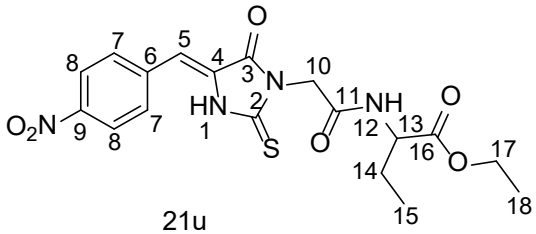

21u

A reaction of (Z)-5-(4-nitrobenzylidene)imidazolidine-2,4-dione **22f** (0.50g, 2.06 mmol) and ethyl 2-(2-chloroacetamido)butanoate **23c** (0.42g, 2.06 mmol) gave compound **21u** as a yellow solid (0.21g, 25.14%); m.p 237-239 ^{o}C; **^{1}H NMR (400 MHz, DMSO) δ_H** ^{1}H NMR (400 MHz, DMSO) δ 11.99 (s, 1H, H-1), 8.74 (d, *J* = 7.4 Hz, 1H, H-12), 8.45 (d, *J* = 8.3 Hz, 2H, H-7), 8.24 (d, *J* = 8.4 Hz, 2H, H-8), 6.85 (s, 1H, H-5), 4.26 (q, *J* = 8.0 Hz, 2H, H-17), 4.15 (q, *J* = 15.5 Hz, 1H, H-13), 4.12 (s, 2H, H-10), 1.86 – 1.38 (m, 2H, H-14), 1.14 (t, *J* = 7.1 Hz, 3H, H-18), 0.83 (t, *J* = 7.3 Hz, 3H, H-15). **^{13}C NMR (101 MHz, DMSO) δ_c** (ppm) ^{13}C NMR (101 MHz, DMSO) δ 172.12 (C-16), 170.72 (C-2), 167.70 (C-11), 167.03 (C-3), 147.18 (C-9), 142.10 (C-4), 141.37 (C-6), 132.71 (C-7), 123.98 (C-5), 117.99 (C-8), 60.97 (C-17), 54.32 (C-13), 33.97 (C-10), 24.97 (C-14), 14.46 (C-18), 10.54 (C-15). **IR** (KBr cm^{-1}): 3304 (N-H), 2980 (C-H), 2858 (C-H), 1739 (C=O), 1715 (C=O), 1651 (C=O),1505 (C=C), 1338 (C=S), 1181 (C-O). **HRMS** (ESI-TOF): m/z [M + H]$^+$ calculated for $C_{18}H_{20}N_4O_6S$: 421.1103; found: 421.1170.

5.6.22. (Z)-ethyl 2-(2-(4-(4-nitrobenzylidene)-5-oxo-2-thioxoimidazolidin-1-yl)acetamido)pentanoate (21v)

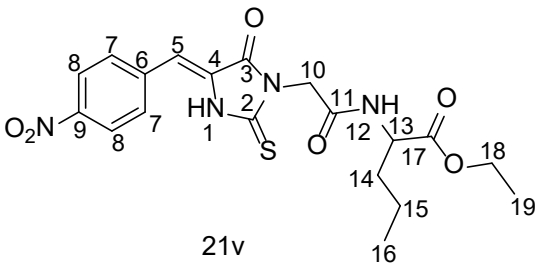

21v

A reaction of (Z)-5-(4-nitrobenzylidene)imidazolidine-2,4-dione **22f** (0.50g, 2.06 mmol) and ethyl 2-(2-chloroacetamido)pentanoate **23e** (0.44g, 2.06 mmol) gave compound **21v** as a yellow solid (0.53g, 61.50%); m.p 211-213 ^{o}C; **^{1}H NMR (400 MHz, DMSO) δ_H** 11.87 (s, 1H, H-1), 8.73 (d, *J* = 7.5 Hz, 1H, H-12), 8.43 (d, *J* = 8.6 Hz, 2H, H-7), 8.22 (d, *J* = 8.7 Hz, 2H, H-8), 6.82 (s, 1H, H-5), 4.33 (q, *J* = 8.1 Hz, 1H, H-13), 4.14 (s, 2H, H-10), 4.06 (q, *J* = 8.8 Hz, 2H, H-18), 1.79 – 1.46 (m, 2H, H-14), 1.34 – 1.19 (m, 2H, H-15), 1.13 (t, *J* = 7.1 Hz, 3H, H-19), 0.72 (t, *J* = 7.3 Hz, 3H, H-16). **^{13}C NMR (101 MHz, DMSO) δ_c** (ppm) 172.32 (C-17), 170.72 (C-2), 167.69 (C-11), 167.04 (C-3), 147.13 (C-9), 142.07 (C-4), 141.37 (C-6), 132.71 (C-7), 123.95 (C-5), 117.95 (C-8), 60.97 (C-18), 52.80 (C-13), 46.20 (C-10), 33.82 (C-14), 18.98 (C-15), 14.42 (C-19), 13.74 (C-16). **IR** (KBr cm^{-1}): 3109 (N-H), 2959 (C-H), 2916 (C-H), 1743 (C=O), 1714 (C=O), 1649 (C=O),1594 (C=C), 1337 (C=S), 1146 (C-O). **HRMS** (ESI-TOF): m/z [M + H]$^{+}$ calculated for $C_{19}H_{22}N_4O_6S$: 435.1260; found: 435.1324.

5.7 Biological assays

5.7.1 General in vitro α-glucosidase assay method

Saccharomyces cerevisiae α-glucosidase (50 μg/mL) and substrate (p-nitrophenyl glucopyranoside) were purchased from Sigma-Aldrich. Enzyme was prepared in potassium monobasic anhydrous phosphate buffer (pH 6.8, 3 mM), and reduced glutathione added prior the assays and the synthesized compounds and were dissolved in DMSO at a final concentration of 100 μM. Samples were sonicated if solubility was a problem and stored at 4°C until required. Sample concentrations tested were 65 and 130 μM. The various concentrations of compounds (10 μL), enzyme solution (20 μL), and potassium phosphate buffer (67 μL), were added in the 96-well plate and incubated at 37 °C for 10 min. Thereafter, the substrate (10 μL, 4 mM) was added to the mixture and allowed to incubate at 37 °C for 20 min followed

by the addition of sodium carbonate (25 µl). Eventually, the change in absorbance was measured by BioTek® PowerWave XS spectrophotometer (Winooski, VT, USA). Epigallacatechin gallate (EGCG) (200 µM) was used as control whereas error bars indicated the standard deviation of the mean.

REFERENCES

1. M Nath, K Bhattacharjee, Y Choudhury. Pleiotropic effects of anti-diabetic drugs: A comprehensive review. *European Journal of Pharmacology*. 2020; **884**:173349.

2. DJ Wexler. Patient education: Type 2 diabetes: Insulin treatment (Beyond the Basics). 2022. https://pro.uptodatefree.ir/Show/1737

3. J Dowarah, VP Singh. Anti-diabetic drugs recent approaches and advancements. *Bioorganic & medicinal chemistry*. 2020;**28**(5):115263.

4. CR Sagandira, AZ Khasipo, MB Sagandira, P Watts. An overview of the synthetic routes to essential oral anti-diabetes drugs. *Tetrahedron*. 2021;**96**:132378.

5. FJ Ndisang, A Vannacci, S Rastogi. Insulin resistance, type 1 and type 2 diabetes, and related complications. *Journal of diabetes research*. 2017. DOI:10.1155/2017/1478294

6. R Swaby, T Randell. Strategies for optimising blood glucose control in diabetes mellitus. *Paediatrics and Child Health*. 2021;**31**(4):146-152.

7. L Espinoza, CR Boychuk. Diabetes, and its treatment, as an effector of autonomic nervous system circuits and its functions. *Current Opinion in Pharmacology*. 2020;**54**:18-26.

8. V Siwan, SM Twigg, D Min. Alterations of CD163 expression in the complications of diabetes: A systematic review. *Journal of Diabetes and its Complications*. 2022:**108150**.

9. MS Rahman, KS Hossain, S Das, S Kundu, EO Adegoke, MA Rahman, MA Hannan, MJ Uddin, MG Pang. Role of insulin in health and disease: an update. *International Journal of Molecular Sciences*. 2021;**22**(12):6403.

10. SL Aronoff, K Berkowitz, B Shreiner, L Want. Glucose metabolism and regulation: beyond insulin and glucagon. *Diabetes spectrum*. 2004;**17**(3):183-190.

11. S Padhi, AK Nayak, A Behera. Type II diabetes mellitus: A review on recent drug-based therapeutics. *Biomedicine & Pharmacotherapy*. 2020;**131**:110708.

12. E Čolak, D Pap. The role of oxidative stress in the development of obesity and obesity-related metabolic disorders. *Journal of Medical Biochemistry*. 2021;**40**(1):1.

13. ML Aitken, MA Szkudlinska, EJ Boyko, KM Utzschneider, SE Kahn. Impaired counterregulatory responses to hypoglycaemia following oral glucose in adults with cystic fibrosis. Diabetologia. 2020;**63**(5):1055-1065.

14. J Ye, J Deng, W Liang, H Luo, W Mei, L Liu, M Wang, Y Shu. Time in range assessed by capillary blood glucose in relation to insulin sensitivity and β-cell function in patients with type 2 diabetes mellitus: A cross-sectional study in China. *Journal of Diabetes Investigation*. 2022; **13**(11). DOI: 10.1111/jdi.13876

15. AM Martin, EW Sun, DJ Keating. Mechanisms controlling hormone secretion in human gut and its relevance to metabolism. *Journal of Endocrinology*. 2020;**244**(1):1-5.

16. H Sun, P Saeedi, S Karuranga, M Pinkepank, K Ogurtsova, BB Duncan, C Stein, A Basit, JC Chan, JC Mbanya, ME Pavkov. IDF Diabetes Atlas: Global, regional and country-level diabetes prevalence estimates for 2021 and projections for 2045. *Diabetes research and clinical practice*. 2022;**183**:109119.

17. JC Chan, LL Lim, NJ Wareham, JE Shaw, TJ Orchard, P Zhang, ES Lau, B Eliasson, AP Kong, M Ezzati, CA Aguilar-Salinas. The Lancet Commission on diabetes: using data to transform diabetes care and patient lives. *The Lancet*. 2020;**396**(10267):2019-2082.

18. DJ Magliano, RM Islam, EL Barr, EW Gregg, ME Pavkov, JL Harding, M Tabesh, DN Koye, JE Shaw. Trends in incidence of total or type 2 diabetes: systematic review. *BMJ*. 2019;**366**. Doi: 10.1136/bmj.l5003

19. E Standl, K Khunti, TB Hansen, O Schnell. The global epidemics of diabetes in the 21st century: Current situation and perspectives. *European journal of preventive cardiology*. 2019;**26**(2):7-14.

20. D Glovaci, W Fan, ND Wong. Epidemiology of diabetes mellitus and cardiovascular disease. *Current cardiology reports*. 2019;**21**(4):1-8.

21. F Bahman, S Taurin. Inhalation of Insulin for Diabetes Management. *Nanotechnology for Diabetes Management*. 2022;**59**:165.

22. Stats SA. Mortality and causes of death in South Africa: Findings from death notification, 2015. https://www.statssa.gov.za

23. N Sahadew, VS Singaram. A diabetes profile of the eight districts in the public health sector, Eastern Cape Province, South Africa. *South African Medical Journal*. 2019;**109**(12):957-962.

24. V Pillay-van Wyk, W Msemburi, R Laubscher, RE Dorrington, P Groenewald, T Glass, B Nojilana, JD Joubert, R Matzopoulos, M Prinsloo, N Nannan. Mortality trends and differentials in South Africa from 1997 to 2012: second National Burden of Disease Study. *The Lancet Global Health*. 2016;**4**(9):e642-e653.

25. J Chiou, RJ Geusz, ML Okino, JY Han, M Miller, R Melton, E Beebe, P Benaglio, S Huang, K Korgaonkar, S Heller. Interpreting type 1 diabetes risk with genetics and single-cell epigenomics. *Nature*. 2021;**594**(7863):398-402.

26. JM Norris, RK Johnson, LC Stene. Type 1 diabetes—Early life origins and changing epidemiology. *The lancet Diabetes & endocrinology*. 2020;**8**(3):226-238.

27. M Mobasseri, M Shirmohammadi, T Amiri, N Vahed, HH Fard, M Ghojazadeh. Prevalence and incidence of type 1 diabetes in the world: a systematic review and meta-analysis. *Health promotion perspectives*. 2020;**10**(2):98.

28. J Lucier, RS Weinstock, C Doerr. Diabetes Mellitus Type 1 (Nursing). 2021.

29. N Chaudhary, N Tyagi. Diabetes mellitus: An Overview. *International Journal of Research and Development in Pharmacy & Life Sciences*. 2018;**7**(4):3030-3033.

30. AA Akil, E Yassin, A Al-Maraghi, E Aliyev, K Al-Malki, KA Fakhro. Diagnosis and treatment of type 1 diabetes at the dawn of the personalized medicine era. *Journal of Translational Medicine*. 2021;**19**(1):1-9.

31. EN Gurzov, PC Ke, U Ahlgren, RS Ribeiro, M Gotthardt. Novel strategies to protect and visualize pancreatic β cells in diabetes. *Trends in Endocrinology & Metabolism*. 2020;**31**(12):905-917.

32. KM Bullard, CC Cowie, SE Lessem, SH Saydah, A Menke, LS Geiss, TJ Orchard, DB Rolka, G Imperatore. Prevalence of diagnosed diabetes in adults by diabetes type—United States, 2016. *Morbidity and Mortality Weekly Report*. 2018;**67**(12):359.

33. E van Duinkerken, CM Ryan. Diabetes mellitus in the young and the old: Effects on cognitive functioning across the life span. *Neurobiology of disease*. 2020;**134**:104608.

34. N Esser, KM Utzschneider, SE Kahn. Early beta cell dysfunction vs insulin hypersecretion as the primary event in the pathogenesis of dysglycaemia. *Diabetologia*. 2020;**63**(10):2007-2021.

35. T Mezza, F Cinti, CM Cefalo, A Pontecorvi, RN Kulkarni, A Giaccari. β-cell fate in human insulin resistance and type 2 diabetes: a perspective on islet plasticity. *Diabetes*. 2019;**68**(6):1121-1129.

36. E Buttermore, V Campanella, R Priefer. The increasing trend of Type 2 diabetes in youth: An overview. Diabetes & Metabolic Syndrome: *Clinical Research & Reviews.* 2021;**15**(5):102253.

37. K Blaslov, FS Naranđa, I Kruljac, IP Renar. Treatment approach to type 2 diabetes: Past, present and future. *World journal of diabetes*. 2018;**9**(12):209.

38. H Ikegami, N Babaya, S Noso. β-Cell failure in diabetes: Common susceptibility and mechanisms shared between type 1 and type 2 diabetes. *Journal of Diabetes Investigation*. 2021;**12**(9):1526-1539.

39. M Roden, GI Shulman. The integrative biology of type 2 diabetes. *Nature*. 2019;**576**(7785):51-60.

40. N Javeed, AV Matveyenko. Circadian etiology of type 2 diabetes mellitus. *Physiology*. 2018;**33**(2):138-150.

41. GI Shulman. Ectopic fat in insulin resistance, dyslipidaemia, and cardiometabolic disease. *New England Journal of Medicine*. 2014;**371**(12):1131-1141.

42. RI Holt. Diagnosis, epidemiology and pathogenesis of diabetes mellitus: an update for psychiatrists. *The British Journal of Psychiatry*. 2004;**184**(S47):55-63.

43. CA Harper, K Smythe, VW Wong, ME Rollo, CE Collins. Comparison of pre-diagnosis dietary intake of women with gestational diabetes mellitus to dietary recommendations. *Midwifery*. 2021;**100**:103032.

44. H Wang, N Li, T Chivese, M Werfalli, H Sun, L Yuen, CA Hoegfeldt, CE Powe, J Immanuel, S Karuranga, H Divakar. IDF diabetes atlas: estimation of global and regional gestational diabetes mellitus prevalence for 2021 by International Association of Diabetes in Pregnancy Study Group's Criteria. *Diabetes Research and Clinical Practice*. 2022;**183**:109050.

45. MZ Banday, AS Sameer, S Nissar. Pathophysiology of diabetes: An overview. *Avicenna Journal of Medicine*. 2020;**10**(04):174-188.

46. N Vrachnis, P Belitsos, S Sifakis, K Dafopoulos, C Siristatidis, KI Pappa, Z Iliodromiti. Role of adipokines and other inflammatory mediators in gestational diabetes mellitus and previous gestational diabetes mellitus. *International journal of endocrinology*;2012. DOI: 10.1155/2012/549748

47. J Zhang, S Ma, C Guo, S Long, S Wu, H Tan. Research progress on etiology of gestational diabetes mellitus. *Global Health Journal*. 2018;**2**(4):19-27.

48. L Yuen, VW Wong. Gestational diabetes mellitus: challenges for different ethnic groups. *World journal of diabetes*. 2015;**6**(8):1024.

49. GB Bolli, F Porcellati, P Lucidi, CG Fanelli. The physiological basis of insulin therapy in people with diabetes mellitus. *Diabetes Research and Clinical Practice*. 2021;**175**:108839.

50. JA Dave, SV Delport. Prescribing insulin in type 1 diabetes mellitus: an update for general practitioners. *South African Family Practice*. 2006;**48**(10):30-33.

51. B Silver, K Ramaiya, SB Andrew, O Fredrick, S Bajaj, S Kalra, BM Charlotte, K Claudine, A Makhoba. EADSG guidelines: insulin therapy in diabetes. *Diabetes therapy*. 2018;**9**(2):449-492.

52. A Sow, D Boiro, PS Sow, B Niang, A Mbaye, AL Barrage, AL Fall, S Dieye, NF Sow, M Gueye, MN Mbaye. Insulin therapy in childhood type 1 diabetes: Knowledge and practice in Senegal. *Archives de Pédiatrie*. 2021;**28**(4):307-310.

53. GE Rayman, AN Lumb, B Kennon, C Cottrell, D Nagi, E Page, D Voigt, HC Courtney, H Atkins, J Platts, K Higgins. Dexamethasone therapy in COVID-19 patients: implications and guidance for the management of blood glucose in people with and without diabetes. *Diabetic Medicine*. 2021;**38**(1):14378

54. F Sousa, P Castro, P Fonte, B Sarmento. How to overcome the limitations of current insulin administration with new non-invasive delivery systems. *Therapeutic delivery*. 2015;**6**(1):83-94

55. RA Rabkin, GM Reaven, CE Mondon. Insulin metabolism by liver, muscle, and kidneys from spontaneously diabetic rats. *American Journal of Physiology-Endocrinology and Metabolism.* 1986;**250**(5):530-537.

56. A Cutruzzolà, M Parise, R Fiorentino, A Romano, V Molinaro, A Gnasso, S Di Molfetta, C Irace . The Effect of Two Different Insulin Formulations on Postprandial Hyperglycemia after High and Low Glycemic-Index Meal in Type 1 Diabetes. *Nutrients*. 2022;**14**(16):3316.

57. Better health channel, https://www.betterhealth.vic.gov.au./health/conditionsandtreatments/diabetes-and-insulin, (accessed November 2022)

58.Medical news today, https https://www.medicalnewstoday.com/articles/316674#types, (Accessed November 2022)

59. CE De Block, J Van Cauwenberghe, N Bochanen, E Dirinck. Rapid-acting insulin analogues: Theory and best clinical practice in type 1 and type 2 diabetes. *Diabetes, Obesity and Metabolism*. 2022;**24**:63-74

60. SJ Brink. Insulin Past, Present, and Future: 100 Years from Leonard Thompson. *Diabetology*. 2022;**3**(1):117-158.

61. HE Turner, DR Matthews. The use of fixed-mixture insulins in clinical practice. *European journal of clinical pharmacology*. 2000;**56**(1):19-25.

62. PF Frias, JP Frias. New basal insulins: a clinical perspective of their use in the treatment of type 2 diabetes and novel treatment options beyond basal insulin. *Current Diabetes Reports*. 2017;**17**(10):1-9.

63. AD Dahlén, G Dashi, I Maslov, MM Attwood, J Jonsson, V Trukhan, HB Schiöth. Trends in antidiabetic drug discovery: FDA approved drugs, new drugs in clinical trials and global sales. *Frontiers in pharmacology*. 2021;**12**:807548.

64. E Lazzaroni, MB Nasr, C Loretelli, I Pastore, L Plebani, ME Lunati, L Vallone, AM Bolla, A Rossi, L Montefusco, E Ippolito. Anti-diabetic drugs and weight loss in patients with type 2 diabetes. *Pharmacological Research*. 2021;**171**:105782.

65 . M Meneses, B Silva, M Sousa, R Sa, P Oliveira, GM Alves. Antidiabetic drugs: mechanisms of action and potential outcomes on cellular metabolism. *Current pharmaceutical design*. 2015;**21**(25):3606-3620.

66. O Grytsai, I Myrgorodska, S Rocchi, C Ronco, R Benhida. Biguanides drugs: past success stories and promising future for drug discovery. *European Journal of Medicinal Chemistry*. 2021;**224**:113726.

67. C Jose, A Pradhan, AR Shabaraya. A Review on Drug Related Problems in Type 2 DM with Combination of Sulfonylureas and Biguanides. *International Journal of Research and Review*. 2021;**8**:271-276

68. RA Maxson, EK McCoy. Noninsulin therapy for diabetes. *Physician Assistant Clinics*. 2020;**5**(2):153-165.

69. FA Al-Omary. Gliclazide. *In Profiles of Drug Substances, Excipients and Related Methodology* 2017;**42**:125-192.

70. D Lu, R Dopart, DA Kendall. Controlled downregulation of the cannabinoid CB1 receptor provides a promising approach for the treatment of obesity and obesity-derived type 2 diabetes. *Cell Stress and Chaperones*. 2016;**21**(1):1-7.

71. PM Sulis, BF Dambrós, A Mascarello, AR Dos Santos, RA Yunes, RJ Nunes, MJ Frederico, FR Barreto Silva. Sulfonyl (thio) urea derivative induction of insulin secretion is mediated by potassium, calcium, and sodium channel signal transduction. *Journal of Cellular Physiology*. 2019;**234**(7):10138-10147

72. S Tyagi, P Gupta, AS Saini, C Kaushal, S Sharma. The peroxisome proliferator-activated receptor: A family of nuclear receptors role in various diseases. *Journal of advanced pharmaceutical technology & research*. 2011;**2**(4):236.

73. MI Morja, PM Chauhan, KH Chikhalia. Iron catalyzed alkynylation of thiohydantoins with terminal alkyne via cross-dehydrogenative coupling (CDC). *Tetrahedron Letters*. 2021;**77**:153148.

74. PG de Carvalho, JM Ribeiro, RP Garbin, G Nakazato, SF Yamada Ogatta, Â de Fátima, M de Lima Ferreira Bispo, F Macedo. Synthesis and antimicrobial activity of thiohydantoins obtained from L-amino acids. *Letters in Drug Design & Discovery*. 2020;**17**(1):94-102.

75. S Jha, JD Silversides, RW Boyle, SJ Archibald. Hydrogen bonded dimers vs. one-dimensional chains in 2-thiooxoimidazolidin-4-one (thiohydantoin) drug derivatives. *CrystEngComm*. 2010;**12**(6):1730-1739.

76. V Deval, A Kumar, V Gupta, A Sharma, A Gupta, P Tandon, KK Kunimoto. Molecular structure (monomeric and dimeric) and hydrogen bonds in 5-benzyl 2-thiohydantoin studied by FT-IR and FT-Raman spectroscopy and DFT calculations. *Spectrochimica Acta Part A: Molecular and Biomolecular Spectroscopy.* 2014;**132**:15-26.

77. A Mezoughi, W Mohammed, ZO Ettarhouni. Recent biological applications and chemical synthesis of thiohydantoins. *Journal of Chemical Reviews*. 2021;**3**(3):196-218.

78. BT Gregg, KC Golden, JF Quinn, DO Tymoshenko, WG Earley, DA Maynard, DA Razzano, WM Rennells, J Butcher. Expedient Lewis acid catalyzed synthesis of a 3-substituted 5-arylidene-1-methyl-2-thiohydantoin library. *Journal of Combinatorial Chemistry*. 2007;**9**(06):1036-1040.

79. ME Jung, S Ouk, D Yoo, CL Sawyers, C Chen, C Tran, J Wongvipat. Structure− activity relationship for thiohydantoin androgen receptor antagonists for castration-resistant prostate cancer (CRPC). *Journal of medicinal chemistry*. 2010;**53**(7):2779-2796.

80. ME Kukushkin, NA Karpov, DE Shybanov, NV Zyk, EK Beloglazkina. A convenient synthesis of 3-aryl-5-methylidene-2-thiohydantoins. *Mendeleev Communications*. 2022;**32**(1):126-128.

81. S Reyes, K Burgess. On formation of thiohydantoins from amino acids under acylation conditions. *The Journal of Organic Chemistry*. 2006;**71**(6):2507-9.

82. ZD Wang, SO Sheikh, Y Zhang. A simple synthesis of 2-thiohydantoins. *Molecules*. 2006;**11**(10):739-750.

83. A Buchynskyy, JR Gillespie, ZM Herbst, RM Ranade, FS Buckner, MH Gelb. 1-Benzyl-3-aryl-2-thiohydantoin derivatives as new anti-Trypanosoma brucei agents: SAR and in vivo efficacy. *ACS medicinal chemistry letters*. 2017;**8**(8):886-891.

84. R Raj, J Gut, PJ Rosenthal, V Kumar. 1H-1, 2, 3-Triazole-tethered isatin-7-chloroquinoline and 3-hydroxy-indole-7-chloroquinoline conjugates: synthesis and antimalarial evaluation. *Bioorganic & Medicinal Chemistry Letters*. 2014;**24**(3):756-759.

85. K Kieć-Kononowicz, E Szymańska. Antimycobacterial activity of 5-arylidene derivatives of hydantoin. *Il Farmaco*. 2002;**57**(11):909-916.

86. J Han, H Dong, Z Xu, J Lei, M Wang. Facile synthesis of 5-arylidene thiohydantoin by sequential sulfonylation/desulfination reaction. *International journal of molecular sciences*. 2013;**14**(6):12484-12495.

87. Khirallah SM, Ramadan HM, Aladl HA, Ayaz NO, Kurdi LA, Jaremko M, Alshawwa SZ, Saied EM. Antidiabetic potential of novel 1,3, 5-trisubstituted-2-thioxoimidazloidin-4-one analogues: insights into α-glucosidase, α-amylase and antioxidant activities. *Pharmaceuticals*. 2022;**15**(12):1576.

88. Bloomgarden ZT. Approaches to treatment of type 2 diabetes. *Diabetes Care*. 2008 ;**31**(8):1697.

89. Chakrabarti R, Rajagopalan R. Diabetes and insulin resistance associated disorders: Disease and the therapy. *Current science*. 2002:1533-8.

90. Martin AE, Montgomery PA. Acarbose: An α-glucosidase inhibitor. *American Journal of Health-System Pharmacy*. 1996;**53**(19):2277-90.

91. Khan MS, Munawar MA, Ashraf M, Alam U, Ata A, Asiri AM, Kousar S, Khan MA. Synthesis of novel indenoquinoxaline derivatives as potent α-glucosidase inhibitors. *Bioorganic & medicinal chemistry*. 2014;**22**(3):1195-200.

92. Li J, Sha Y. Aconvenient synthesis of amino acid methyl esters. *Molecules*. 2008;**13**(5):1111-9.

93. Shmatova OI, Shevchenko NE, Balenkova ES, Röschenthaler GV, Nenajdenko VG. Friedel–Crafts alkylation of natural amino acid-derived pyrroles with CF3-substituted cyclic imines. *Mendeleev Communications*. 2013;**2**(23):92-3.

94. Tropiano M, Blackburn OA, Tilney JA, Hill LR, Placidi MP, Aarons RJ, Sykes D, Jones MW, Kenwright AM, Snaith JS, Sørensen TJ. Using remote substituents to control solution structure and anion binding in lanthanide complexes. *Chemistry–A European Journal*. 2013;**19**(49):16566-71.

95. Burgy G, Tahtouh T, Durieu E, Foll-Josselin B, Limanton E, Meijer L, Carreaux F, Bazureau JP. Chemical synthesis and biological validation of immobilized protein kinase inhibitory Leucettines. European Journal of Medicinal Chemistry. 2013;**62**:728-37.

96. Zaitseva ER, Smirnov AY, Mishin AS, Baranov MS. Synthesis and Optical Properties of the New Acetylene Kaede Chromophore Analog. *Russian Journal of Bioorganic Chemistry.* 2020;**46**:458-61.

97. Brun E, Safer A, Carreaux F, Bourahla K, L'helgoua'ch JM, Bazureau JP, Villalgordo JM. Microwave-assisted condensation reactions of acetophenone derivatives and activated methylene compounds with aldehydes catalyzed by boric acid under solvent-free conditions. *Molecules*. 2015;**20**(6):11617-31.

98. Kaczor A, Szemerédi N, Kucwaj-Brysz K, Dąbrowska M, Starek M, Latacz G, Spengler G, Handzlik J. Computer-aided search for 5-arylideneimidazolone anticancer agents able to overcome ABCB1-based multidrug resistance. *ChemMedChem*. 2021;**16**(15):2386-401.

99. Singh V, Singh A, Singh G, Verma RK, Mall R. Benzoxazolyl linked benzylidene based rhodanine and analogs as novel antidiabetic agents: synthesis, molecular docking, and in vitro studies. *Medicinal Chemistry Research*. 2021;**30**(10):1905-14.

100. AAmmar Y, AM Sh El-Sharief M, M Ghorab M, A Mohamed Y, Ragab A, Y Abbas S. New imidazolidineiminothione, imidazolidin-2-one and imidazoquinoxaline derivatives: Synthesis and evaluation of antibacterial and antifungal activities. *Current Organic Synthesis*. 2016 ;**13**(3):466-75.

101. Gawas PP, Bora A, Reji RP, Cb SK, Ramakrishna B, Nalluri V, Jayaraman SV, Sivalingam Y, Nutalapati V. Tuning the π-Conjugation of 2-Thiohydantoins toward a Rigorously Defined Detection of Volatile Organic Compounds by Surface Photovoltage. *ACS Applied Electronic Materials*. 2022;**4**(5):2313-25.

102. Tundis R, Loizzo MR, Menichini F. Natural products as α-amylase and α-glucosidase inhibitors and their hypoglycaemic potential in the treatment of diabetes: an update. *Mini reviews in medicinal chemistry*. 2010;**10**(4):315-31.

103. Roskar I, Molek P, Vodnik M, Stempelj M, Strukelj B, Lunder M. Peptide modulators of alpha-glucosidase. *Journal of Diabetes Investigation*. 2015;**6**(6):625-31.

104. Rose DR, Chaudet MM, Jones K. Structural studies of the intestinal α-glucosidases, maltase-glucoamylase and sucrase-isomaltase. *Journal of pediatric gastroenterology and nutrition*. 2018;**66**:S11-3.

Appendix

Selected ^{1}H, ^{13}C, dept NMR, IR spectra and biological assays charts

A1: ^{1}H and ^{13}C NMR spectra of ethyl 2-(2-chloroacetamido)butanoate

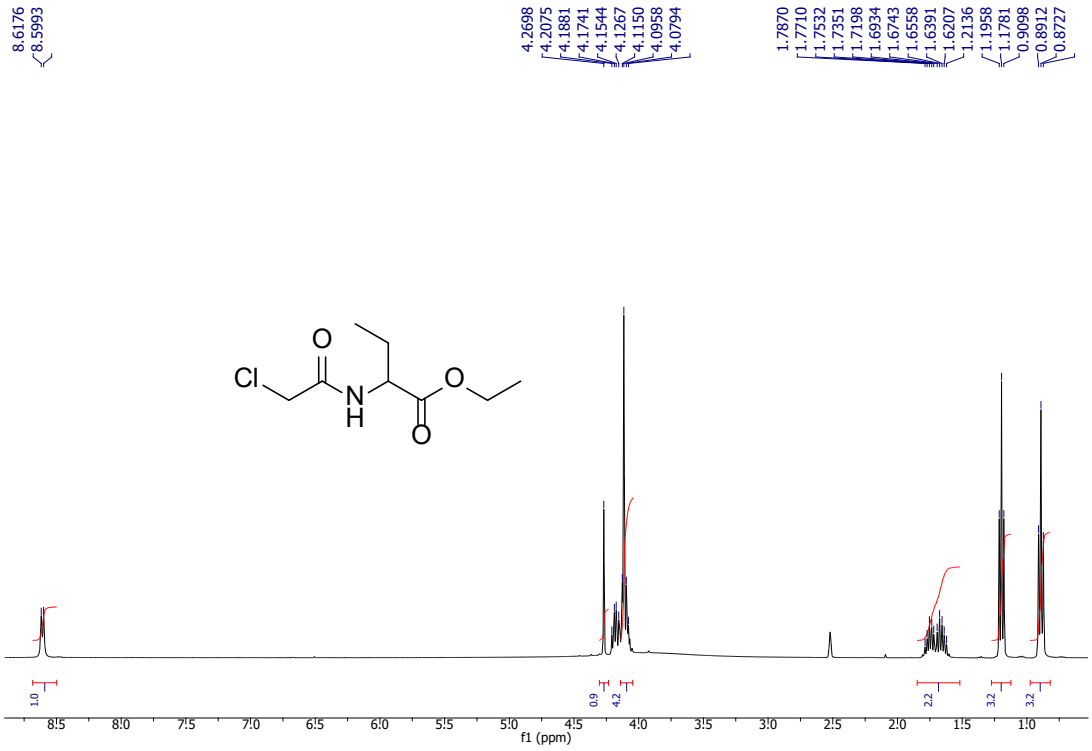

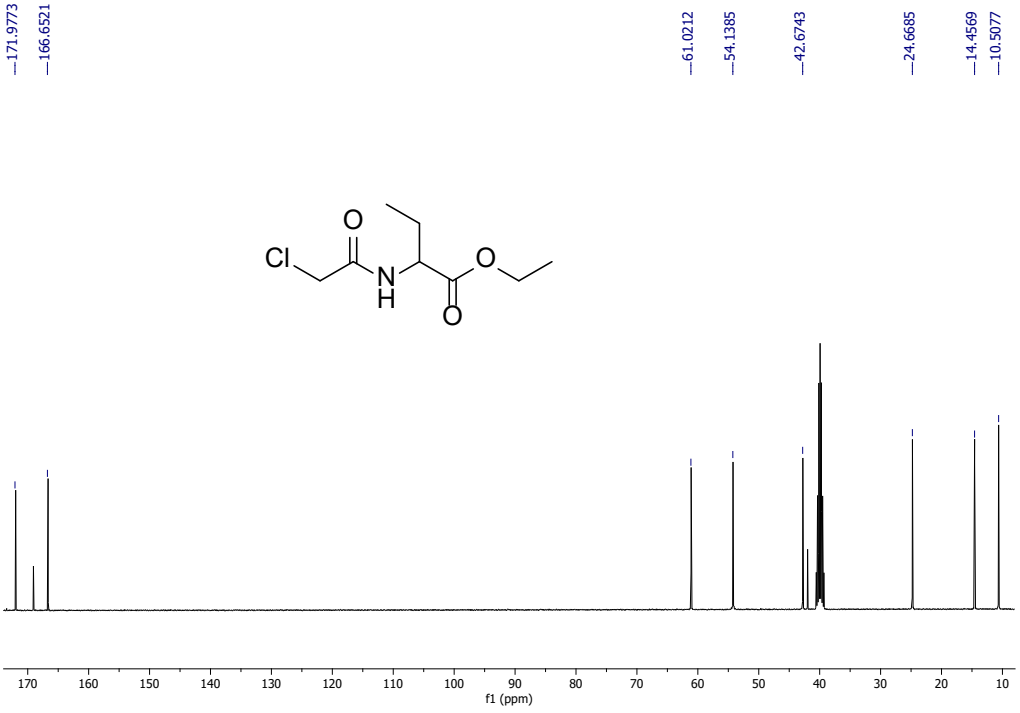

A2: ^{1}H and ^{13}C NMR of 2-thiohydantoin

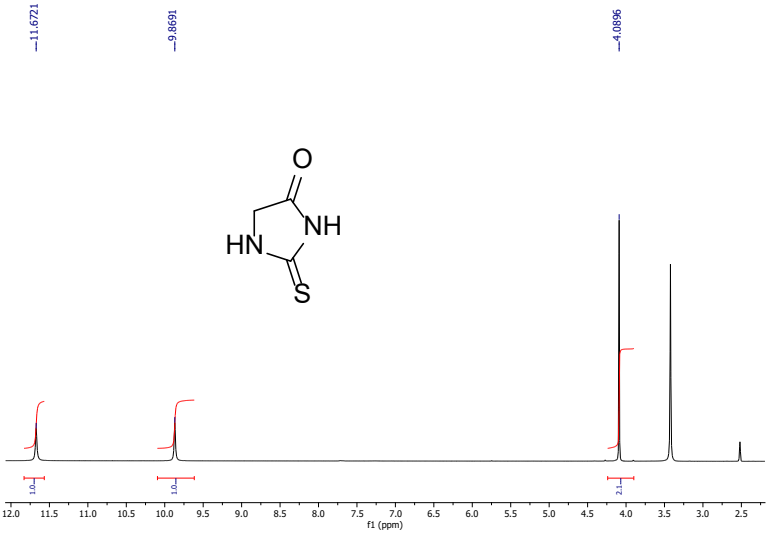

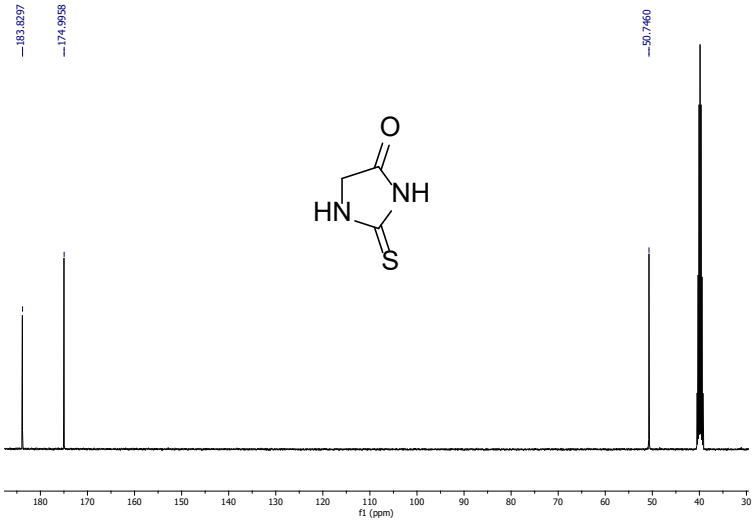

A3: ^{1}H and ^{13}C NMR of (Z)-5-(4-methylbenzylidene)-2-thioxoimidazolidin-4-one

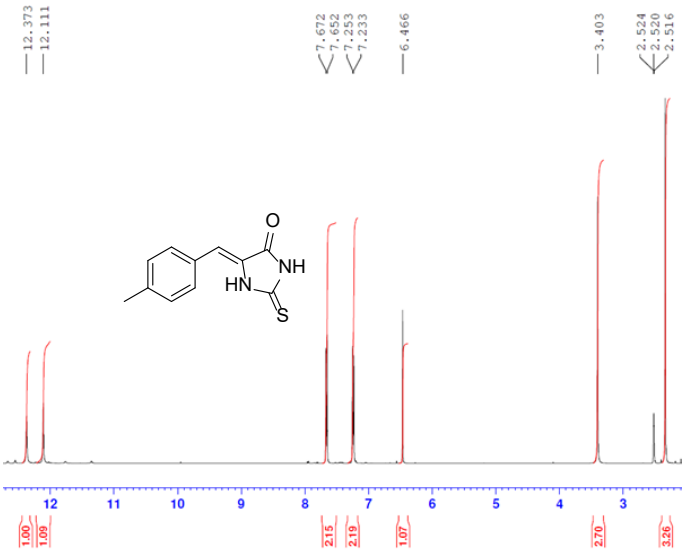

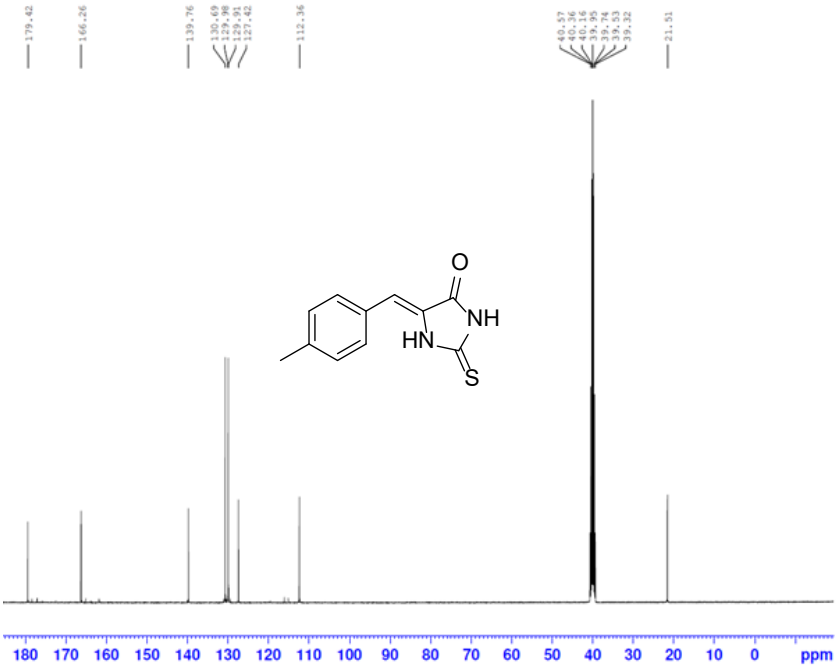

A4: Dept 135 NMR and IR spectra

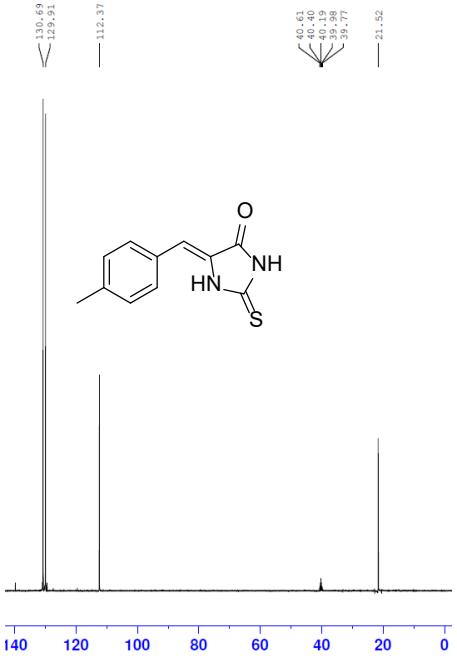

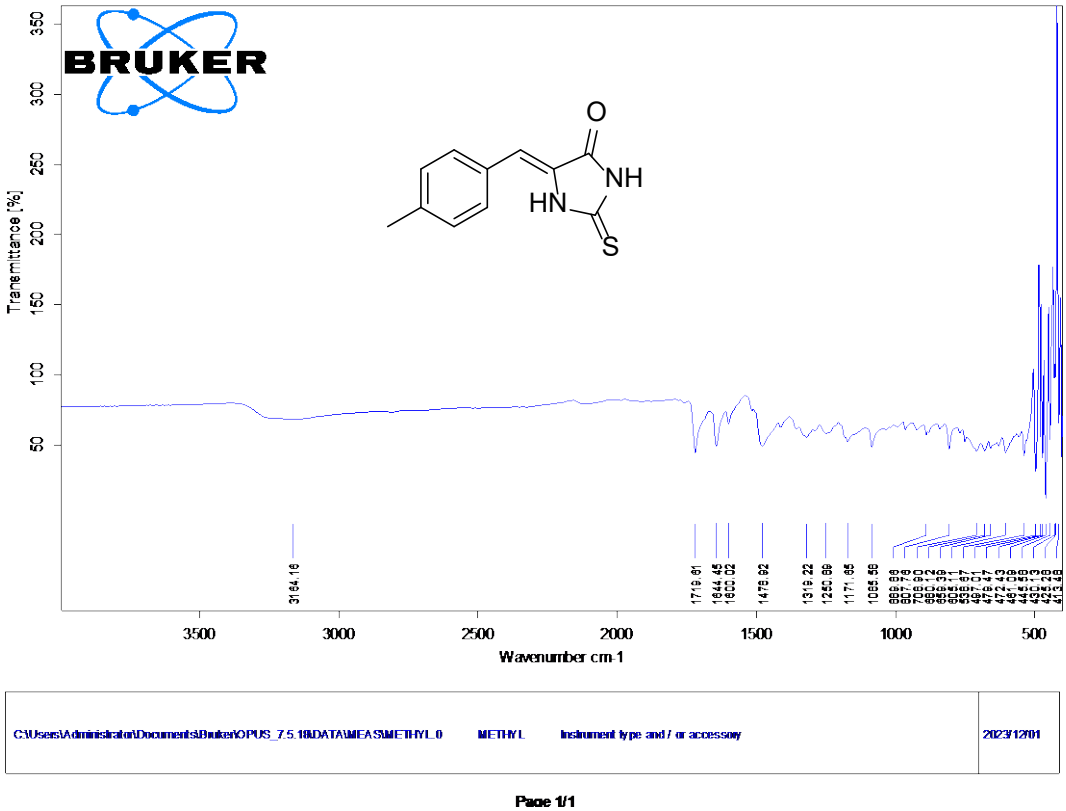

C:\Users\Administrator\Documents\Bruker\OPUS_7.5.18\DATA\MEAS\METHYL.0 METHYL Instrument type and / or accessory 2023/12/01

Page 1/1

A5: ^{1}H and ^{13}C NMR spectra of (Z)-5-(4-hydroxybenzylidene)-2-thioxoimidazolidin-4-one

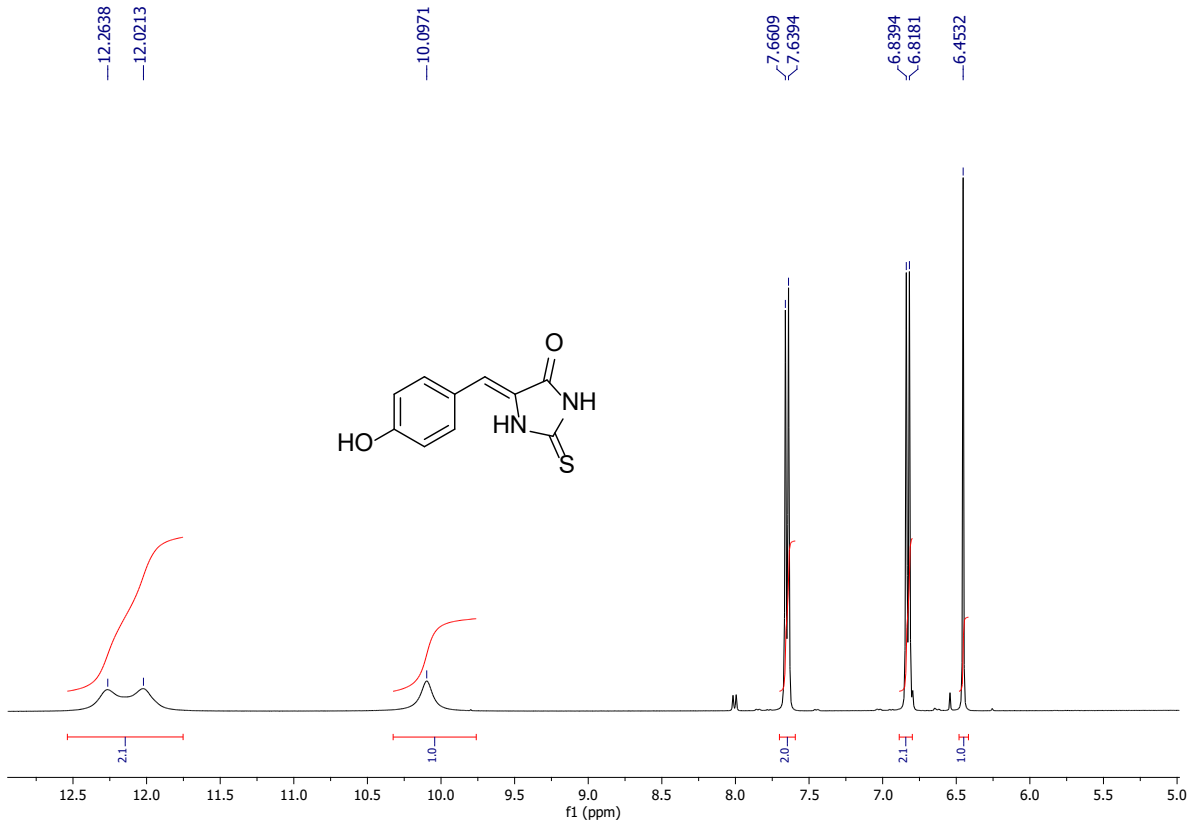

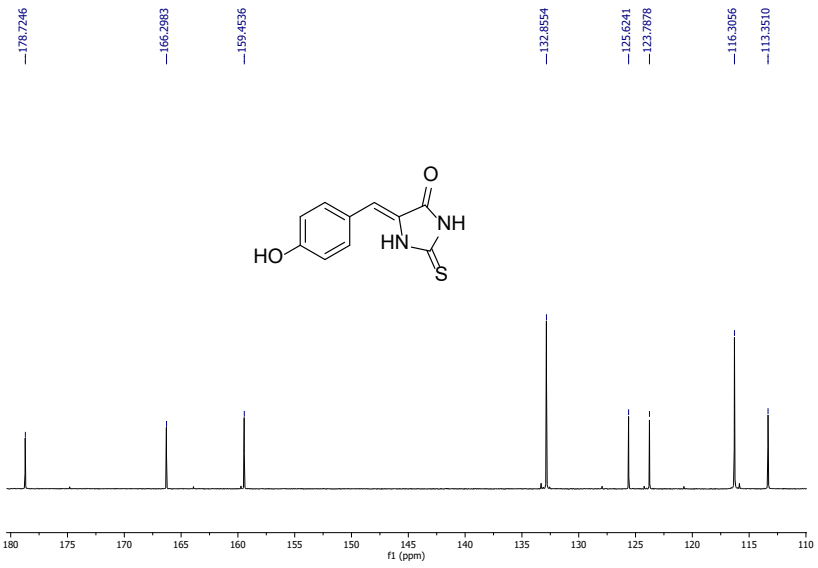

A6: dept 135 NMR and IR spectra of (Z)-5-(4-hydroxybenzylidene)-2-thioxoimidazolidin-4-one

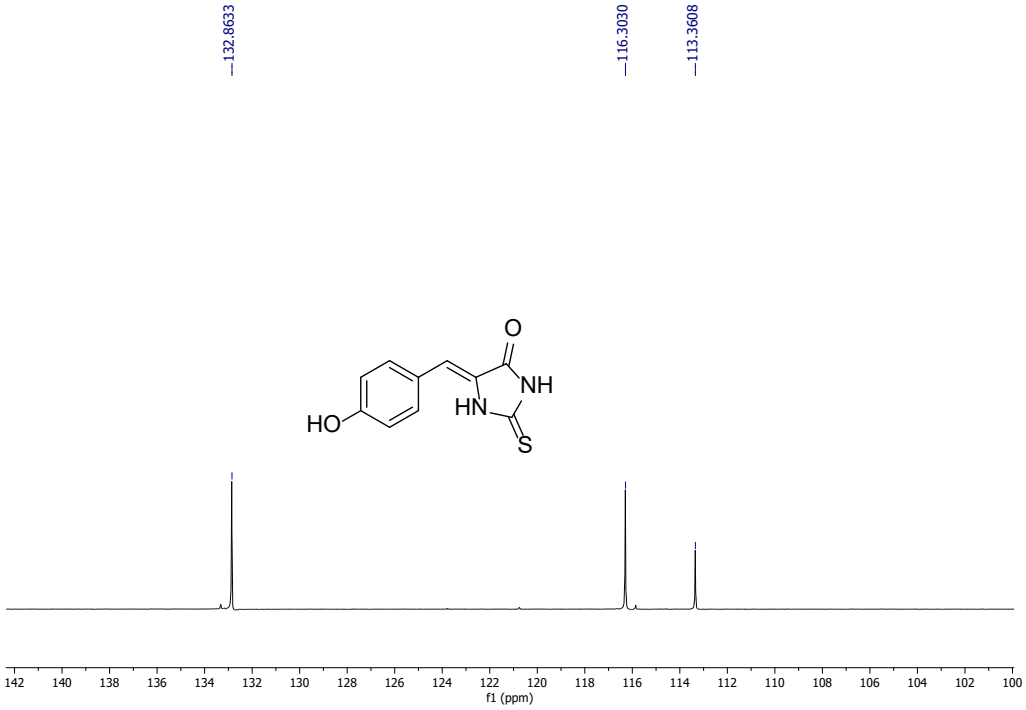

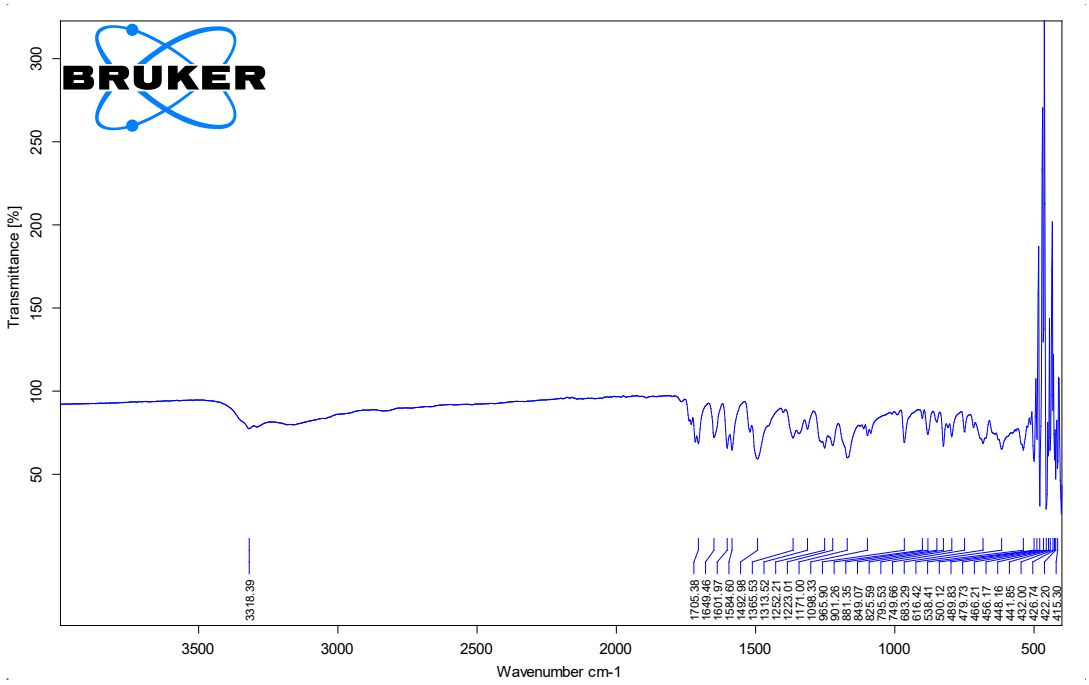

C:\Users\Administrator\Documents\Bruker\OPUS_7.5.18\DATA\MEAS\UTA-95-1.0	UTA-95-1	Instrument type and / or accessory	2023/12/01

Page 1/1

A7: ^{1}H and ^{13}C NMR spectra of (Z)-ethyl 2-(2-(4-(4-methoxybenzylidene)-5-oxo-2-thioxoimidazolidin-1-yl)acetamido)butanoate

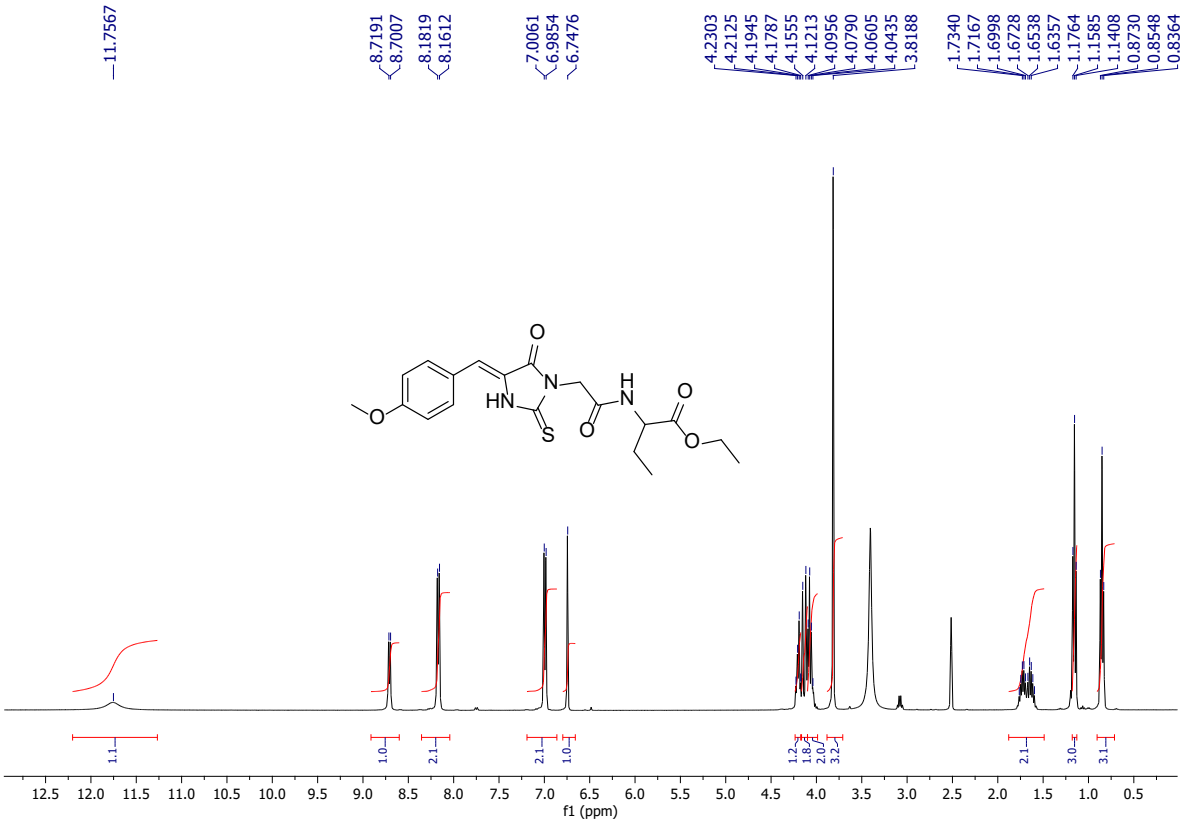

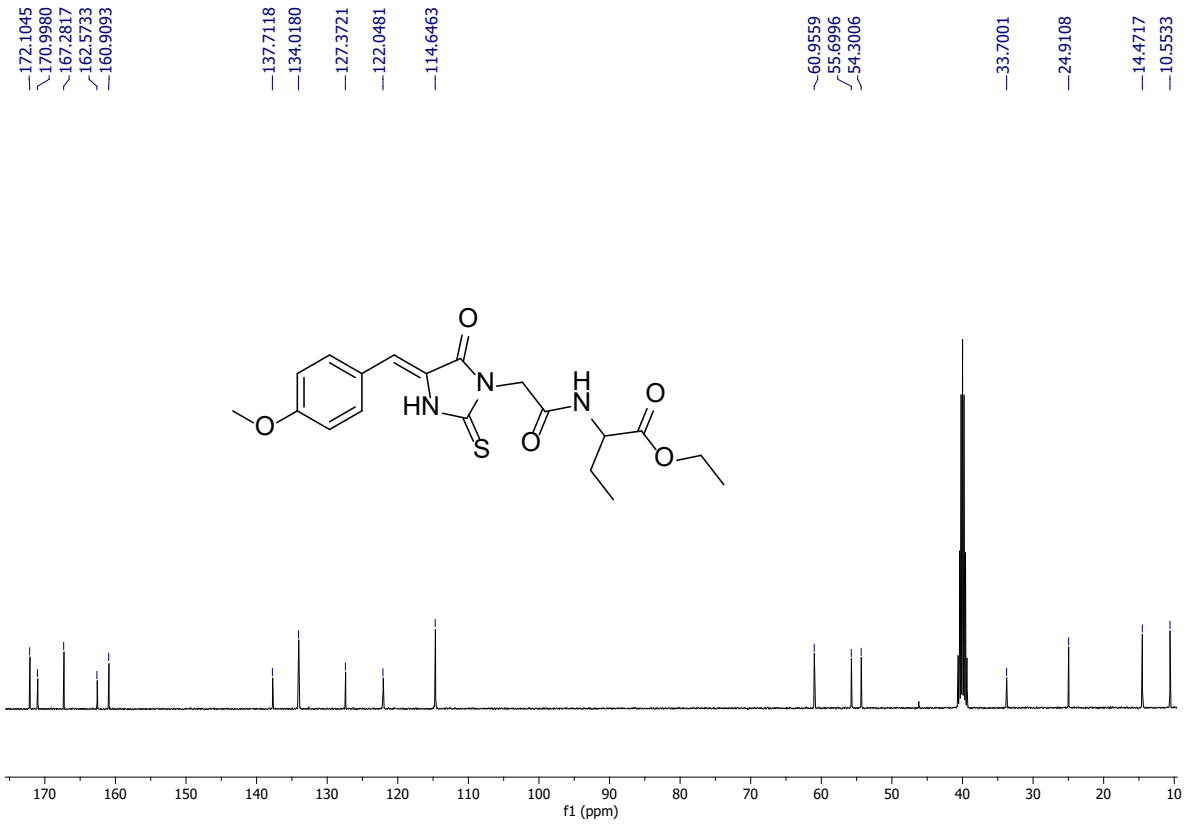

A8: Dept 135 NMR and IR Spectra of (Z)-ethyl 2-(2-(4-(4-methoxybenzylidene)-5-oxo-2-thioxoimidazolidin-1-yl)acetamido)butanoate

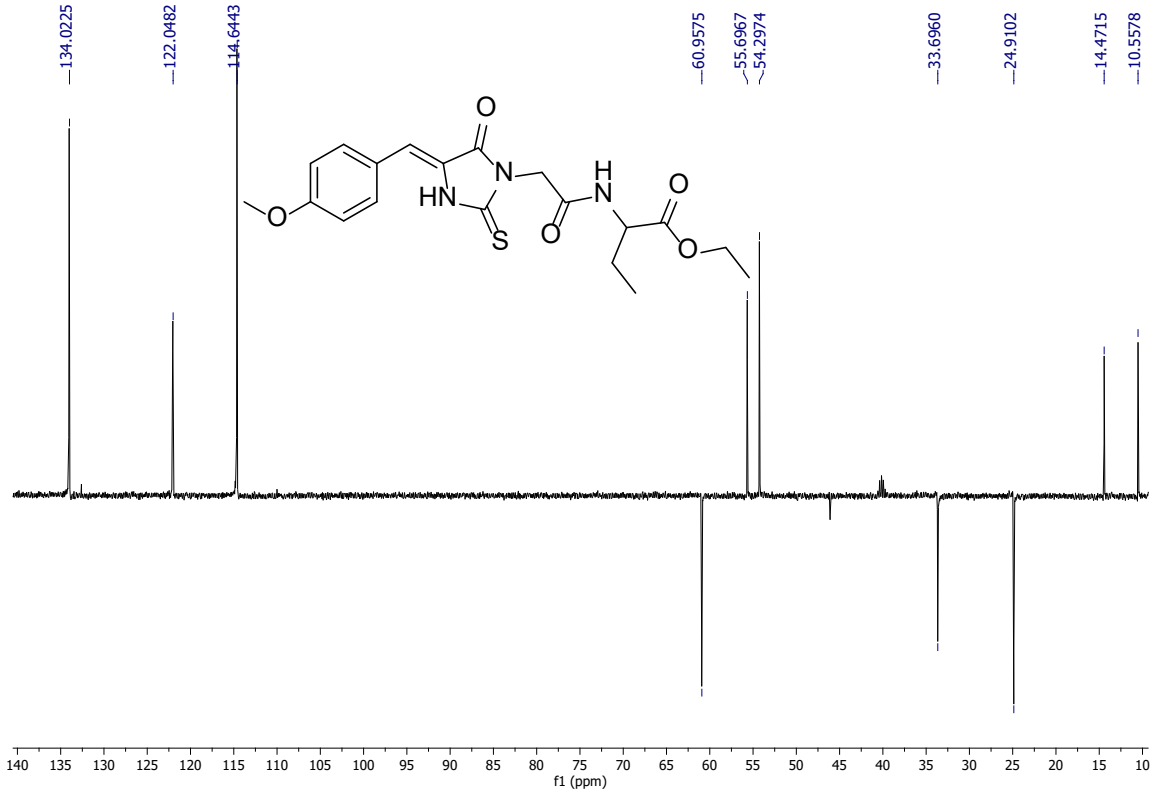

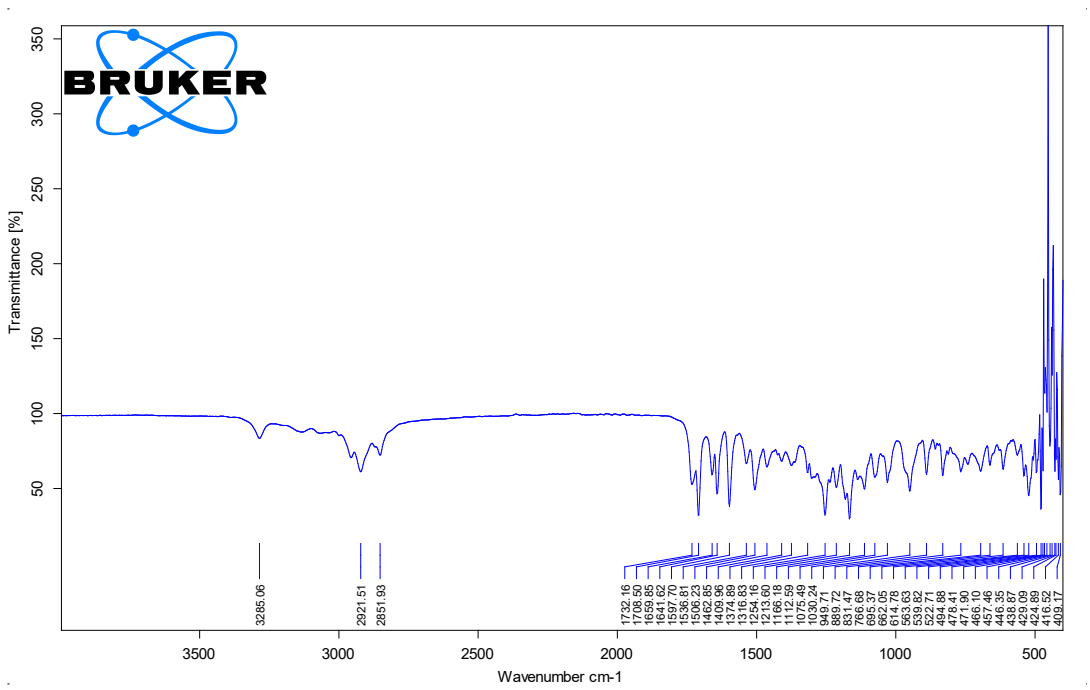

C:\Users\Administrator\Documents\Bruker\OPUS_7.5.18\DATA\MEAS\A3-7.0	A3-7	Instrument type and / or accessory	2023/12/05

Page 1/1

A9: ^{1}H and ^{13}C NMR spectra of (Z)-ethyl 2-(2-(4-(4-methylbenzylidene)-5-oxo-2-thioxoimidazolidin-1-yl)acetamido)propanoate

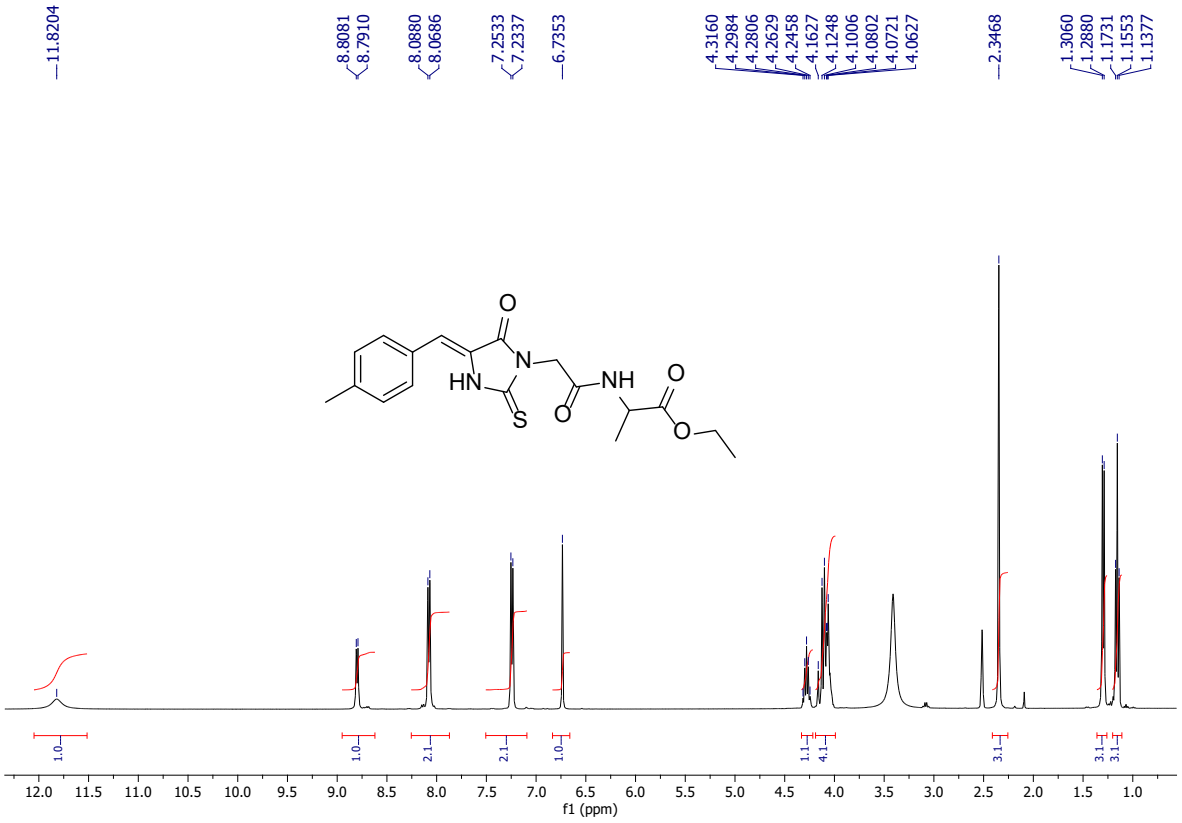

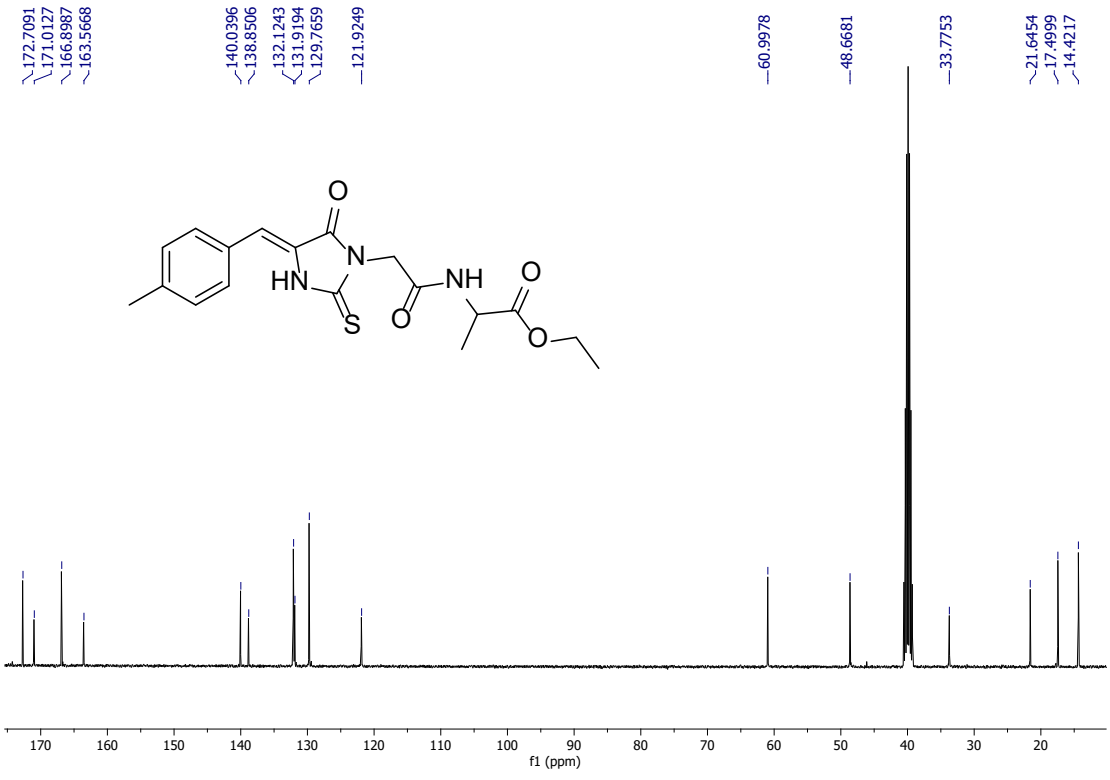

A10: Dept 135 NMR and IR spectra of (Z)-ethyl 2-(2-(4-(4-methylbenzylidene)-5-oxo-2-thioxoimidazolidin-1-yl)acetamido)propanoate

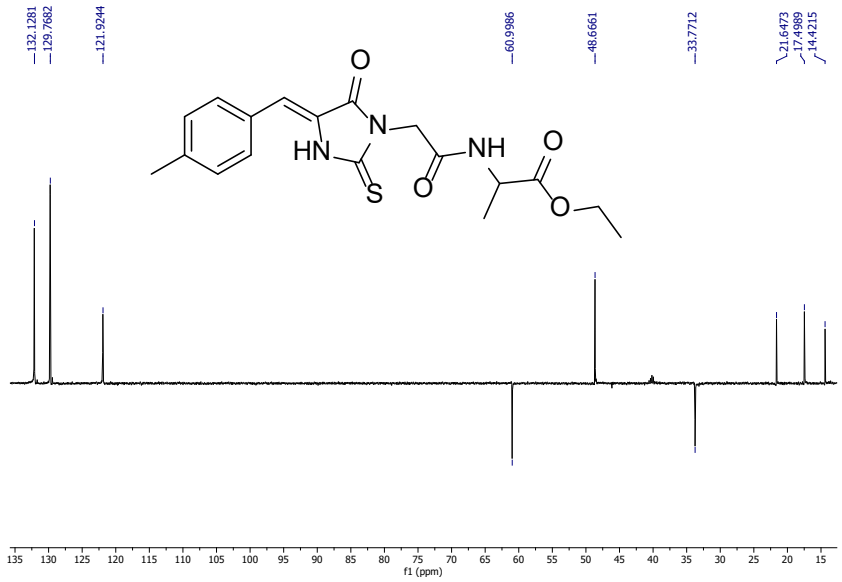

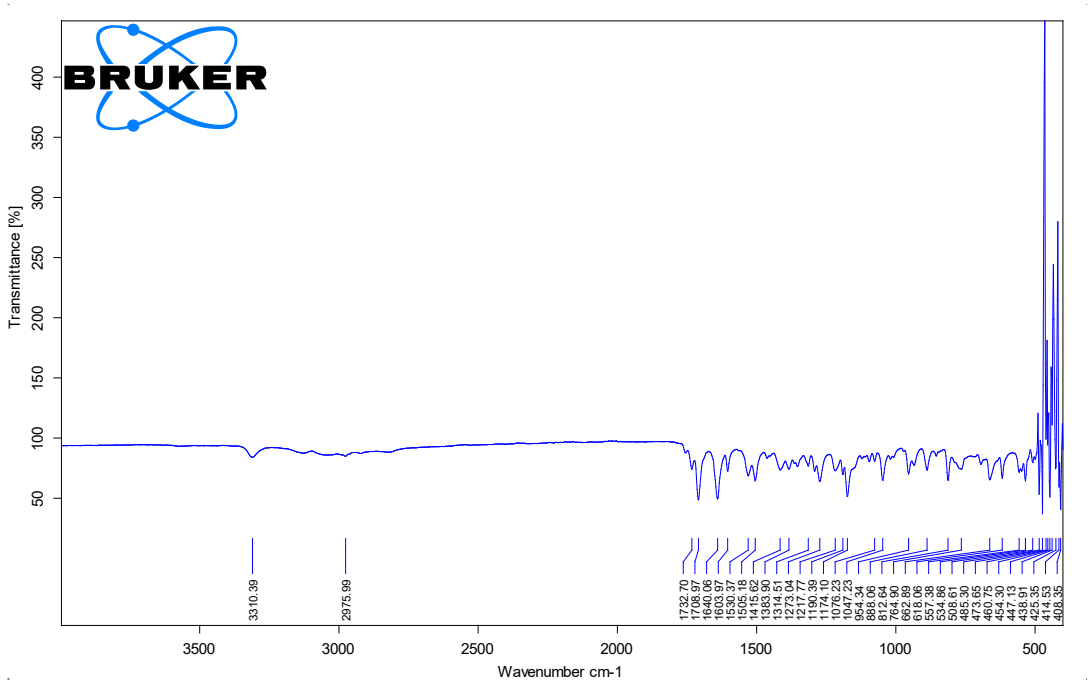

C:\Users\Administrator\Documents\Bruker\OPUS_7.5.18\DATA\MEAS\A1-9.0	A1-9	Instrument type and / or accessory	2023/12/05

Page 1/1

A11: ^{1}H and ^{13}C NMR spectra of (Z)-ethyl 2-(2-(4-(4-fluorobenzylidene)-5-oxo-2-thioxoimidazolidin-1-yl)acetamido)pentanoate

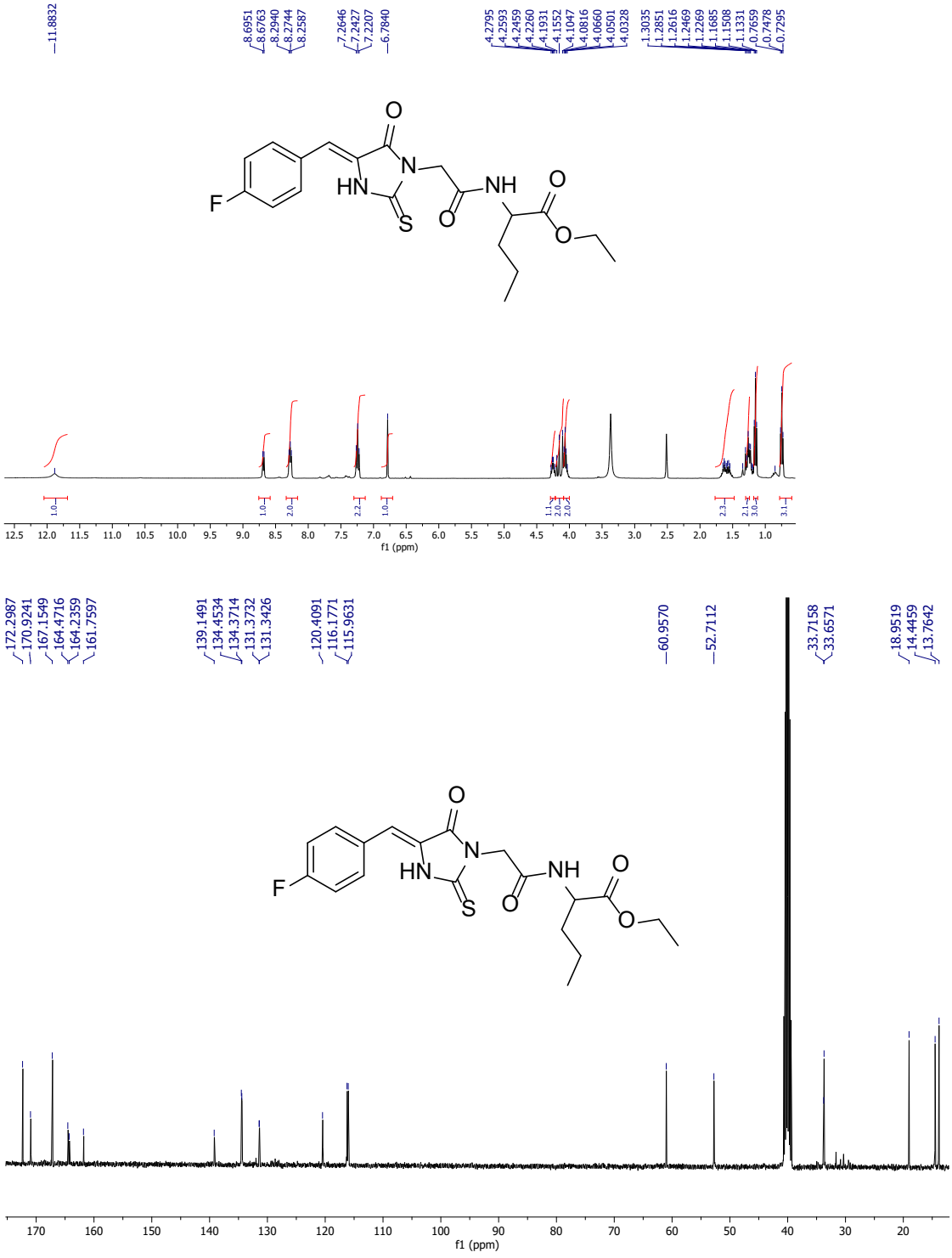

A12: Dept 135 NMR and IR spectra

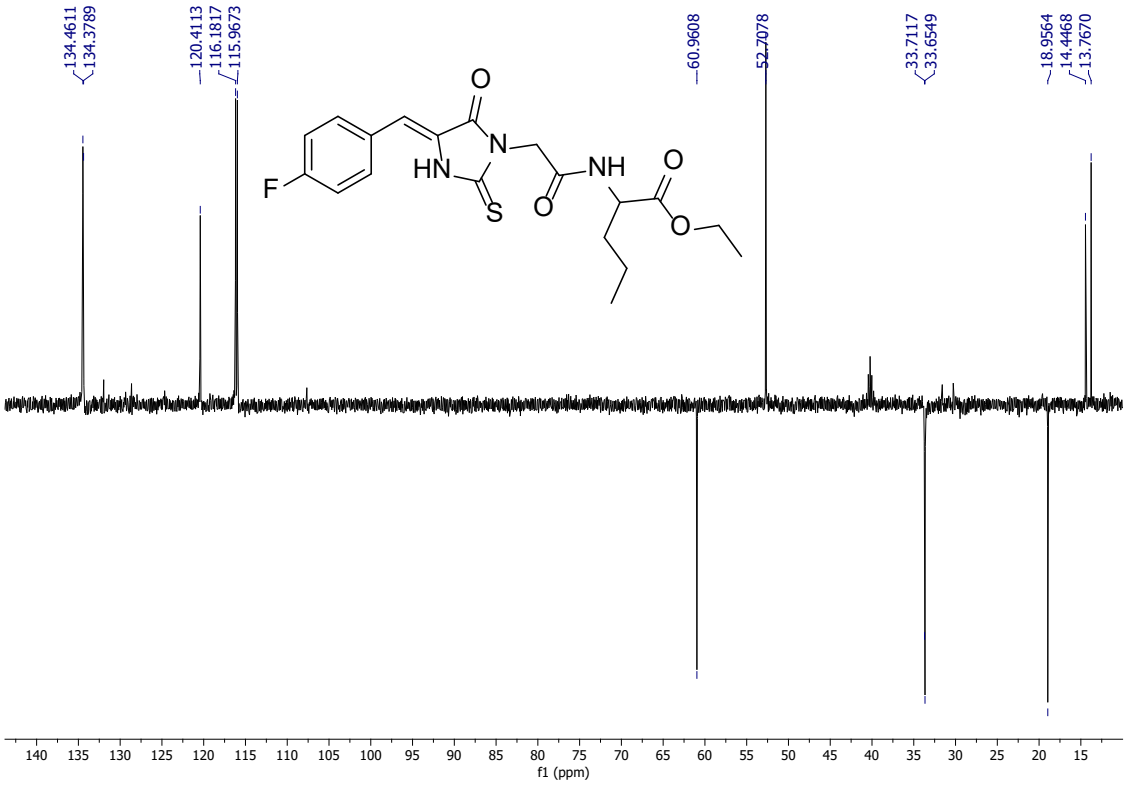

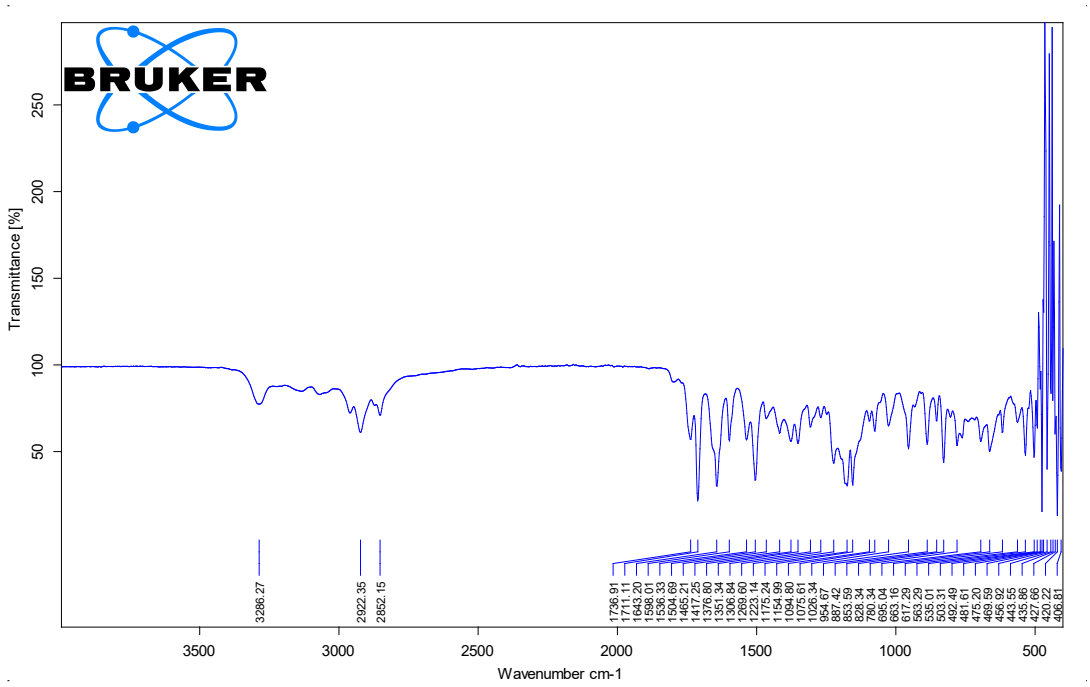

C:\Users\Administrator\Documents\Bruker\OPUS_7.5.18\DATA\MEAS\A1-13.0	A1-13	Instrument type and / or accessory	2023/12/05

Page 1/1

A13: % α-glucosidase charts for thiohydantoin derivatives